2017-06-01

Aerodynamic Drag On Intermodal Rail Cars

Philip Donovan Kinghorn
Brigham Young University

Aerodynamic Drag On Intermodal Rail Cars

Philip Donovan Kinghorn

A thesis submitted to the faculty of
Brigham Young University
in partial fulfillment of the requirements for the degree of

Master of Science

R. Daniel Maynes, Chair
Julie Crockett
Steven E. Gorrell

Department of Mechanical Engineering

Brigham Young University

ABSTRACT

Aerodynamic Drag On Intermodal Rail Cars

Philip Donovan Kinghorn
Department of Mechanical Engineering, BYU
Master of Science

The freight rail industry is essential to the US infrastructure and there is significant motivation to improve its efficiency. The aerodynamic drag associated with transport of commodities by rail is becoming increasingly important as the cost of diesel fuel increases. For intermodal railcars a significant amount of aerodynamic drag is a result of the large distance between containers that often occurs and the resulting pressure drag resulting from the separated flow that results due to their non-streamlined shape.

This thesis reports on research that has been done to characterize the aerodynamic drag on intermodal train builds and allow their builds to be optimized for fuel efficiency. Data was obtained through wind tunnel testing of G-scale (1/29) models. Drag on these models was measured using a system of isolated load cell balances and the wind tunnel speed was varied from 20 to 100 mph.

Several common intermodal scenarios were explored and the aerodynamic drag for each was characterized. These scenarios were the partial loading of containers on rail cars, the influence of the gap between containers, the use of a streamlined container near the front of the train, and the inclusion of semi-trailers on railcars. For each case multiple build configurations were tested and the drag results were compared to determine the optimal build for each scenario.

Keywords: aerodynamics, railcars, intermodal, wind tunnel, train

ACKNOWLEDGMENTS

I would like to offer sincere gratitude to Dr. Daniel Maynes, Dr. Julie Crockett, and Dr. Steven Gorrell for their help and assistance on this project and throughout my graduate school experience. I would also like to thank Wayne Kennedy for his guidance and direction throughout this project. I want to express my gratitude for the love and support of my wife Keolanani and our children Emma and Landon.

TABLE OF CONTENTS

LIST OF TABLES

LIST OF FIGURES

NOMENCLATURE

A_D	Drag area in cm^2
c	Confidence level for the Student's t score
C_d	Drag coefficient
$e_{1,k}$	Element of error for the k-th term
F_D	Force of drag in newtons
L	Characteristic length in cm
n	Number of datasets
P	Atmospheric air pressure
ΔP	Pressure difference between the total pressure and the static pressure
R	Ideal gas constant
Re	Reynolds number
T	Air temperature in K
$t_{\nu,c}$	Student's t score
U	Air velocity
u_s	Systematic uncertainty
u_r	Random uncertainty
U_x	Total uncertainty
u_{s,C_d}	Systematic uncertainty of C_d
u_{r,C_d}	Random uncertainty of C_d
U_{C_d}	Total uncertainty of C_d
Θ_x	Absolute sensitivity coefficient
μ	Dynamic viscosity in Ns/m^2
ν	Degrees of freedom for the Student's t score
ρ	Air density in kg/m^3
σ_x	Standard deviation
$\sigma_{\bar{x}_n}$	Standard deviation of the mean

CHAPTER 1. INTRODUCTION

1.1 Motivation

Freight railroads are very important to our society, which relies heavily each day on the transportation of goods. These goods are moved around the world with an ever increasing network of ships, planes, trains, trucks, and even drones and the rail industry is an essential part to this transportation network. In the United States, natural resources, agricultural products, automobiles, and commodities are all moved throughout the country by rail. The Association of American Railroads refers to the rail industry as the backbone of the US economy and it is widely recognized as the best freight rail system in the world [1]. A recent study analyzed the economic and fiscal impact of the US rail industry. The results showed that in 2014 the rail industry supported approximately 1.5 million jobs, \$88.4 billion in wages, and \$273.6 billion in output to the economy [2]. Clearly this backbone industry is essential to the US infrastructure and there is significant motivation to improve its efficiency.

Freight locomotives are powered by diesel generators which power electric motors. Fuel cost is one of the highest operating costs for rail companies and so variations in diesel fuel prices

Figure 1.1: Image of an intermodal train of well cars loaded with containers.

Figure 1.2: Image of two well car models with articulated trucks.

can have a significant impact on the industry. Union Pacific is one of the largest rail companies in North American and in 2015 spent around $2 billion in fuel costs [3]. As diesel prices have risen, rail companies have become increasingly interested in improving the fuel efficiency of their trains. Fuel efficiency can be increased by reducing the resistant forces that act against the forward movement of the train. The resistant forces are dominated by frictional resistance due to relative motion between wheels and track and the aerodynamic drag. As these forces increase, there is a direct increase in the energy and fuel required to operate the train.

The focus of this research is the resistance resulting from aerodynamic drag. At low speeds the aerodynamic drag may only make up a small percentage of the total resistant forces. However, the drag increases proportional to the velocity squared and so as the train velocity increases the drag becomes more significant. Consequently, at high speeds the majority of the resistant forces acting against the train may be from drag, with some studies reporting that it can be as high as 90% [4].

An investigation into the reduction of aerodynamic drag becomes increasingly important in the case of intermodal rail cars. Intermodal trains are made up of some number of locomotives that are followed by a series of flat spine cars and recessed well cars which are loaded with shipping containers and semi-trailers as shown in Fig. 1.1. The well cars may be individual rail cars or in a set of three or five with articulated trucks (wheel assembly). This mean that each car in the set shares a set of trucks with the well car in front of it as seen in Fig. 1.2. This type of train travel at greater velocities than any other type of freight train so the negative effect of aerodynamic drag is much greater. Intermodal traffic is also the fastest growing type of freight that is being transported [1]. Thus, a reduction in drag could result in a significant improvement in fuel efficiency and revenue generation for intermodal traffic.

Reducing the aerodynamic drag on intermodal rail cars is challenging because there are many constraints that severely limit what can actually be changed. The containers loaded onto intermodal cars are standardized with the many of them required to meet standards set by the International Organization for Standardization (ISO). This makes changing the shape or aerodynamic profile of the containers impossible. Add-on devices like those seen on semi-trailers, which will be discussed later, are impractical because the large number of cars in a typical train (60-100). Train yards where trains are loaded, unloaded and put together are optimized to move the containers as quickly as possible. Changes in the building and tearing down of a train consist to optimize the aerodynamic drag of the completely built train set is possible. However, the build/tear down processes must be fast enough so that increases in aerodynamics more than offset the penalty associated with slowing of the system.

This thesis reports on measurements performed in a large wind tunnel on the campus of Brigham Young University. The purpose of the experiments is to characterize the aerodynamic drag that exists on intermodal train cars for the most likely loading configurations that are realized. The results provide a tabulation of aerodynamic drag data that allow optimization of the train build process to make sure the train is built to minimize aerodynamic resistance. A typical intermodal train may have 60-100 well cars. Each well car may have two intermodal containers, with one stacked on the other, a single container, or it may be empty. Each of these configurations results in a much different aerodynamic drag on this car and on the cars immediately in front of and behind it. Further, there are three standard intermodal container sizes and all can be transported on a single train. Thus, gap width between successive containers can show large variation and sometimes there will be large containers stacked on small containers and vice-versa. These situations and other similar scenarios are considered in this thesis to allow the train builder to optimize the train build process.

1.2 Literature Review

Aerodynamics is the study of the fluid/solid interaction as an object moves through a fluid. It can better be explained as the study of the forces that result from these interactions. Typically, the working fluid is air and much of our knowledge of aerodynamics has come from studying aircraft and airfoils. Understanding the aerodynamic forces of lift and drag are essential to the flight of any aircraft. While useful, the aerodynamic principles of aircrafts cannot be directly applied to ground vehicles such as trains and trucks. Moving so close to the ground makes the flow dynamics of ground vehicles significantly different to the flow around an aircraft [5].

In the case of ground vehicles, the most relevant aerodynamic force is drag. The drag opposes the forward motion of the vehicle and reduces its efficiency. Aerodynamic drag is the sum of two component forces, pressure drag and friction drag. Friction drag is a result of the shear stress, τ_w, on an object. This occurs in the fluid boundary layer which forms on the surface of the object as a result of the no-slip condition. Friction drag is calculated by integrating τ_w over the surface area and it scales with Reynolds number. Pressure drag results from a pressure difference on the front and back of an object as it moves through a fluid. At the back of the object the flow separates which creates a low pressure region of vortices. The magnitude of the low pressure region scales with the size of the vortices that form. [6–8]. These two components together make up the total aerodynamic drag on an object. However when pressure drag is present it typically makes up the majority of the drag and the friction drag has little effect.

In general ground vehicles such as trains and truck-trailers are classified aerodynamically as bluff bodies. Bluff bodies have a blocky or rectangular shape with sharp edges. The flow profile of bluff bodies usually causes flow separation and vortex shedding resulting in a large amount of pressure drag [9–11]. Pressure drag is generally the dominant source of aerodynamic drag for bluff bodies.

Many studies have been performed with the interest of reducing the aerodynamic drag on truck-trailer vehicles [11-15]. These studies often focus on a few specific areas of the truck-trailer. Many aim to reduce drag caused by the height difference of the trailer and cab. These suggest a curved front faring on the top of the cab to direct the flow of air up over the trailer. The drag reduction for the faring studies varies but one study reported a 16.6% drag reduction [12].

Another area of interest is the trailing edge of the trailer. The air coming off the back of the trailer causes vortices and a low pressure region to form. Studies suggest that the drag could be reduced by reducing the trailer back area with deployable fins. Experimental data showed that the fins reduced the drag on the trailer by 19% [13]. CFD measurements of the same fins resulted in the drag being reduced by 15% [14]. The underside of the trailer has also been studied significantly using side skirts to prevent flow under the trailer. Trailer side skirts have been reported to reduce the drag on the truck-trailer by 13% [15].

The desire for high speed passenger trains has led to significant train specific aerodynamic research [16–19]. The aim with high speed trains is to avoid flow separation along the train. This is done by streamlining the leading locomotive and closing the gaps between rail cars. While similar streamlining would be desirable for freight trains, the current constraints of the industry make it impractical.

Many drag reduction methods used for high speed trains and truck-trailers may not be directly applicable to freight trains but many of the principles learned may be helpful in improving efficiency. Although a perfectly streamlined solution for freight trains is not currently feasible, significant progress has been made to reduce drag and improve efficiency. These studies generally focus on small changes that can be retro fitted to existing rail cars. One study investigated coal carrying rail cars which are similar to a box car with an open top. The open top results in high drag which could be reduced if the cars were covered [20]. Reductions in the drag as large as 40% were reported. Another study looked at the underside of the coal cars and the unloading mechanism. By streamlining the underside, a drag reduction of 10-15% was observed [21]. Research on auto carrying rail cars reported a 14% reduction in drag if the corrugated roof was replaced or covered with a flat material. The drag was shown to be further reduced by 15% by installing a skirt to prevent flow under the rail car [22].

A few studies have focused specifically on reducing the drag of intermodal rail cars. One study performed by the Association of American Railroads (AAR) investigated several aspects of intermodal rail cars in a wind tunnel. A streamlined design of an intermodal well car was tested and showed a 14% reduction in drag compared to the non-streamlined car. The study also reported that the drag on a well car could be reduced 16% by completely sealing all gaps in the cars floor. A device to fill the gap between successive intermodal containers was also tested at three different gap widths. The resulting drag reduction ranged from 14 (far spacing) to 34% (closest spacing). The study also showed that the drag on a rail car in a unit train (a train made up of all one type of rail car) depends on its position in the train. The drag decreases exponentially until about the 10th car and after remained relatively constant [23, 24]. Based on the findings of the AAR another study reviewed the loading practices of intermodal rail cars and developed an algorithm with computational data to minimize the load gaps along the train and reduce drag. The algorithm was then used to create a system to image and evaluate the aerodynamic efficiency of passing trains [25–28].

In this study similar methods will be explored to reduce gaps between loads and determine optimal loading configurations for drag reduction . The aim of this research is to characterize the drag on the central cars of an intermodal train. The drag is relatively constant along these cars and they make up the bulk of the train. Using 1/29th scale models of intermodal rail cars allows for wind tunnel tests to be performed on a longer train than previous studies. This will allow for a more representative drag reading for the central cars. Further this research will examine the drag relationship of different types of intermodal rail cars in the same train.

1.3 Contribution

The contribution of this research will be to characterize the aerodynamic drag on intermodal train builds and allow their build to be optimized for fuel efficiency. The work will focus on addressing the overall drag for following common scenarios:

- Empty and single-stacked well car loading cases, when these cars are surrounded by cars with double-stacked containers
- The influence that gap distance between intermodal containers exert on the overall drag
- Reduction in the drag that can be realized by employing a streamlined shape add-on for the first and last container carrying cars
- The drag that exists when traditional intermodal containers are replaced with semi-trailers that are loaded onto spine cars

For all scenarios the drag will be measured on model railcars in a wind tunnel. The drag for each test scenario will be quantified by calculating an average drag coefficient, which will be compared to determine the most efficient intermodal configurations.

1.4 Thesis Outline

This thesis is structured in the following manner. Chapter 2 describes the methodology. It details the wind tunnel testing protocol, the train models and all loading scenarios considered, the instrumentation used to collect data, and a presentation of the experimental uncertainty associated with all results. Chapter 3 presents the results and compares them to baseline conditions. The results are discussed for all scenarios and optimal configurations are specified. Lastly, Chapter 4 provides conclusions of the research and discusses future work that should be conducted in this area.

CHAPTER 2. METHODOLOGY

2.1 Experimental Setup

Wind tunnels have been used for some time to study aerodynamic forces on an object and provide a controlled environment for aerodynamic tests to be performed. However, the size constraints of wind tunnels often necessitate the use of scale models for the experiment. The data collected is then correlated to the full scale using non-dimensional analysis. For this experiment, all of the data was collected using the large wind tunnel at Brigham Young University, whose test section is shown in Fig. 2.1. The test section of this wind tunnel is approximately 5.1 m in length with a width of 1.22 m and a height of 0.61 m.

The wind tunnel operates at 18 discrete velocity settings, nine speeds in both a high and low gear. For this experiment only speeds 2 through 8 in the high gear were used. This created a range of air speed between approximately 35 m/s to 50 m/s that was explored. The air velocity, U, inside the wind tunnel is used in equation 2.1 to calculate the non-dimensional Reynolds number.

$$Re = \frac{UL\rho}{\mu} \tag{2.1}$$

L is the characteristic length, μ is the air viscosity, and ρ is the air density. The characteristic length, L, used in these calculations was the height of two stacked container models. Air viscosity, μ, was found using a temperature dependent relation from the DIPPR chemical database. Air density was calculated using the ideal gas relation shown in equation 2.2

$$\rho = \frac{P}{RT} \tag{2.2}$$

where R is the air ideal gas constant, (287 J/kg·K), and temperature was measured with a thermocouple mounted in the wind tunnel test section. The local atmospheric pressure, P, was recorded from the BYU weather station before each test.

Figure 2.1: The test track and model system was constructed and secured to the wind floor. The track was used to simulate the flow past actual rail cars and each rail car was fastened to the test track. Force data was collected from individual intermodal rail cars with a system of load cells.

Air speed, U, was measured with a pitot probe mounted on the ceiling of the test section near the front opening. The pitot probe was connected to a differential pressure transducer and velocity was calculated with equation 2.3

$$U = \sqrt{\frac{2\Delta P}{\rho}} \tag{2.3}$$

ΔP is the pressure difference between the total pressure and the static pressure and was measured by the differential pressure transducer connected to the pitot probe. Again, the air density, ρ, was calculated from equation 2.2. The velocities tested resulted in Reynolds numbers ranging from 1.9×10^5 to 2.8×10^5. The drag coefficient, C_d, was calculated using Eqn. 2.4

$$C_d = \frac{F_D}{\frac{1}{2}\rho U^2 A_D} \tag{2.4}$$

F_D is the drag force measured on the rail car model by the load cells and A_D is the drag area. The projected frontal area of two stacked container models was used for the drag area of all experiments.

Figure 2.2: Sections of channel aluminum were used for the rail car track. These sections could be rearranged or replaced to accommodate different rail car lengths.

Figure 2.3: G-Scale locomotive train model. These models were purchased from a model train manufacturer and placed at the front of the wind tunnel test track. Drag on the locomotives was not measured in this study.

2.1.1 Test Track

One of the challenges of using a wind tunnel to study the drag on trains is that it is difficult to simulate real world conditions. As a train travels down the track there is relative motion between the train and the ground which results in the air flowing past the train having a uniform flow profile. In the test section of a wind tunnel the flow is uniform except near the walls, ceiling, and floor

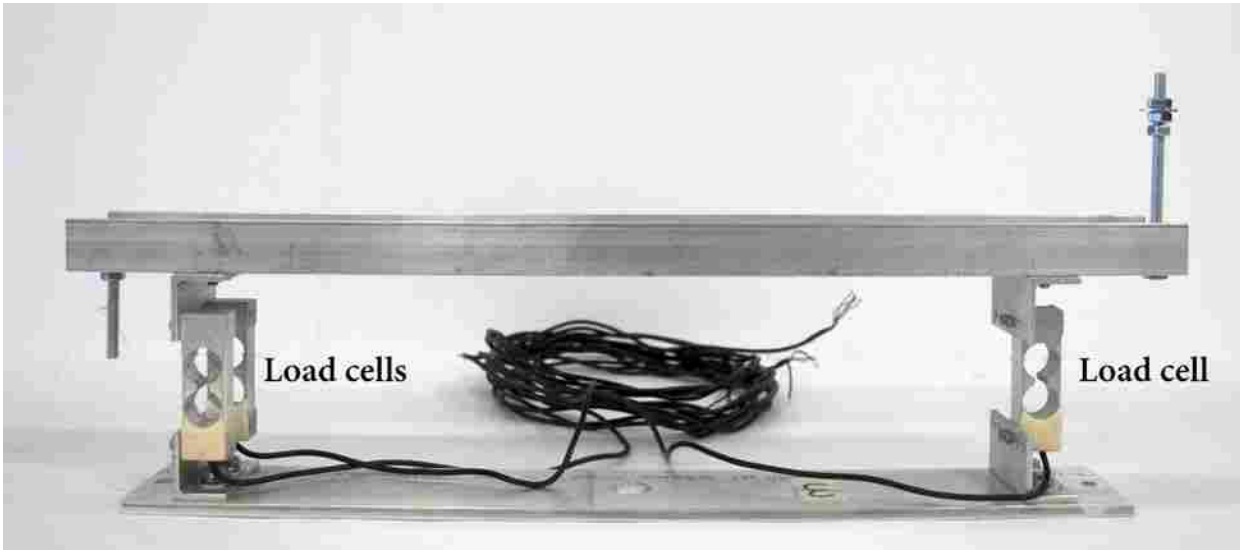

Figure 2.4: Drag data was collected from rail cars fastened to test cells like the one shown here. Each test section used three 19.6 N. load cells with the sum of the three outputs being recorded. The load cells were regularly calibrated with a set of weights to record force measurements in newtons.

where a boundary layer forms and reduces the velocity of the flow. If train models were mounted on the floor of the test section for testing then the results would be affected by the boundary layer. To remedy this, a simulated test track was constructed and fastened to the wind tunnel test section shown in Fig. 2.1 and 2.2. The shape of the test track positioned the train models in the middle of the wind tunnel test section where the flow profile is uniform and not affected by the boundary layers at the walls, ceiling, or floor. Sections of aluminum channel were used as the simulated track. Two locomotive models, similar to the one shown in Fig. 2.3, were fastened with wire at the front of the track. Each of the intermodal rail cars were secured to the track behind the locomotives with a 1/4” diameter bolt mounted to the cars and mounted on the channel.

The test apparatus was made by fastening three 19.6 N load cells (Transducer Techniques LSP2) to a single section of track as shown in Fig. 2.4. Force data was recorded as the sum of the three load cell outputs. The load cells in the test section were calibrated using a pulley and weights system for forces between 0 N and 9.8 N. Calibration validation was performed regularly during testing and the load cells were re-calibrated if an error in excess of 2.5% existed. The average calibration error was approximately 0.5%.

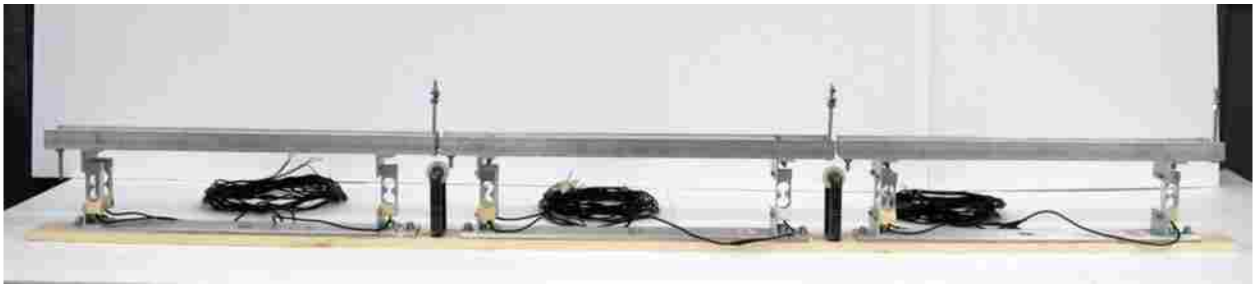

Figure 2.5: Three consecutive test sections were used to measure multiple rail cars in one tests. Each test section was calibrated separately. The pulleys used in calibration can be seen in this image.

The original test rig had a single load cell test section and would record force data for a single rail car. It was later determined that simultaneous measurements from multiple cars was desired so the test track was rebuilt to include three consecutive load cell test sections, each with a separate rail car model mounted on them. The new test track, which is shown in Fig. 2.5, and this revised system, greatly reduced the required number of tests needed to understand the aerodynamic interaction of consecutive rail cars. The experiment error was also reduced because data for each rail car configuration could be collected in a single test instead of multiple separate tests.

2.1.2 Train Models

There can be a lot of variation in the types and sizes of cars and containers when building an intermodal train. For this experiment, we tested some of the most common configurations as well as a few specialty cases. All of the tests were completed with 1/29th scale (G-scale) models of the rail cars. These models were either purchased from a model train manufacturer or custom built by a model maker. The following list outlines the types of model train components that were used in these experiments.

- Well Cars and Containers
  - 40 ft. models
  - 48 ft. models
  - 53 ft. models
- Specialty Components
  - Union Pacific Arrowedge®
  - 40 ft. smooth container
  - Foam boxes to vary gap length
  - Semi-Trailers on spine cars
  - Locomotives

Figure 2.6: Image of 48 ft. well car model. Length refers to the recessed well and not the total rail car length.

The well car is a specific intermodal freight transportation carriage for shipping containers. These specialized rail cars have a lowered platform between the trucks that the shipping containers are mounted to. The size of the well car is referenced by the length of this lowered mounting platform. Since the well car platform is lower to the tracks, it allows containers to be stacked while maintaining a lower clearance height. Well cars may be individual rail cars or come as articulated sets of either five or three. In articulated sets, well cars share the trucks of the car in front of them.

For this experiment three lengths of well cars were used: 40 ft., 48 ft., and 53 ft. The 40 ft. well cars were modified at BYU from a set of five 48 ft. well cars. The 48 ft. cars were purchased

Figure 2.7: Image of two 40 ft. articulated well car models loaded with double stacked 40 ft. containers.

Figure 2.8: 40 ft. corrugated container model stacked on a 48 ft. container model. Actual model lengths are approximately 42 cm and 50 cm respectively.

from USA Trains and a set of three 53 ft. well cars were purchased from a specialized model maker.

The container models used in this experiment correspond to the lengths of the well cars used and are three common container sizes used in the United States. The models were purchased from USA Trains in lengths of 40 and 48 ft. The 48 ft. containers were extended in the middle to build a set of 53 ft. containers. Figure 2.8 shows a 40 ft. container stacked on a 48 ft. container. The 53 ft. containers are shown loaded in the 53 ft. well cars in Fig. 2.9. The actual lengths of the model containers were 42 cm, 50 cm, and 56 cm.

Figure 2.9: Image of a 53 ft. well car model loaded with double stacked 53 ft. containers. Actual container model length is approximately 55 cm.

Figure 2.10: Image of the Union Pacific Arrowedge® model used to reduce the drag on the first and last container cars. The Arrowedge® is stacked on a 48 ft. container loaded in a 48 ft. well car.

The Arrowedge®, show in Fig. 2.10, is a container for increasing aerodynamics of stacked intermodal shipping containers on well cars. It was designed and developed by Union Pacific and undergraduate BYU engineering students. Its purpose is to increase fuel savings by decreasing drag on the train. It is used on the first and last container cars, in opposing directions, in a train to reduce the aerodynamic drag on those cars. The Arrowedge® model was purchased from a model builder and was tested at both the front and rear of the test track with 48 ft. well cars loaded with 48 ft. double stacked containers.

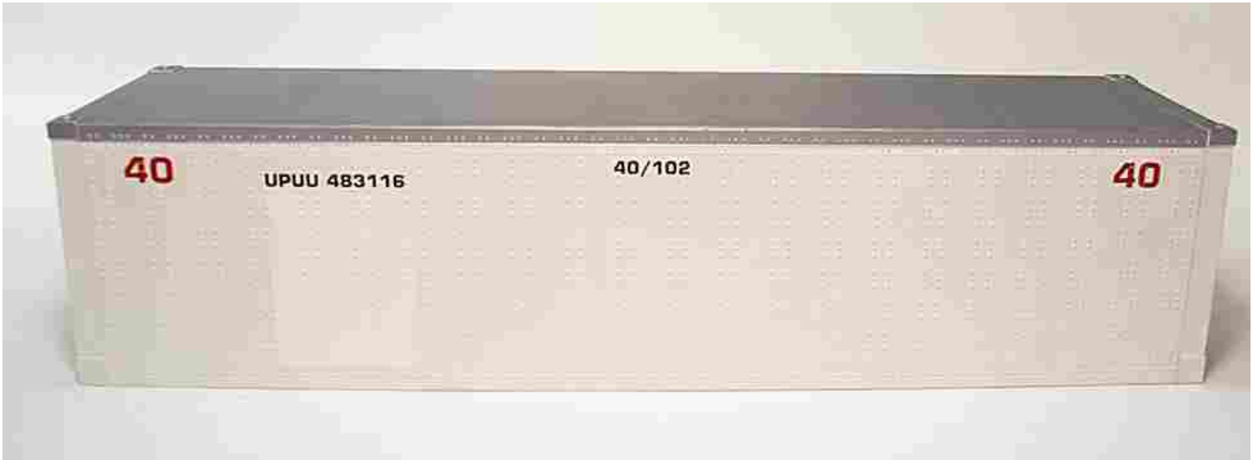

Figure 2.11: 40 ft. container model with a smooth roof and riveted sides.

Standard intermodal containers are constructed with corrugated sides which may increase the amount of aerodynamic drag on the container. To explore the influence of container design, a less common container design was tested and compared to the standard corrugated containers. These containers have a smooth roof and riveted sides as seen in Fig. 2.11. A set of these container models, in the 40 ft. length, were purchased and tested. The results were compared to tests with the 40 ft. corrugated containers.

For this study, one scenario that was explored in testing was the influence of the gap between containers on the drag. Sets of foam containers with varying lengths were constructed and tested. The containers were made with a hot wire CNC machine to have the same height and width as standard double stacked container models and were loaded into the 48 ft. well cars for testing. Six gap lengths were tested and three of these are shown in Fig. 2.12. Three sets of containers were designed with the same dimensions as standard double stacked container sizes: 20 ft., 40 ft., and 48 ft. containers. The last three sets were designed to extend past the recessed well of the rail car and test a smaller gap length. One of these is shown in the bottom panel of Fig. 2.12. The gap length, L_g, was normalized by the gap length of a 48 ft. container in a 48 ft. well car.

Semi-trailers can be shipped on a train when loaded on a Spine Car. To investigate this scenario two semi-trailer models were purchased from a model builder. The trailers that were tested were identical 48 ft. semi-trailers loaded onto 53 ft. spine cars. The actual length of the trailer models, shown in Fig. 2.13, was 50 cm. The trailers and spine cars were tested with both

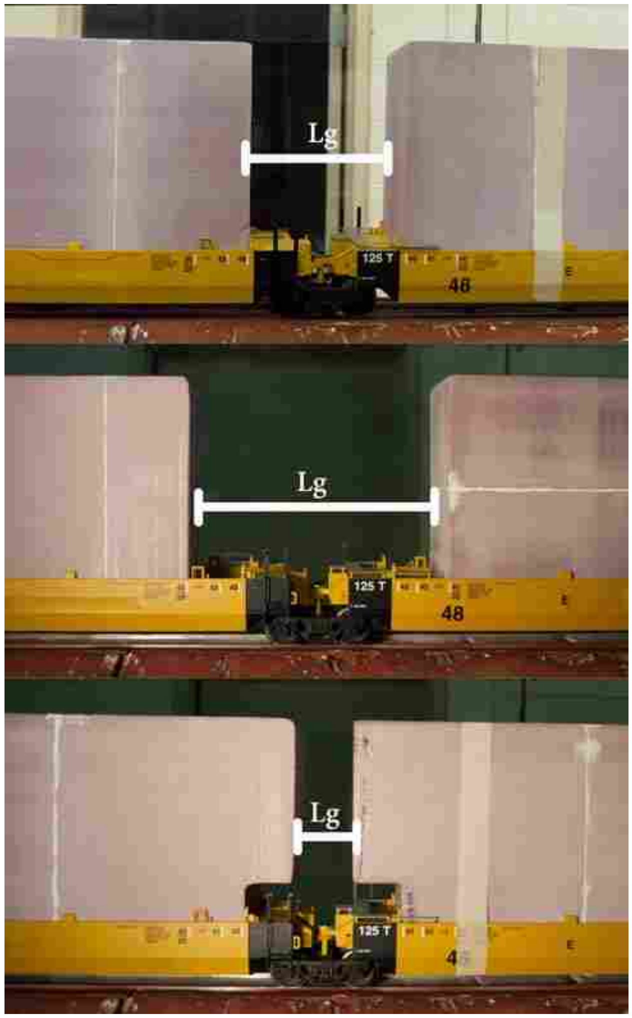

Figure 2.12: Foam containers constructed to study the drag effect of the load gap. Three of the five lengths are shown here.

the 53 ft. and the 48 ft. well cars. A semi-trailer side skirt was constructed and attached to one of the trailer models to examine influence if side skirts are left on when a trailer is loaded on a train. The side skirts are designed to reduce the drag on a trailer while it is driving on the road and their drag effect on a train is unknown.

Locomotive models like the one seen in Fig. 2.3 were positioned at the front of the test track for each wind tunnel test. The drag on the locomotives was not an aspect of this experiment and was not measured. They were used only to condition the flow and better simulate the flow of air past rail cars trailing a locomotive. The models were standard G-scale models purchased from USA Trains.

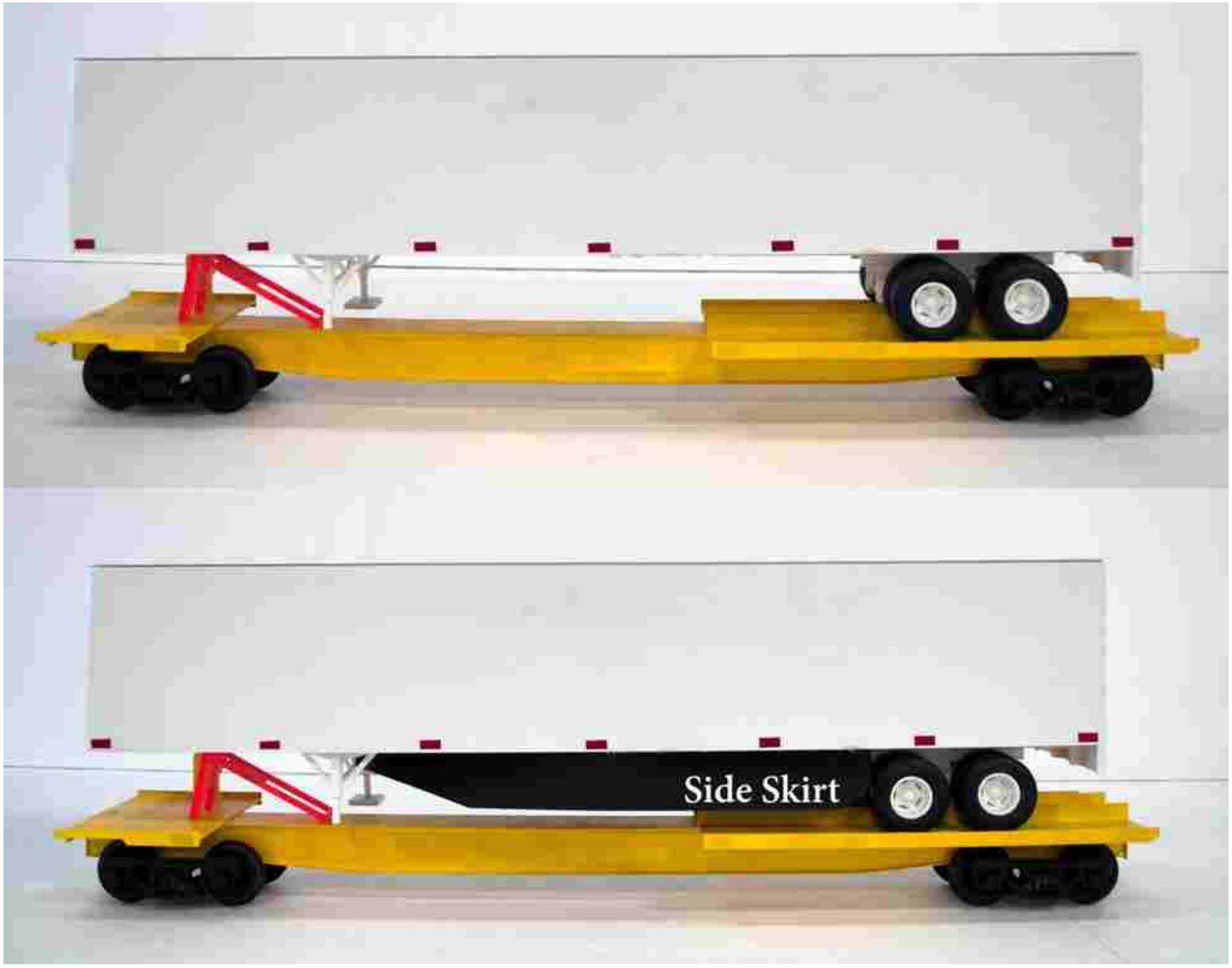

Figure 2.13: Side images of a semi-trailer on a 53' spine car model. The top panel shows a semi-trailer without a side skirt and the bottom panel shows a semi-trailer with a side skirt.

2.2 Experimental Procedure

Locomotive rail car models were secured to the track using a small gage wire and the intermodal rail car models were bolted to the track with 1/4 in. bolts. Container models were secured to the well cars using a small steel rod which was inserted through holes drilled in the sides of the well car and the container. When two stacked containers were needed the containers were bolted together. The bolts were placed through the inside of both containers so they did not interrupt the air flow. Models were checked thoroughly to insure that they were aligned correctly. A level was used to check vertical alignment and the models were inspected visually for horizontal alignment. Once the rail car models were secured the wind tunnel was closed and the load cells from each test section were zeroed.

As stated before, the load cells were regularly calibrated using a weight and pulley system. A set of known weights were hung from the load cells and the resulting sensor output was measured. The force-voltage data was fit to a linear curve and the slope of the line provided the constants to scale the load data. Weights ranging from 100g to 1000g were used in either 100g or 200g increments. This range of weights exceeded the range that was measured during any of the experiments. Load cells were calibrated in both increasing and decreasing increments to determine if any hysteresis existed. The calibration results showed no sign of hysteresis in the load cells.

All of the data and measurements for the experiments were recorded with a National Instruments data acquisition system and then data was processed using the LabView software package. For each test the wind tunnel was run twice through speeds 2 through 8 in the high gear and in random order. At each speed setting all measurements were sampled at 1 kHz and an average over 30 second was recorded. After all data had been recorded the drag coefficient, C_d, and the Reynolds number, Re, were calculated with Eqns. 2.1 and 2.4.

2.3 Uncertainty Analysis

Uncertainty for a set of experimental data is a measure of the error associated with the data measurements. Experimental uncertainty is a combination of systematic and random error [29]. Systematic error is introduced by the measurement devices in an experiment and their inability to measure the true value of a parameter. All measurement devices will show some variability when measuring a parameter. This variability is seen in the form of elemental errors, e_k, such as hysteresis or non-linearity. A given instrument may show multiple elemental errors and these need to be combined to determine the total systematic uncertainty, u_s, for the instrument. Elemental errors are combined using the root-sum-squares method or RSS method. The RSS method is shown in Eqn. 2.5.

$$u_s = \pm\sqrt{e_1^2 + e_3^2 + ... + e_k^2} \tag{2.5}$$

Random error is a result of experimental conditions and is evidenced by a scattering of the collected data. Experimental procedures, variations in the test environment, and the repeatability of the experiment may all contribute to the random error of a data set. These types of errors are often unavoidable but the overall effect or random error on a data set may be reduced by averaging over a large set of data point and by collecting multiple sets of data for each experiment. The random uncertainty for a set of data, u_r, is calculated using Eqn. 2.6.

$$u_r = \pm t_{\nu,c}\sigma_x \tag{2.6}$$

Where σ_x is the standard deviation of the data set, $t_{\nu,c}$ is the Students t-score which is based on the degrees of freedom, ν, and the confidence level, c. Generally, a confidence level of 95 percent is used, which is the case for this study.

To find the total uncertainty, U_x, for a given measured parameter the systematic uncertainty, u_s, and random uncertainty, u_r, for parameter need to be combined. This can be done by again using the RSS method as shown in Eqn. 2.7

$$U_x = \pm\sqrt{u_s^2 + u_r^2} \tag{2.7}$$

U_x is the total uncertainty for a single parameter and this method may be used to find the uncertainty of all the parameters that are measured directly in the experiment. When the desired parameter is the result of an equation that contains several measured parameters, then additional statistical methods must be used to determine the uncertainty of the calculated value. The goal of this study was to measure the aerodynamic drag coefficient, C_d, for intermodal rail cars which cannot be measured directly. The drag coefficient is calculated using Eqn. 2.4. The equation may be modified so that it only contains parameters that were measured directly in the experiment. The result is shown in Eqn. 2.8.

$$C_d = \frac{F_D}{\Delta P A_D} \tag{2.8}$$

F_D is the drag force on the rail car models measured in newtons. ΔP is the differential pressure measured from the pressure transducer in pascals. A_D is the drag area which was the frontal area of two stacked container models.

To calculate the systematic uncertainty for, C_d, the systematic uncertainty for each of the parameters in Eqn. 2.8 are combined using a method similar to the RSS method. This method requires the calculation of an absolute sensitivity coefficient for each parameter along with that parameter's systematic uncertainty, $u_{s,x}$. The absolute sensitivity coefficient, Θ_x, is the partial derivative of the C_d equation with respect to the parameter x, as shown in Eqn. 2.9.

$$\Theta_x = \frac{\partial C_d}{\partial x} \tag{2.9}$$

After $u_{s,x}$ and Θ_x are calculated for each measured parameter in the drag coefficient equation, then the systematic uncertainty for Cd can be calculated using Eqn. 2.10.

$$u_{s,C_d} = \sqrt{(\Theta_{F_D} u_{s,F_D})^2 + (\Theta_{\Delta P} u_{s,\Delta P})^2 + (\Theta_{A_D} u_{s,A_D})^2} \tag{2.10}$$

The random error for the result calculated from multiple datasets can be calculated by modifying Eqn. 2.6 to calculate the random error for multiple data sets instead of a single set of data points. This is shown in Eqn. 2.11

$$u_{r,C_d} = \pm t_{\nu,c} \frac{\sigma_{\bar{x}_n}}{\sqrt{n}} \tag{2.11}$$

where

$$\nu = n - 1 \tag{2.12}$$

The Student's t is based on the degrees of freedom, ν, and a confidence level of 95%. $\sigma_{\bar{x}_n}$ is the standard deviation of the means.

The total uncertainty for C_D can be calculated by modifying Eqn. 2.7, substituting u_{s,C_D} for u_s and u_{r,C_D} for u_r. The result is shown in Eqn. 2.13

$$U_{C_D} = \sqrt{u_{s,C_D}^2 + u_{r,C_D}^2} \tag{2.13}$$

In each experimental test case for this study a mean C_d was calculated from the data for each speed at which the wind tunnel was operated. These mean C_d values were then averaged to find a mean C_d for the entire dataset. Multiple datasets were obtained for every test case in the study and the C_d values were averaged resulting in an absolute mean C_d for a given test scenario. Uncertainty analysis was performed for both the single test section track and the three test section track using a Student's t score based on a confidence interval of 95%. The average total uncertainty of the C_d values for the single test section track was shown to be approximately 0.85%. The average uncertainty of the C_d values for the three test section track were 0.74%, 0.88%, and 1.3%; or an average of 0.98%. The measured data was also shown to be very repeatable. Similar test configurations were tested on both the single test section track and the three test section track with several months of time between tests. These tests resulted in C_d values that were nearly identical.

CHAPTER 3. RESULTS AND DISCUSSION

In this chapter the results of the wind tunnel tests will be presented and discussed. Shown in Fig. 3.1 are test results where the drag coefficient was measured for a central car in a set of five intermodal 48 foot well car models. Each well car was loaded with two stacked 48 foot containers. This configuration was used as a baseline for comparison with many of the other tests that were conducted. The graph provides the drag coefficient(C_d) plotted as a function of Reynolds number(Re) for two repeat wind tunnel tests. Each test consisted of seven discrete speeds run through two times, for a total of four measurements at each nominal speed.

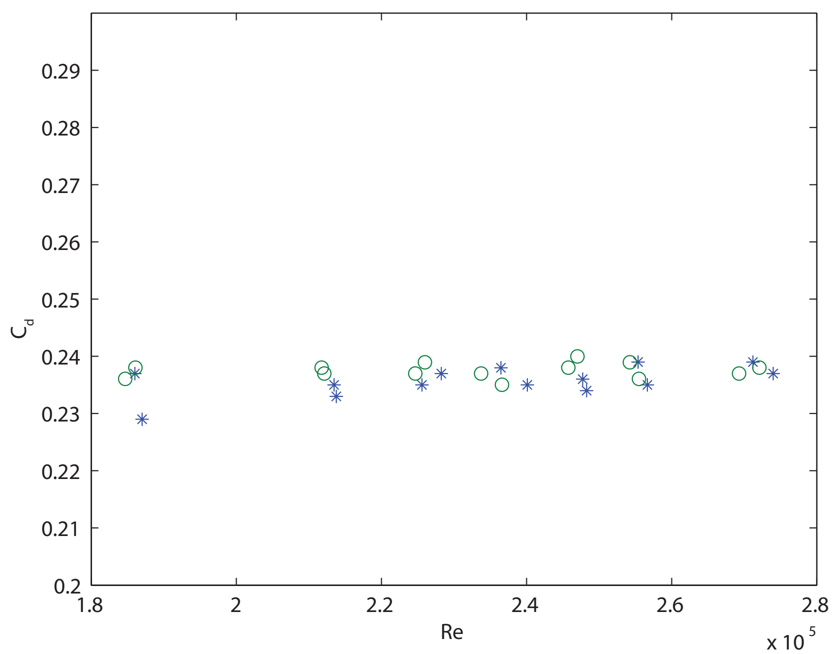

Figure 3.1: Average drag coefficient as a function of Reynolds number for a representative test case of a centrally placed well car in a set of five well cars.

The data shows very little variation in C_d with varying Re (speed). In this case the maximum variation is approximately 3% compared to the average value across all Reynolds numbers. Since the C_d is relatively constant across the range of Re tested it was determined that these data points could be averaged resulting in a single C_d value for a given test configuration. From here on, averaging over a similar number of data points will be presented to describe the results for the various test configurations.

3.1 Baseline Tests

The first few sets of tests with the 48 foot well cars were conducted using the first test track described in chapter 2. Force measurements were recorded on a single rail car in each test. The track setup was generally the same for each test case with two locomotive models at the front followed by the set of five 48 foot well cars. The third and central well car of the set (5th car in the train) was placed on the test section for all the tests.

The goal of the first set of tests with the 48 foot (model length of 19.9 in.) well car models was to explore three different sized and types of containers that are commonly used and to quantify how the drag on the car is changed for these scenarios. These tests were performed using the single test section track described in chapter 2. All data was collected in the wind tunnel using a set of five 48 foot well cars with two leading locomotives as described previously. Three container configurations were tested and these are shown in Fig 3.2.

The height and width for all container models was the same at 4 in. and 6.5 in., respectively. The length of the 48 foot container models was 19.9 in. and the length of the 40 foot models was 16.6 in. In the first case, each well car was loaded with two stacked 48 foot containers with standard corrugation on the top and sides. In the next case, the cars were loaded with two stacked 40 foot containers with standard corrugation. In the third case, the cars were loaded with two stacked 40 foot containers of a different and much less common type. These last containers have a smooth roof and riveted sides rather than the corrugation seen on most shipping containers. An average drag coefficient was calculated for each of these cases and the results are presented in Table 3.1.

In comparing the measured C_d values for the three scenario, we see the importance of container matching. Container matching is a process of matching the length of the container with the length of the well car. When 40 foot containers are placed in a 48 foot well cars the resulting

Figure 3.2: Images of container models utilized in the 48 foot well car models. Corrugated 40 foot containers are shown in the top panel; smooth 40 foot containers are shown in the middle panel; corrugated 48 foot containers are shown in the bottom panel.

Table 3.1: Average drag coefficient results for tests run with 48 foot well car models loaded with 40 foot and 48 foot containers.

Container Type	Average Drag Coefficient	Percent Drag Reduction
40 foot Corrugated	0.28	Baseline
40 foot Smooth	0.26	7.14 %
48 foot Corrugated	0.23	17.9 %

drag coefficient is 0.28. The drag coefficient is reduced by 17.9% to a C_d value of 0.23 when 48 foot containers are loaded into the 48 foot well cars. Reducing the distance between the loads reduces the size of the vortices at the point of separation which reduces the pressure drag on the rail cars. This was further explored in other parts of the research. The containers with the smooth roof resulted in 7.1% less drag than the standard corrugated containers. This is due to the elevated drag caused by flow separation off of the corrugation.

3.2 Partial Loads

Loading configurations on an intermodal train are dynamic and changing due to loading and unloading of containers at each train yard. This sometimes results in single stacked containers or empty well cars interspersed with double stacked cars. Such loading results in an increase in aerodynamic drag on the train. Since several configurations of empty loads are possible, it becomes important to understand which configurations incur the greatest and least amount of drag. This will allow operators to choose the optimal configuration for a given situation. In order to investigate this, wind tunnel tests were conducted on various partial load configurations using three different lengths of well cars.

Tests were conducted with 40, 48, and 53 foot length (model lengths of 16.6, 19.9, and 21.9 in.) well cars with containers of corresponding length. All of these tests were conducted using the three car test section track. A set of five well cars with two leading locomotives was used with the 40 and 48 foot cars. Only a set of three 53 foot well cars was available and so these cars were placed on the three car test section track with a 48 foot well car placed in front of and behind the 53 foot cars, in a similar configuration to the 40 and 48 foot cars. In all cases the drag coefficient was measured for each of the three cars mounted on the test sections. A container weighted drag coefficient was calculated using Eqn. 3.1.

$$C_{d,n} = \frac{(C_{d1} + C_{d2} + ... + C_{dn})}{c} \tag{3.1}$$

Where n is the number of cars in the system and c is the total number of containers loaded.

For each car length a baseline was established with all cars loaded with two stacked containers. Varying configurations were then tested in which one, two, three, or four containers were removed. This resulted in a total of ten tested configurations as shown in Fig. 3.3.

3.2.1 40 foot well cars

The drag coefficient results for the 40 foot well car tests are shown in Fig. 3.3. The drag coefficient for each of the three cars is shown, however in some cases this does not represent the change in drag for the whole set of five cars. In cases where an empty load is adjacent to the first or last car in the set, the drag on those cars would also be affected. In order include the drag on the first and last car in the analysis the following assumptions were made:

1. The set of five cars is centrally placed in a unit train of similar fully loaded well cars.

2. The drag on a rail car is only affected by its own configuration and that of the cars directly in front of and behind it.

3. The drag coefficient for the first or last car can be estimated using results from one of the configurations shown in Fig. 3.3. For example when a single container is removed directly in front of an untested car the C_d of the untested car would be equivalent to C_d value for the third car in configuration number 1.

The validity of these assumptions can be shown with closer examination of the data in Fig. 3.3. In the baseline configuration (configuration 0) the C_d values for the three test cars are nearly uniform. If assumption two were not true and the drag on a rail car is affected by more than the cars directly in front of and behind it then a higher C_d value would be expected for test cars one and three.

Using the above assumptions, a container weighted drag coefficient was calculated for the entire set of five well cars for these partial load configurations and is shown in Fig. 3.4. The weighted drag coefficient for each configuration was compared to the baseline case to calculate a percent increase of $C_{d,n}$. For the 40 foot well car results several trends were observed. As expected the $C_{d,n}$ increased as more containers were removed. When only one container is removed the car location is irrelevant. When two containers are removed there are three possible configurations. The results show that configuration number two has the lowest $C_{d,n}$ of the three, with an increase of 30%. Configurations three and four increase $C_{d,n}$ by 45% and 47% respectively. This suggests that if two containers are to be removed they should not be removed from the same car but from two adjacent cars. When three containers are removed, configuration five, with an increase of

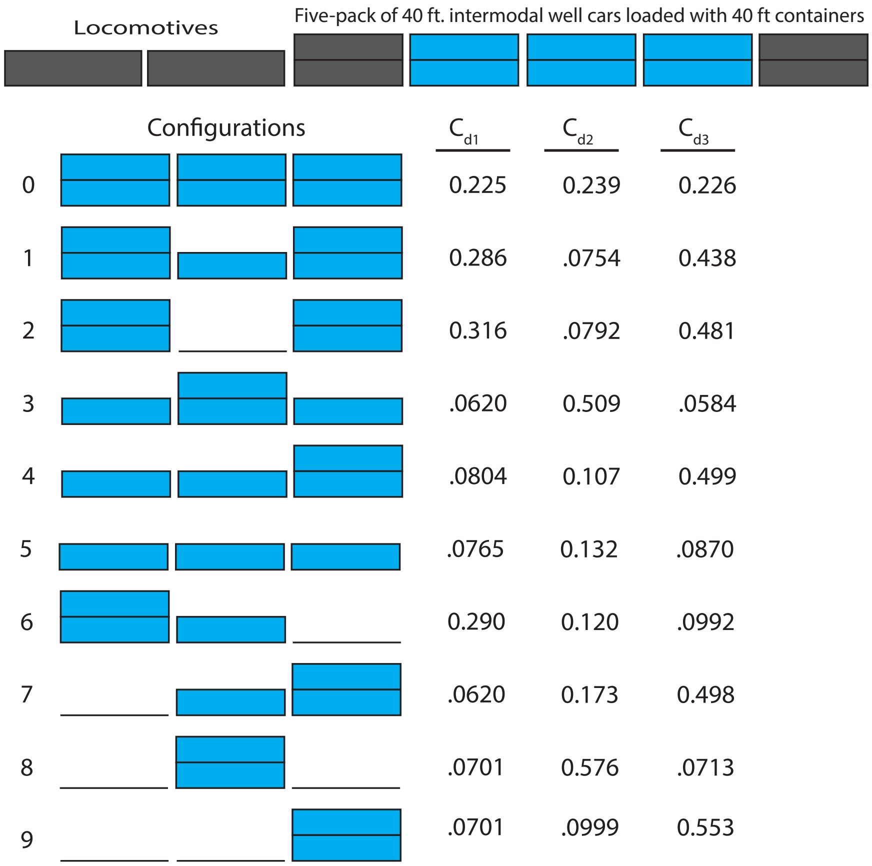

Figure 3.3: Average drag coefficients for partial load configurations with a set of five 40 foot well cars.

27% is very favorable over configurations six and seven, which show increases of 51% and 59%. In the case of four removed containers, configuration number nine increases $C_{d,n}$ by 84%, which is significantly better than the 120% increase of configuration number eight. All of these results show that a single long gap between loads is favorable to multiple gaps of shorter length. When a container is removed leaving and empty slot this increases the size of the vortices at points of flow separation which increases the pressure drag on the rail car. Some configurations also result in new regions of flow separation. The flow separates each time the it has to move up or down in configurations 6 or 7. This results in more low pressure vortices and a significant increase in pressure drag.

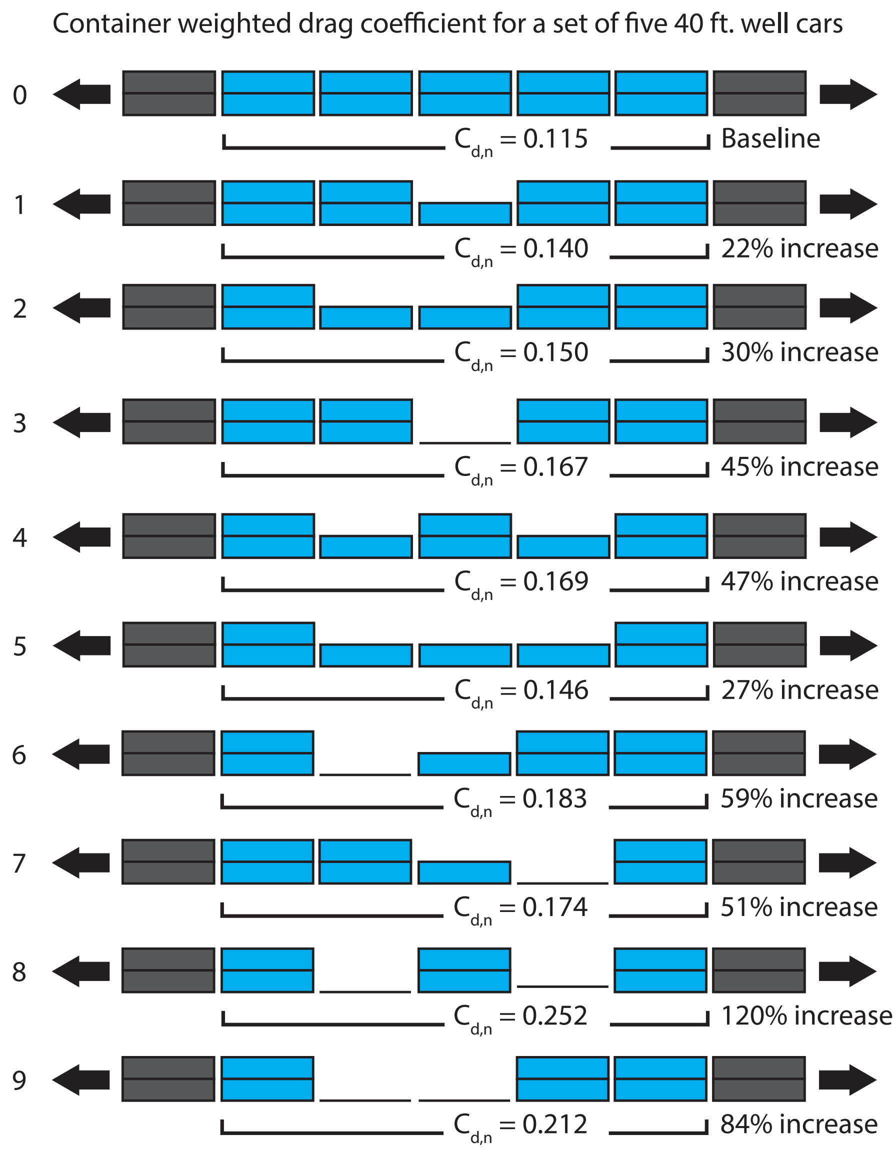

Figure 3.4: Container weighted drag coefficients for a set of five 40 foot well cars in several partial load configurations.

3.2.2 48 foot well cars

The drag coefficient results for the 48 foot well cars tests are shown in Fig. 3.5. The same assumptions used with the 40 well cars were used to calculate a container weighted $C_{d,n}$ for the set of five 48 foot well cars. These results are shown in Fig. 3.6. The same trends were observed in these results as with the 40 foot well car results. Configurations number one, two, five, and nine remained the most favorable for their respective number of missing containers (one, two, three, and four). However, while the trends remained the same, the magnitudes of the $C_{d,n}$ values were greater for nearly all of the 48 foot well car results. This suggests that partial loads have a greater influence on the drag of the longer 48 foot well cars.

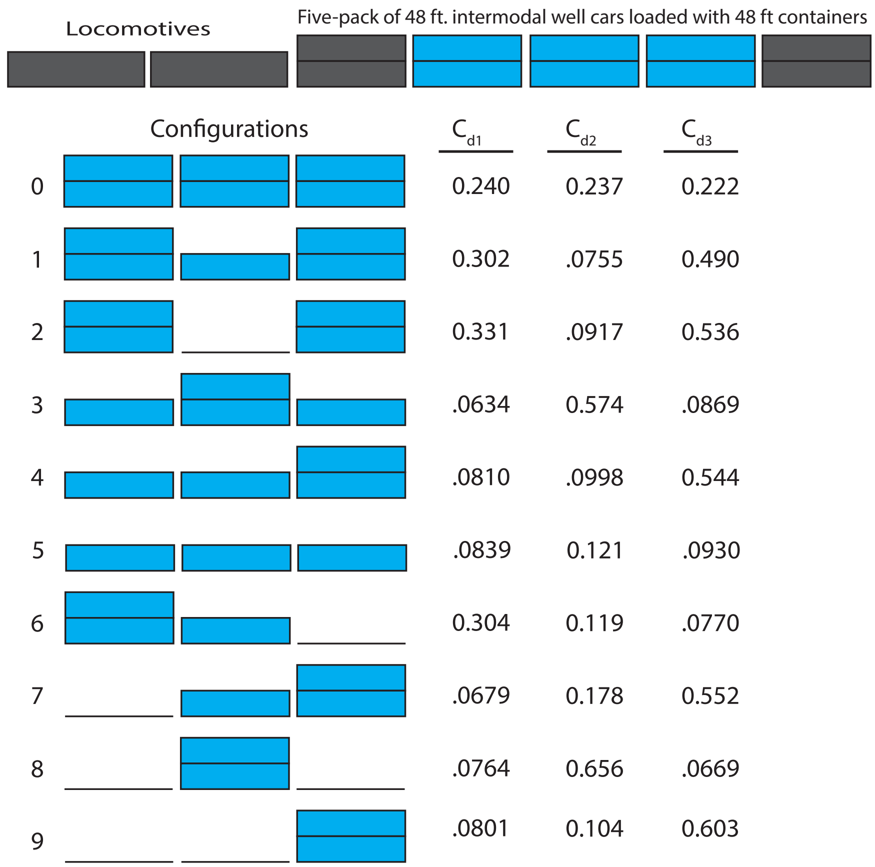

Configuration	C_{d1}	C_{d2}	C_{d3}
0	0.240	0.237	0.222
1	0.302	.0755	0.490
2	0.331	.0917	0.536
3	.0634	0.574	.0869
4	.0810	.0998	0.544
5	.0839	0.121	.0930
6	0.304	0.119	.0770
7	.0679	0.178	0.552
8	.0764	0.656	.0669
9	.0801	0.104	0.603

Figure 3.5: Average drag coefficients for partial load configurations with a set of five 48 foot well cars.

3.2.3 53 foot well cars

The drag coefficient results for the 53 foot well cars tests are shown in Fig. 3.7. Since only a 3-pack of 53 foot well cars was available, assumptions 1 and 3 could not be used. For this reason a 5-pack analysis similar to the 40 and 48 foot well car tests could not be conducted. Instead the container weighted $C_{d,n}$ could only be applied to the three test cars. For this reason, the trends differ greatly from those of the 40 and 48 foot well cars. For example, configurations 3, 5

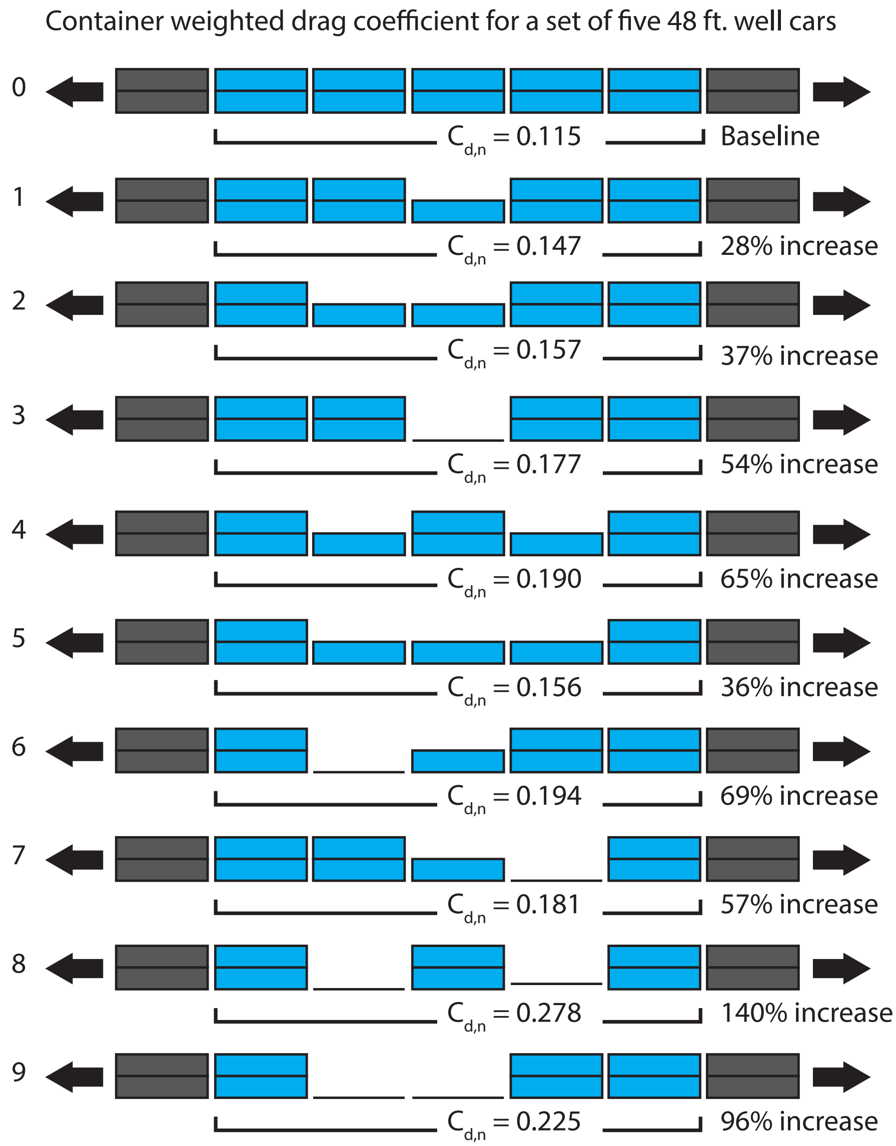

Figure 3.6: Container weighted drag coefficients for a five-pack of 48 foot well cars in several empty load configurations.

and 7 have the lowest container weighted $C_{d,n}$ for their respective number of missing containers. However, due to the limits of the 53 foot configurations, the drag effect on the car in front and behind the set of three was not included in this analysis. If a test were conducted with a set of five 53 foot well cars, it is predicted that the same trends would be observed as with the other car lengths.

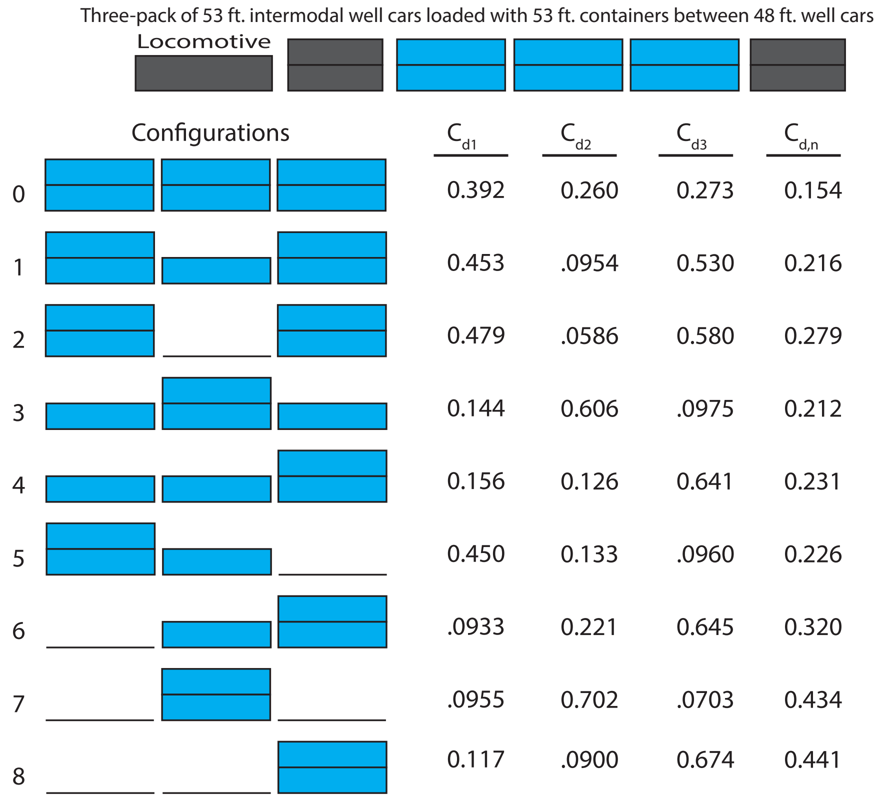

Configuration	C_{d1}	C_{d2}	C_{d3}	$C_{d,n}$
0	0.392	0.260	0.273	0.154
1	0.453	.0954	0.530	0.216
2	0.479	.0586	0.580	0.279
3	0.144	0.606	.0975	0.212
4	0.156	0.126	0.641	0.231
5	0.450	0.133	.0960	0.226
6	.0933	0.221	0.645	0.320
7	.0955	0.702	.0703	0.434
8	0.117	.0900	0.674	0.441

Figure 3.7: Average drag coefficients for partial load configurations with a three-pack of 53 foot well car models. The last column shows the container weighted drag coefficients for the three-pack of well cars.

3.3 Container Gap Experiment

This experiment was conducted using the single test car section track and a set of five 48 foot well cars. In place of the container models that were used in other testing, sets of foam models were constructed as described in chapter 2 and shown in Fig. 3.8. Six sets of five foam models were built at six different lengths. The height and width of each model was equivalent to the height and width of two double stacked container models. The length of the first three sets corresponded to the lengths of 20, 40, and 48 foot (8.28, 16.6, and 19.9 in. model dimensions) containers. The remaining three sets had lengths of 21.1, 22.7, and 24.2 inches

The six sets of containers resulted in container gap lengths of 40, 20, 12, 9, 5, and 1 cm. The 40, 20, and 12 cm cases corresponded to the gap width of a 20 ft, 40 ft, and 48 ft containers. Three of the six gap lengths are shown in Fig. 3.9. The 12 cm gap was chosen as the baseline because

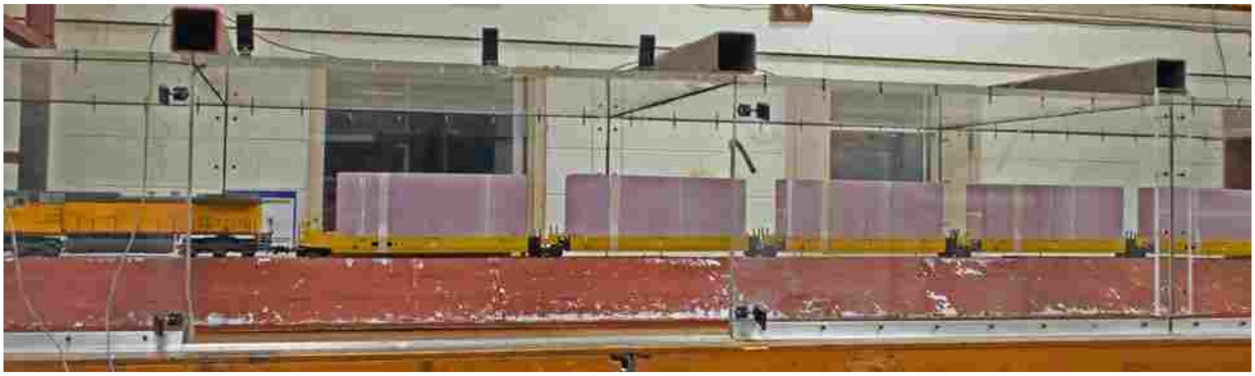

Figure 3.8: Foam containers constructed to study the effect of the container gap on the drag.

this is the resulting gap when 48 foot containers are loaded into 48 foot well cars. A normalized gap length, Lg, was calculated by dividing each gap length by the baseline length. The average C_d values based on the normalized gap length are shown in Table 3.2. The percent deviation from the baseline for each case is also shown. The data was then graphed and fit to a curve as shown in Fig. 3.10. The equation of the curve is shown in Eqn. 3.2.

Table 3.2: Average C_d value with normalized gap width. The third column shows the percent deviation from the baseline.

Lg	C_d	% from baseline
3.33	0.403	38%
1.67	0.348	19%
1	0.292	Baseline
0.75	0.279	-4.5%
0.42	0.245	-16%
.083	0.139	-52%

$$C_d = 0.4115e^{0.01152Lg} - 0.2294e^{-0.6744Lg} \tag{3.2}$$

The graph and trend line show that as the container gap length is reduced shorter than the baseline the drag on the rail car is reduced at an increasing rate. This suggests that even small reductions in the container gap would result in favorable drag reduction. This is because reducing

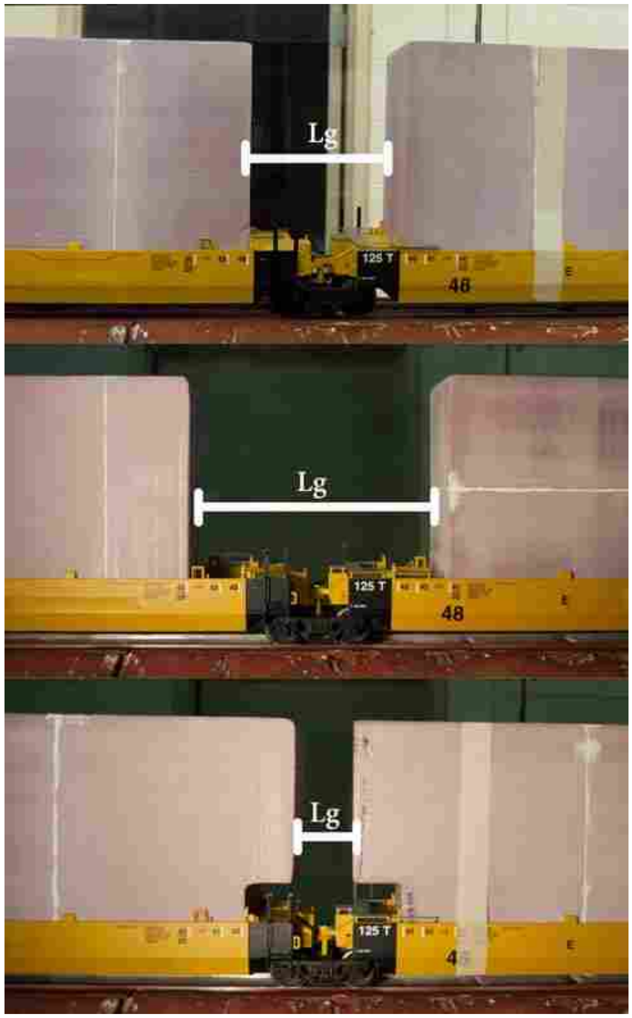

Figure 3.9: Foam containers constructed to study the effect of the container gap on the drag. Three of the six lengths tested are shown above.

the gap distance between loads reduces the size of the vortices at the points of flow separation which reduces the pressure drag on the rail car. The following section focuses on a practical way to reduce the container gap length by using a longer container for the top container in a stack.

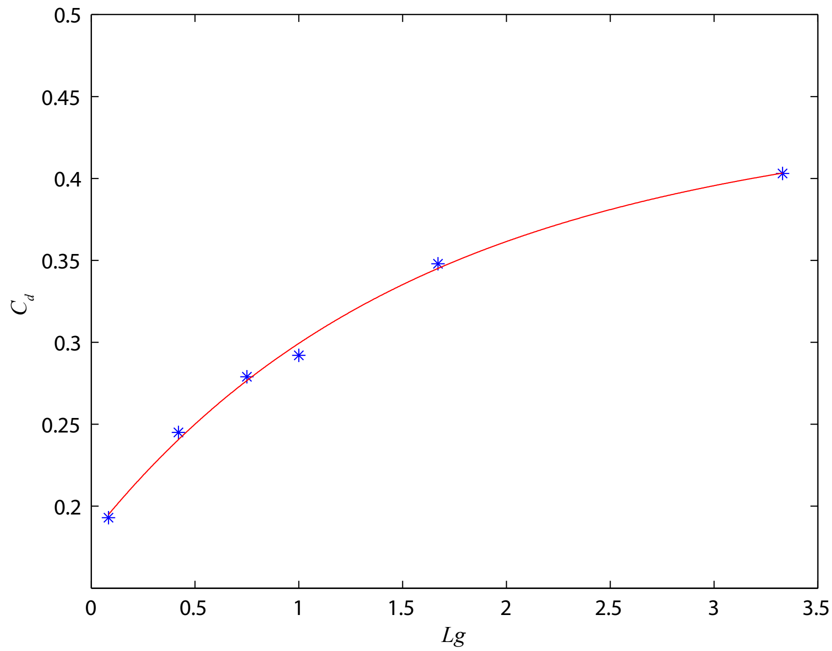

Figure 3.10: Average C_d as a function of normalized container gap width Lg, for containers loaded on 48 foot well cars.

3.4 Mixed Loading

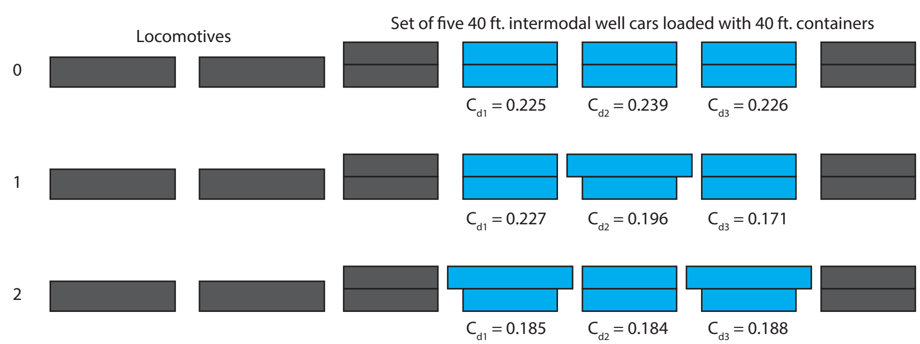

Figure 3.11: Average C_d values for configurations where a 53 ft. container is loaded onto a 40 ft. container in a set of 40 ft. well cars.

To reduce the gap distance between loads, 53 foot containers can be stacked on top of 40 foot containers loaded into 40 foot well cars. To test the effect that this has on the drag of the railcars, 53 foot containers were tested with a set of five 40 foot well cars in two configurations as shown in Fig. 3.11. Configuration 1 used only one 53 foot container on the third and central well car and configuration 2 used 53 foot containers on the second and fourth well cars. This test utilized the three car test section track and the average C_d values for the three test cars for configurations 1, 2, and a baseline case are shown in Fig. 3.11.

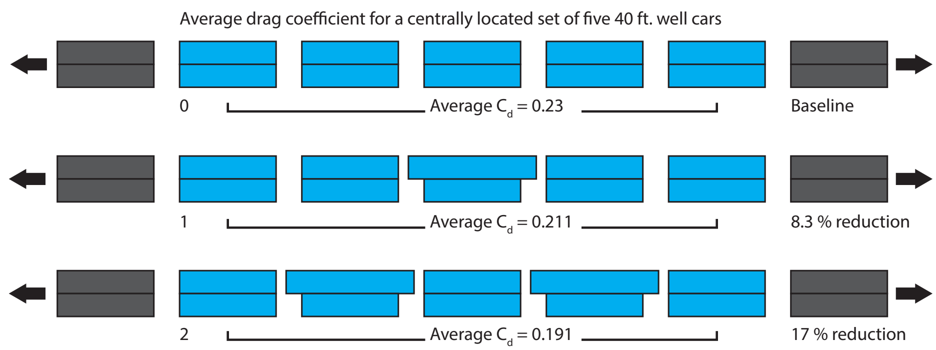

Figure 3.12: Average C_d values for a set of 40 ft. well cars with mixed loading. The percent deviation from the baseline is shown for each case.

The same assumptions used in the partial loads section were applied to this data to then calculate an average C_d for the set of five 40 foot well cars in these configurations. These results along with the percent deviation from the baseline are shown in Fig. 3.12. The results show that adding a single 53 foot container to a set of well cars reduces the average drag on the set by 8.3%. Configuration 2 with two 53 foot containers reduces the average C_d of the well car set by 17%. If configuration 2 was applied to each well car set in a unit train of 100 well cars the potential drag reduction for the whole train could be approximately 17%.

3.5 Arrowedge®

The first well car in an intermodal train (directly following the leading locomotives) has a higher drag than any of the following well cars. This is due in large part to the height of two double stacked containers in a well car being significantly higher than the height of the leading locomotives. This height difference incurs a large amount of pressure drag on the first well car. To reduce drag on the first well car a streamlined faring called the Arrowedge® was developed by the rail company Union Pacific in 2013. The streamlined profile aimed to reduce the amount of drag caused by the height transition. A scale model of the Arrowedge® was tested in this research to quantify the drag reduction of this design. These tests were performed with the 48 foot well cars and the single test section track, as shown in Fig. 3.13. The Arrowedge® was tested at both front and the rear of the train mounted on top of a 48 foot container. The drag on the car behind the Arrowedge® was also measured to determine what, if any, effect the Arrowedge® has on trailing rail cars. Average C_d results for the Arrowedge® in both configurations are shown in Table 3.3.

Figure 3.13: Image of the model that was tested at both the front(top panel) and the rear of the train(bottom panel).

Table 3.3: Average drag coefficient results for tests run with the Arrowedge® model.

Car Position	First well car		Last well car	
Container Type	Standard container	Arrowedge®	Standard container	Arrowedge®
Average C_d	0.56	0.27	0.32	0.23
% Reduction in Drag	51.7 %		30.1%	

Tests with the Arrowedge® at the front of the train resulted in 52% drag reduction compared to the case where the leading container car consisted of a double stack of 48 foot containers. When tested at the rear of the train, mounted in the reverse direction, the drag on the last well car was reduced by 30% compared to a car with double stacked 48 foot containers. Interestingly the effect on the drag for the 2nd car from the front was negligible. These results show that the Arrowedge® can significantly reduce the drag on the first well car, but that it has little to no effect on other cars in the train. The Arrowedge® is a great example of how streamlining an object can result in a large drag reduction. The streamlined shape reduces the pressure drag by reducing the frontal area where the pressure is highest and reducing flow separation. It should be noted that further research by a different team at BYU redesigned the Arrowedge® to significantly reduce production costs but keep similar drag reduction [30].

3.6 Trailers

Semi trailers are often transported on intermodal trains. They are loaded onto spine cars that are coupled to other types of intermodal rail cars. They also contribute to the aerodynamic drag of the train, so studies were conducted to determine the affects of common trailer loading configurations. Tests were conducted using the three car test section track with 53 foot well cars in the configuration shown in Fig. 3.14. Two semi trailers were tested in four configurations which varied whether each trailer was facing forwards($\Leftarrow$) or backwards($\Rightarrow$). For example the trailer configuration shown in Fig. 3.14, with two trailers facing forwards, would be represented with $\Leftarrow\Leftarrow$. Results for this study are shown in the top half of Table 3.4. Configuration 2 $\Leftarrow\Rightarrow$ gave the smallest C_d, while configuration 3 $\Rightarrow\Leftarrow$ showed the highest C_d. This suggests that when two trailers are loaded onto rail cars, they should be configured so that the wheel assembly of the trailers are adjacent to one another. The wheel assembly of the trailers disturbs the flow and causes flow separation which increase the pressure drag. In configurations where the wheel assemblies of the two trailers are far apart two separate regions of separation occur. In the optimal case the two wheel assemblies are close together and result in a single region of separation which reduces the pressure drag on both trailers.

Semi trailers are often equipped with side skirts to reduce drag when they are driven on the road but the effect side skirts exert on drag when these trailers are loaded onto rail cars has

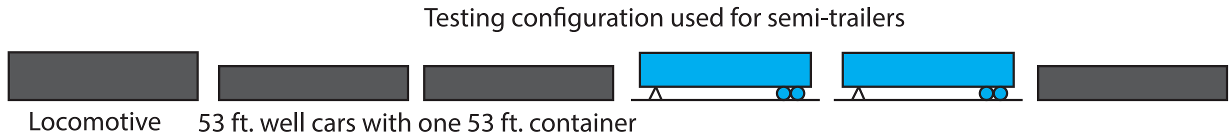

Figure 3.14: Diagram of the testing setup for semi-trailers among 53 foot well cars.

Table 3.4: Average drag coefficients for semi-trailer in multiple configurations with 53 foot well cars.

Configuration	C_{d1}	C_{d2}	Average
1 $\Leftarrow\Leftarrow$	0.400	0.344	0.372
2 $\Leftarrow\Rightarrow$	0.389	0.330	0.360
3 $\Rightarrow\Leftarrow$	0.488	0.367	0.428
4 $\Rightarrow\Rightarrow$	0.470	0.353	0.412
With skirting			
1s $\Leftarrow\Leftarrow$	0.396	0.322	0.359
2s $\Leftarrow\Rightarrow$	0.383	0.314	0.349
3s $\Rightarrow\Leftarrow$	0.489	0.333	0.411
4s $\Rightarrow\Rightarrow$	0.467	0.324	0.396

not been explored. To examine this in a preliminary way, semi trailers with side skirts were tested in identical configurations as described above. The results of these tests are shown in the bottom half of Table 3.4. Configuration 2 again had the lowest C_d while configuration 3 had the highest. All trailers with side skirts showed lower average C_d values than those without skirts in the same loading configuration. This shows that when trailers are loaded onto a train the side skirts should not be removed but remain attached. In general the side skirts decreased the C_d values by 3.1 to 4.0%, depending on the combined trailer positions.

CHAPTER 4. CONCLUSION

The objective of this research was to characterize the aerodynamic drag on intermodal train builds and allow their build to be optimized for fuel efficiency. The results presented in the previous chapter illustrate that the drag can be optimized in many ways. Four scenarios were investigated, the partial loading of well cars, the influence of the gap between containers, use of the Arrowedge® addition, and the inclusion of semi trailers among well cars.

The results for partial loading of well cars shows that close attention should be paid to container configurations whenever containers are removed. Partial loads will always result in an increase of drag but that increase can be minimized by choosing the best loading configuration. With the 40 foot well cars, when two containers were removed the drag increase ranged from 30-47%. When three containers were removed the increase ranged from 27-59%. When four container were removed the increase ranged from 84-120%. Similar results were observed with the 48 foot well cars. These results showed that when containers are removed for a set of well cars the best option is to remove them from adjacent cars, creating one large gap as opposed to several smaller ones.

The influence of the container gap length was illustrated in several of the results. First, the baseline results highlight the importance of container matching. Here a 17.9% reduction in drag occurred when 48 foot containers were loaded into 48 foot well cars instead of 40 foot containers. The data from the container gap experiment showed that the drag coefficient relates to the gap length with an exponential function; as the gap width increases the C_d value increases as well. Three gap lengths shorter than a baseline width were explored and resulted in reductions in the drag of 4.5%, 16%, and 52%.

The test data for the mixed loading of 40 and 53 foot containers in 40 foot well cars showed possibilities for significant reductions in drag. With the addition of just one 53 foot container placed on one 40 foot container, the average drag on a set of five well cars was reduced by 8.3%.

When two 53 foot containers were placed on two 40 foot containers, the average drag on a set of well cars was reduced by 17%.

The data from the streamlined Arrowedge® shows that it has a significant effect on the drag of the car it is loaded onto, but negligible influence on surrounding cars. At the front of the train the Arrowedge® showed a 51.7% reduction in the drag on the leading well car and a 30.1% reduction for the drag on the well car at the rear of the train.

4.1 Future Work

There remain several aspects of intermodal trains that could be investigated to reduce aerodynamic drag. This research focused mainly on the gap distance between loads and on partial loading configurations and very little on design changes to containers or rail cars. The results from the Arrowedge® highlight the benefit of streamlining and new more streamlined designs could be applied to well cars a containers. Other modifications could be added to existing well cars like side skirts or covers to make the rail cars more aerodynamic.

The results from the partial loads tests gives insight into how and in what configuration containers should be loaded and unloaded. This could be further expanded to examine the interaction between multiple sets of well cars with partial loads. Ultimately an aerodynamic model could be developed for the loading configuration of an entire intermodal train. This would aid controllers in maintaining the most aerodynamic container configuration possible.

The gap length between containers is a large contributor to the drag on well cars. Reducing the container gap may significantly reduce drag but introduces several logistical problems. Time required to attach and remove a gap filling device to a 100 car train could outweigh the potential aerodynamic benefit. The use a mixed loading is one solution to this but future research could investigate a practical gap filling device.

REFERENCES

[1] Staff, 2010. "High speed railroading." *The Economist*, 6. 1, 2

[2] Irani, D., and ECONOMIST, C., 2016. "Economic and fiscal impact analysis of class i railroads.". 1

[3] Staff, 2015. 2015 investor fact book Tech. rep., Union Pacific Corporation. 2

[4] Paul, J., Johnson, R., and Yates, R., 2009. "Application of cfd to rail car and locomotive aerodynamics." *The Aerodynamics of Heavy Vehicles II: Trucks, Buses, and Trains*, pp. 259–297. 2

[5] Hucho, W.-h., and Sovran, G., 1993. "Aerodynamics of road vehicles." *Annual review of fluid mechanics,* **25**(1), pp. 485–537. 4

[6] Hucho, W.-H., 1998. *Aerodynamics of road vehicles: from fluid mechanics to vehicle engineering*., 4 ed. Elsevier. 4

[7] Anderson, J. D. J., 2008. *Introduction to flight*., 6 ed. McGraw-Hill. 4

[8] Munson, B. R., Okiishi, T. H., Huebsch, W. W., and Rothmayer, A. P., 2013. *Fundamentals of fluid mechanics*., 7 ed. John Wiley and Sons, Inc. 4

[9] Irwin, P. A., 2008. "Bluff body aerodynamics in wind engineering." *Journal of Wind Engineering and Industrial Aerodynamics,* **96**(6), pp. 701–712. 4

[10] Roshko, A., 1993. "Perspectives on bluff body aerodynamics." *Journal of Wind Engineering and Industrial Aerodynamics,* **49**(1-3), pp. 79–100. 4

[11] Bearman, P., 2009. "Bluff body flow research with application to road vehicles." *The aerodynamics of heavy vehicles ii: trucks, buses, and trains*, pp. 3–13. 4

[12] Modi, V., Hill, S. S., and Yokomizo, T., 1995. "Drag reduction of trucks through boundary-layer control." *Journal of wind engineering and industrial aerodynamics,* **54**, pp. 583–594. 4

[13] Ortega, J., and Salari, K., 2004. "An experimental study of drag reduction devices for a trailer underbody and base." In *34th AIAA Fluid Dynamics Conference and Exhibit*, p. 2252. 4

[14] Hyams, D. G., Sreenivas, K., Pankajakshan, R., Nichols, D. S., Briley, W. R., and Whitfield, D. L., 2011. "Computational simulation of model and full scale class 8 trucks with drag reduction devices." *Computers & Fluids,* **41**(1), pp. 27–40. 4

[15] McCallen, R. C., Salari, K., Pointer, W. D., Browand, F., Ross, J., Slezak, L., Routbort, J., Ortega, J., Castellucci, P., Chang, J., Singh, S., Dringenberg, E., Radovich, C., Merzel, T., Plocher, D., Storms, B., Clarke, R. M., and Carrington, K., 2006. "Aerodynamic drag reduction." *Annual Progress Report for Heavy Vehicle Systems Optimization Program,* **1**, pp. 1–59. 5

[16] Tian, H.-q., 2009. "Formation mechanism of aerodynamic drag of high-speed train and some reduction measures." *Journal of Central South University of Technology,* **16**(1), pp. 166–171. 5

[17] Yang, X., Jin, J., and Shi, G., 2013. "Preliminary study on streamlined design of longitudinal profile of high-speed train head shape." *Procedia-Social and Behavioral Sciences,* **96**, pp. 1469–1476. 5

[18] Orellano, A., and Sperling, S., 2009. "Aerodynamic improvements and associated energy demand reduction of trains." In *The Aerodynamics of Heavy Vehicles II: Trucks, Buses, and Trains*. Springer, pp. 219–231. 5

[19] Raghunathan, R. S., Kim, H.-D., and Setoguchi, T., 2002. "Aerodynamics of high-speed railway train." *Progress in Aerospace sciences,* **38**(6), pp. 469–514. 5

[20] Adams, A., Burr, J., Campbell, M., Jones, A., Peterson, E., Spear, M., Wells, K., and Maynes, D., 2011. Aerodynamic coal car covers capstone report Tech. rep., Brigham Young University, 5. 5

[21] Saunders, J., Watkins, S., Kumar, H., et al., 1991. "Aerodynamics to save energy for unit-train freight wagons." In *Conference on Railway Engineering 1991: Demand Management of Assets; Preprints of Papers*, Institution of Engineers, Australia, p. 98. 5

[22] Condie, R., 2014. "Aerodynamic improvements for auto-carrying railcars." Master's thesis, Brigham Young University, 5. 5

[23] Paul, J., Smith, T., Gielow, M., and Gielow, R., 1983. "3/10 scale wind tunnel test of skeletonized and well-type intermodal rail cars." *Livonia, Michigan, Airflow Sciences Corporation Report R-83-019,* **1**. 5

[24] Paul, J., 1984. Wind tunnel tests of 3 10 scale well and skeleton type articulated intermodal railcars Tech. rep. 5

[25] Lai, Y.-C., and Barkan, C., 2005. "Options for improving the energy efficiency of intermodal freight trains." *Transportation Research Record: Journal of the Transportation Research Board*(1916), pp. 47–55. 6

[26] Lai, Y.-C., Barkan, C. P., and Önal, H., 2008. "Optimizing the aerodynamic efficiency of intermodal freight trains." *Transportation Research Part E: Logistics and Transportation Review,* **44**(5), pp. 820–834. 6

[27] Lai, Y.-C., Ouyang, Y., and Barkan, C. P., 2008. "A rolling horizon model to optimize aerodynamic efficiency of intermodal freight trains with uncertainty." *Transportation Science,* **42**(4), pp. 466–477. 6

[28] Lai, Y.-C., Barkan, C. P., Drapa, J., Ahuja, N., Hart, J. M., Narayanan, P., Jawahar, C., Kumar, A., Milhon, L., and Stehly, M., 2007. "Machine vision analysis of the energy efficiency of intermodal freight trains." *Proceedings of the Institution of Mechanical Engineers, Part F: Journal of Rail and Rapid Transit,* **221**(3), pp. 353–364. 6

[29] Figliola, R. S., and Beasley, D., 2015. *Theory and design for mechanical measurements*. John Wiley & Sons. 19

[30] Adams, D., Carruth, J., Cloward, J., Linn, J., Millerberg, J., Schaff, A., Terry, A., and Hepworth, A., 2016. Arrowedge intermodal fairing capstone summary Tech. rep., Brigham Young University, 4. 38

APPENDIX A. DATA TABLES

Baseline Results											
40 foot Corrugated		Test: 1							Test: 2		
D (lbs)	*T (K)*	*V (m/s)*	*ρ (kg/m³)*	*Re*	C_d	*D (lbs)*	*T (K)*	*V (m/s)*	*ρ (kg/m³)*	*Re*	C_d
1.33	302	47.2	0.983	2.61E+05	0.276	1.60	300	50.1	0.990	2.80E+05	0.299
1.73	304	52.4	0.980	2.87E+05	0.292	1.07	301	41.7	0.989	2.33E+05	0.289
0.36	301	24.9	0.988	1.38E+05	0.260	1.28	302	45.4	0.986	2.52E+05	0.291
1.62	304	51.9	0.979	2.85E+05	0.278	0.69	301	33.8	0.987	1.88E+05	0.282
0.73	303	35.1	0.983	1.94E+05	0.271	1.14	302	43.0	0.985	2.38E+05	0.289
1.41	304	48.6	0.980	2.67E+05	0.276	1.69	303	50.4	0.982	2.77E+05	0.315
0.96	303	40.2	0.981	2.21E+05	0.274	0.31	302	24.0	0.984	1.33E+05	0.256
1.20	303	44.7	0.981	2.46E+05	0.277	0.91	303	38.7	0.982	2.13E+05	0.286
1.08	303	42.6	0.981	2.34E+05	0.273	1.36	304	46.8	0.979	2.56E+05	0.294
40 foot Smooth		Test: 1							Test: 2		
D (lbs)	*T (K)*	*V (m/s)*	*ρ (kg/m³)*	*Re*	C_d	*D (lbs)*	*T (K)*	*V (m/s)*	*ρ (kg/m³)*	*Re*	C_d
1.23	297	46.0	1.003	2.63E+05	0.269	1.20	303	45.4	0.981	2.49E+05	0.248
0.91	298	39.8	1.000	2.26E+05	0.267	1.08	304	43.0	0.979	2.36E+05	0.247
1.11	298	43.9	0.999	2.49E+05	0.267	0.87	304	38.3	0.979	2.10E+05	0.246
1.00	298	42.0	0.998	2.38E+05	0.264	0.64	304	32.6	0.979	1.78E+05	0.245
1.47	298	50.0	0.997	2.83E+05	0.274	1.57	305	50.4	0.975	2.74E+05	0.265
1.29	299	47.4	0.995	2.67E+05	0.268	0.97	305	40.8	0.974	2.22E+05	0.247
0.66	299	34.6	0.995	1.95E+05	0.258	1.46	306	50.2	0.972	2.71E+05	0.250
1.56	299	50.0	0.995	2.82E+05	0.290	0.32	305	22.5	0.974	1.22E+05	0.241
0.31	299	24.8	0.994	1.40E+05	0.236	1.26	306	46.8	0.971	2.53E+05	0.248
48 foot Corrugated		Test: 1							Test: 2		
D (lbs)	*T (K)*	*V (m/s)*	*ρ (kg/m³)*	*Re*	C_d	*D (lbs)*	*T (K)*	*V (m/s)*	*ρ (kg/m³)*	*Re*	C_d
0.41	301	27.1	0.986	1.51E+05	0.222	0.40	298	28.2	0.998	1.60E+05	0.235
0.28	301	22.0	0.986	1.22E+05	0.218	0.76	302	39.1	0.986	2.17E+05	0.236
0.98	302	43.1	0.981	2.38E+05	0.225	0.95	303	43.5	0.983	2.40E+05	0.236
1.06	303	45.3	0.978	2.48E+05	0.223	1.12	304	47.1	0.980	2.58E+05	0.239
0.88	304	41.2	0.975	2.25E+05	0.221	0.27	303	24.1	0.983	1.33E+05	0.216
1.30	305	50.4	0.973	2.74E+05	0.224	1.03	304	45.5	0.978	2.49E+05	0.236
1.41	305	50.7	0.971	2.75E+05	0.238	1.35	305	50.5	0.976	2.75E+05	0.251
1.15	306	47.2	0.970	2.55E+05	0.224	1.27	305	50.3	0.975	2.74E+05	0.238
0.78	306	38.7	0.970	2.09E+05	0.222	0.85	305	41.6	0.975	2.27E+05	0.233

Figure A.1: Wind tunnel results from baseline tests. Re and C_d calculated with $L = 10.48cm$ and $A_D = 191.8cm^2$

40 ft. Partial Loads Results															
Configuration: 0	Test: 1		T = 298 K		ρ = 0.99 kg/m^3			Test: 2		T = 296 K			ρ = 0.99 kg/m^3		
D1 (N)	*D2 (N)*	*D3 (N)*	*V (m/s)*	*Re*	C_{d1}	C_{d2}	C_{d3}	*D1 (N)*	*D2 (N)*	*D3 (N)*	*V (m/s)*	*Re*	C_{d1}	C_{d2}	C_{d3}
4.01	4.27	3.99	43.2	2.4E+05	0.225	0.240	0.224	3.73	4.02	3.79	41.5	2.4E+05	0.227	0.244	0.230
4.61	4.95	4.62	46.8	2.6E+05	0.222	0.238	0.222	4.04	4.34	4.12	43.2	2.5E+05	0.227	0.243	0.231
2.46	2.69	2.44	34.0	1.9E+05	0.224	0.245	0.223	5.26	5.49	5.31	49.7	2.8E+05	0.223	0.233	0.226
5.23	5.56	5.27	49.8	2.8E+05	0.223	0.237	0.225	3.24	3.50	3.35	39.2	2.2E+05	0.222	0.239	0.229
3.66	3.91	3.64	41.6	2.3E+05	0.224	0.240	0.223	2.48	2.64	2.48	34.1	1.9E+05	0.224	0.238	0.224
3.15	3.41	3.19	38.9	2.2E+05	0.221	0.238	0.223	4.76	5.11	4.90	47.2	2.7E+05	0.224	0.241	0.231
4.28	4.53	4.23	45.2	2.5E+05	0.222	0.235	0.219	4.45	4.63	4.45	45.3	2.6E+05	0.228	0.237	0.228
3.19	3.44	3.17	39.0	2.2E+05	0.222	0.240	0.220	2.49	2.63	2.50	33.9	1.9E+05	0.227	0.240	0.228
2.41	2.62	2.43	33.9	1.9E+05	0.221	0.241	0.223	5.31	5.60	5.38	49.6	2.8E+05	0.227	0.239	0.230
3.60	3.91	3.61	41.1	2.3E+05	0.225	0.244	0.225	3.18	3.44	3.26	38.7	2.2E+05	0.223	0.241	0.229
4.36	4.63	4.31	45.2	2.5E+05	0.225	0.239	0.223	4.46	4.67	4.42	45.1	2.6E+05	0.230	0.241	0.228
3.86	4.12	3.84	43.0	2.4E+05	0.221	0.236	0.220	3.70	3.89	3.67	41.2	2.3E+05	0.229	0.241	0.227
5.27	5.53	5.20	49.6	2.8E+05	0.227	0.238	0.224	4.70	4.98	4.70	46.5	2.6E+05	0.228	0.242	0.228
4.59	4.90	4.59	46.8	2.6E+05	0.223	0.238	0.223	4.04	4.24	4.04	43.0	2.4E+05	0.230	0.241	0.230
Configuration: 1	Test: 1		T = 300 K		ρ = 0.99 kg/m^3			Test: 2		T = 297 K			ρ = 1.0 kg/m^3		
D1 (N)	*D2 (N)*	*D3 (N)*	*V (m/s)*	*Re*	C_{d1}	C_{d2}	C_{d3}	*D1 (N)*	*D2 (N)*	*D3 (N)*	*V (m/s)*	*Re*	C_{d1}	C_{d2}	C_{d3}
6.77	1.74	10.14	49.7	2.8E+05	0.288	0.074	0.430	4.17	1.10	6.30	38.8	2.2E+05	0.289	0.076	0.436
4.73	1.21	7.26	41.5	2.3E+05	0.289	0.074	0.443	5.66	1.48	8.64	45.3	2.6E+05	0.289	0.076	0.441
5.65	1.48	8.60	45.2	2.5E+05	0.291	0.077	0.443	6.75	1.71	10.37	49.9	2.8E+05	0.284	0.072	0.435
4.10	1.04	6.24	39.1	2.2E+05	0.283	0.072	0.430	4.66	1.17	7.19	41.4	2.3E+05	0.285	0.071	0.440
5.03	1.27	7.65	43.2	2.4E+05	0.285	0.072	0.433	5.11	1.40	7.90	43.2	2.5E+05	0.286	0.078	0.442
3.15	0.84	4.76	34.1	1.9E+05	0.285	0.076	0.432	3.12	0.86	4.87	34.0	1.9E+05	0.284	0.078	0.443
5.98	1.55	9.00	46.7	2.6E+05	0.289	0.075	0.434	6.09	1.64	9.46	46.8	2.7E+05	0.291	0.078	0.451
5.47	1.34	8.34	45.2	2.5E+05	0.283	0.069	0.431	5.05	1.40	7.78	43.1	2.4E+05	0.285	0.079	0.440
5.05	1.27	7.67	43.0	2.4E+05	0.288	0.073	0.437	3.99	1.10	6.17	38.6	2.2E+05	0.280	0.077	0.433
4.66	1.21	7.09	41.2	2.3E+05	0.291	0.076	0.442	3.05	0.88	4.72	33.7	1.9E+05	0.280	0.080	0.434
4.13	1.04	6.39	38.8	2.2E+05	0.290	0.073	0.448	5.85	1.60	9.09	46.7	2.6E+05	0.281	0.077	0.437
3.13	0.86	4.75	33.7	1.9E+05	0.291	0.080	0.442	5.50	1.48	8.45	44.9	2.6E+05	0.285	0.077	0.438
6.73	1.72	10.07	49.7	2.8E+05	0.288	0.074	0.431	4.57	1.26	7.07	40.9	2.3E+05	0.287	0.079	0.444
5.89	1.46	8.97	46.6	2.6E+05	0.287	0.071	0.437	6.71	1.77	10.24	49.6	2.8E+05	0.286	0.076	0.436
Configuration: 2	Test: 1		T = 299 K		ρ = 0.99 kg/m^3			Test: 2		T = 297 K			ρ = 0.99 kg/m^3		
D1 (N)	*D2 (N)*	*D3 (N)*	*V (m/s)*	*Re*	C_{d1}	C_{d2}	C_{d3}	*D1 (N)*	*D2 (N)*	*D3 (N)*	*V (m/s)*	*Re*	C_{d1}	C_{d2}	C_{d3}
5.13	1.28	7.78	41.2	2.3E+05	0.315	0.078	0.478	6.13	1.55	9.26	44.7	2.6E+05	0.319	0.081	0.482
6.09	1.50	9.27	45.2	2.5E+05	0.313	0.077	0.477	7.43	1.85	11.35	49.3	2.8E+05	0.321	0.080	0.490
5.56	1.36	8.39	43.1	2.4E+05	0.315	0.077	0.476	5.60	1.41	8.50	43.2	2.4E+05	0.315	0.079	0.479
3.39	0.86	5.14	33.8	1.9E+05	0.311	0.079	0.472	5.12	1.31	7.80	41.1	2.3E+05	0.318	0.081	0.485
4.49	1.13	6.80	38.5	2.2E+05	0.318	0.080	0.482	3.41	0.88	5.18	33.9	1.9E+05	0.312	0.081	0.474
6.52	1.54	9.81	46.5	2.6E+05	0.316	0.075	0.475	6.43	1.62	9.77	46.4	2.6E+05	0.314	0.079	0.477
7.43	1.79	11.32	49.4	2.8E+05	0.321	0.077	0.488	4.53	1.18	6.94	38.7	2.2E+05	0.317	0.082	0.485
3.34	0.88	5.12	33.7	1.9E+05	0.310	0.081	0.475	6.15	1.56	9.51	45.0	2.6E+05	0.318	0.081	0.492
5.48	1.30	8.35	43.0	2.4E+05	0.312	0.074	0.476	7.34	1.82	11.15	49.3	2.8E+05	0.317	0.078	0.482
6.54	1.59	9.93	46.7	2.6E+05	0.316	0.077	0.479	3.42	0.91	5.22	33.6	1.9E+05	0.318	0.084	0.485
4.47	1.11	6.81	38.6	2.2E+05	0.316	0.079	0.481	6.47	1.59	9.75	46.2	2.6E+05	0.318	0.078	0.479
6.05	1.50	9.27	45.1	2.5E+05	0.313	0.078	0.480	5.07	1.28	7.76	41.0	2.3E+05	0.318	0.080	0.486
5.04	1.27	7.70	40.9	2.3E+05	0.317	0.080	0.484	5.62	1.42	8.44	42.7	2.4E+05	0.323	0.082	0.484
7.34	1.82	11.06	49.6	2.8E+05	0.315	0.078	0.475	4.42	1.13	6.73	38.3	2.2E+05	0.315	0.081	0.480

Figure A.2: Wind tunnel results from partial loads tests with 40 ft. well cars. Re and C_d calculated with $L = 10.48cm$ and $A_D = 191.8cm^2$

40 ft. Partial Loads Results Continued															
Configuration: 3		Test: 1	T = 300 K		ρ = 0.99 kg/m^3			Test: 2		T = 298 K			ρ = 0.99 kg/m^3		
D1 (N)	*D2 (N)*	*D3 (N)*	*V (m/s)*	*Re*	C_{d1}	C_{d2}	C_{d3}	*D1 (N)*	*D2 (N)*	*D3 (N)*	*V (m/s)*	*Re*	C_{d1}	C_{d2}	C_{d3}
1.16	8.88	1.05	43.2	2.4E+05	0.065	0.499	0.059	0.94	7.33	0.85	38.5	2.2E+05	0.066	0.516	0.060
1.44	11.56	1.36	49.6	2.8E+05	0.062	0.497	0.058	0.71	5.54	0.63	33.7	1.9E+05	0.066	0.513	0.058
0.87	7.40	0.85	39.3	2.2E+05	0.059	0.507	0.058	1.06	8.98	0.97	42.7	2.4E+05	0.061	0.515	0.056
0.69	5.57	0.64	34.1	1.9E+05	0.063	0.507	0.059	1.30	10.45	1.21	46.5	2.6E+05	0.064	0.509	0.059
1.00	8.09	0.94	41.3	2.3E+05	0.062	0.500	0.058	1.24	9.83	1.13	44.9	2.5E+05	0.064	0.511	0.059
1.16	10.52	1.17	46.9	2.6E+05	0.056	0.506	0.056	1.03	8.24	0.95	40.9	2.3E+05	0.065	0.517	0.060
1.21	9.67	1.15	45.2	2.5E+05	0.062	0.500	0.059	1.39	11.98	1.42	49.5	2.8E+05	0.060	0.515	0.061
1.01	8.07	0.92	41.2	2.3E+05	0.063	0.502	0.057	1.22	10.28	1.16	46.2	2.6E+05	0.060	0.507	0.057
1.29	11.89	1.32	49.5	2.8E+05	0.056	0.513	0.057	0.99	8.08	0.94	40.9	2.3E+05	0.062	0.508	0.059
1.23	9.82	1.14	45.3	2.5E+05	0.063	0.507	0.059	0.66	5.45	0.62	33.6	1.9E+05	0.061	0.508	0.058
1.12	8.85	1.08	43.1	2.4E+05	0.064	0.504	0.061	1.08	8.81	1.02	42.5	2.4E+05	0.063	0.513	0.059
1.17	10.46	1.17	46.6	2.6E+05	0.057	0.511	0.057	1.17	9.89	1.11	44.5	2.5E+05	0.062	0.522	0.058
0.85	7.19	0.79	38.7	2.2E+05	0.060	0.506	0.056	0.90	7.22	0.80	38.4	2.2E+05	0.064	0.516	0.057
0.69	5.48	0.61	33.7	1.9E+05	0.064	0.508	0.057	1.46	11.71	1.39	49.2	2.8E+05	0.064	0.510	0.060
Configuration: 4		Test: 1	T = 297 K		ρ = 0.99 kg/m^3			Test: 2		T = 298 K			ρ = 0.99 kg/m^3		
D1 (N)	*D2 (N)*	*D3 (N)*	*V (m/s)*	*Re*	C_{d1}	C_{d2}	C_{d3}	*D1 (N)*	*D2 (N)*	*D3 (N)*	*V (m/s)*	*Re*	C_{d1}	C_{d2}	C_{d3}
1.90	2.50	11.84	49.7	2.8E+05	0.081	0.106	0.504	1.57	2.08	9.50	45.1	2.6E+05	0.081	0.107	0.489
1.60	2.16	10.60	47.1	2.7E+05	0.076	0.103	0.504	1.17	1.56	6.89	38.7	2.2E+05	0.082	0.109	0.482
1.21	1.57	7.34	39.2	2.2E+05	0.083	0.107	0.503	1.58	2.13	10.28	46.3	2.6E+05	0.077	0.104	0.502
1.40	1.91	8.88	43.2	2.4E+05	0.079	0.108	0.501	0.91	1.18	5.34	33.6	1.9E+05	0.084	0.110	0.496
1.33	1.75	8.15	41.5	2.3E+05	0.081	0.107	0.499	1.41	1.86	8.66	42.8	2.4E+05	0.081	0.107	0.496
1.59	2.07	9.79	45.2	2.6E+05	0.082	0.107	0.504	1.26	1.70	8.05	41.0	2.3E+05	0.079	0.106	0.504
0.90	1.20	5.58	34.1	1.9E+05	0.082	0.109	0.505	1.84	2.46	11.48	49.4	2.8E+05	0.079	0.106	0.493
1.58	2.06	9.77	45.0	2.5E+05	0.082	0.107	0.507	1.20	1.67	7.90	41.0	2.3E+05	0.075	0.105	0.494
1.63	2.17	10.36	46.7	2.6E+05	0.079	0.105	0.500	1.42	1.87	8.60	42.9	2.4E+05	0.081	0.107	0.493
0.87	1.17	5.45	33.9	1.9E+05	0.080	0.107	0.500	0.85	1.15	5.25	33.4	1.9E+05	0.079	0.108	0.492
1.19	1.53	7.19	38.7	2.2E+05	0.083	0.108	0.505	1.58	2.08	9.66	44.9	2.5E+05	0.082	0.108	0.503
1.36	1.83	8.93	42.9	2.4E+05	0.078	0.105	0.510	1.62	2.17	10.28	46.3	2.6E+05	0.079	0.106	0.503
1.31	1.73	7.94	41.0	2.3E+05	0.082	0.108	0.497	1.16	1.55	6.91	38.4	2.2E+05	0.083	0.110	0.492
1.86	2.48	11.91	49.8	2.8E+05	0.079	0.105	0.507	1.89	2.48	11.33	49.3	2.8E+05	0.082	0.107	0.490
Configuration: 5		Test: 1	T = 298 K		ρ = 0.99 kg/m^3			Test: 2		T = 297 K			ρ = 1.0 kg/m^3		
D1 (N)	*D2 (N)*	*D3 (N)*	*V (m/s)*	*Re*	C_{d1}	C_{d2}	C_{d3}	*D1 (N)*	*D2 (N)*	*D3 (N)*	*V (m/s)*	*Re*	C_{d1}	C_{d2}	C_{d3}
1.47	2.26	1.58	43.3	2.5E+05	0.082	0.126	0.088	1.48	2.33	1.62	43.0	2.5E+05	0.083	0.131	0.092
1.52	2.43	1.71	45.2	2.6E+05	0.078	0.124	0.088	1.16	1.91	1.29	38.8	2.2E+05	0.081	0.133	0.090
1.72	2.80	1.99	49.6	2.8E+05	0.074	0.120	0.085	0.92	1.45	0.96	33.9	1.9E+05	0.084	0.133	0.087
1.63	2.60	1.89	46.9	2.6E+05	0.078	0.124	0.090	1.67	2.68	1.90	46.7	2.6E+05	0.081	0.129	0.092
1.17	1.83	1.27	39.0	2.2E+05	0.080	0.126	0.088	1.52	2.49	1.72	45.1	2.5E+05	0.079	0.128	0.089
1.28	2.05	1.41	41.4	2.3E+05	0.079	0.126	0.086	1.34	2.14	1.47	41.1	2.3E+05	0.084	0.133	0.091
0.92	1.42	0.98	33.9	1.9E+05	0.085	0.130	0.090	1.84	2.97	2.12	49.4	2.8E+05	0.079	0.128	0.091
1.71	2.64	1.91	46.8	2.6E+05	0.082	0.127	0.092	1.27	2.09	1.46	41.1	2.3E+05	0.079	0.130	0.091
1.17	1.84	1.28	38.8	2.2E+05	0.082	0.129	0.090	1.47	2.33	1.63	42.8	2.4E+05	0.084	0.133	0.093
1.53	2.29	1.60	43.0	2.4E+05	0.087	0.130	0.091	1.92	3.07	2.17	49.8	2.8E+05	0.081	0.130	0.092
1.60	2.49	1.78	45.2	2.5E+05	0.082	0.128	0.092	1.60	2.64	1.85	46.4	2.6E+05	0.077	0.128	0.089
0.92	1.42	0.97	33.7	1.9E+05	0.085	0.132	0.090	1.11	1.87	1.25	38.6	2.2E+05	0.078	0.131	0.088
1.27	2.01	1.38	40.9	2.3E+05	0.080	0.126	0.086	0.87	1.43	0.95	33.7	1.9E+05	0.080	0.132	0.087
1.80	2.93	2.13	49.7	2.8E+05	0.077	0.125	0.091	1.64	2.56	1.80	44.9	2.5E+05	0.085	0.133	0.094

Figure A.3: Wind tunnel results from partial loads tests with 40 ft. well cars. *Re* and C_d calculated with $L = 10.48cm$ and $A_D = 191.8cm^2$

40 ft. Partial Loads Results Continued

Configuration: 6	Test: 1		T = 298 K		ρ = 0.99 kg/m^3				Test: 2		T = 299 K			ρ = 0.99 kg/m^3			
D1 (N)	*D2 (N)*	*D3 (N)*	*V (m/s)*	*Re*	C_{d1}	C_{d2}	C_{d3}	*D1 (N)*	*D2 (N)*	*D3 (N)*	*V (m/s)*	*Re*	C_{d1}	C_{d2}	C_{d3}		
4.28	1.82	1.45	38.9	2.2E+05	0.294	0.125	0.100	4.17	1.74	1.40	38.8	2.2E+05	0.290	0.121	0.097		
6.07	2.52	2.09	46.9	2.7E+05	0.288	0.120	0.099	6.80	2.81	2.39	49.6	2.8E+05	0.291	0.120	0.102		
5.20	2.12	1.72	43.2	2.4E+05	0.292	0.119	0.096	3.12	1.34	1.05	33.8	1.9E+05	0.288	0.124	0.097		
3.19	1.34	1.08	34.0	1.9E+05	0.289	0.122	0.098	5.55	2.29	1.92	45.1	2.5E+05	0.286	0.118	0.099		
6.84	2.79	2.41	49.7	2.8E+05	0.290	0.118	0.102	5.97	2.49	2.02	46.5	2.6E+05	0.291	0.121	0.098		
5.69	2.32	1.92	45.2	2.6E+05	0.292	0.119	0.099	4.69	1.92	1.59	41.1	2.3E+05	0.292	0.119	0.099		
4.72	1.91	1.62	41.2	2.3E+05	0.291	0.118	0.100	5.03	2.17	1.74	42.9	2.4E+05	0.288	0.124	0.100		
5.12	2.08	1.75	43.0	2.4E+05	0.291	0.118	0.099	5.65	2.31	1.91	45.0	2.5E+05	0.293	0.120	0.099		
5.65	2.33	1.95	45.2	2.6E+05	0.290	0.120	0.100	4.04	1.65	1.35	38.7	2.2E+05	0.285	0.116	0.095		
6.08	2.46	2.06	46.4	2.6E+05	0.297	0.120	0.100	3.09	1.33	1.03	33.6	1.9E+05	0.289	0.124	0.097		
4.60	1.89	1.60	41.1	2.3E+05	0.286	0.118	0.100	5.98	2.49	2.09	46.4	2.6E+05	0.292	0.122	0.102		
4.15	1.67	1.41	38.7	2.2E+05	0.292	0.117	0.099	6.68	2.79	2.36	49.4	2.8E+05	0.289	0.121	0.102		
6.84	2.68	2.29	49.6	2.8E+05	0.291	0.114	0.098	4.61	1.90	1.53	41.0	2.3E+05	0.290	0.119	0.096		
3.09	1.31	1.07	33.7	1.9E+05	0.286	0.121	0.099	5.05	2.15	1.78	42.8	2.4E+05	0.291	0.124	0.103		
Configuration: 7	Test: 1		T = 296 K		ρ = 1.0 kg/m^3				Test: 2		T = 299 K			ρ = 0.98 kg/m^3			
D1 (N)	*D2 (N)*	*D3 (N)*	*V (m/s)*	*Re*	C_{d1}	C_{d2}	C_{d3}	*D1 (N)*	*D2 (N)*	*D3 (N)*	*V (m/s)*	*Re*	C_{d1}	C_{d2}	C_{d3}		
1.29	3.46	9.81	45.6	2.6E+05	0.065	0.173	0.490	1.04	2.89	8.00	41.3	2.3E+05	0.064	0.178	0.494		
0.92	2.51	7.21	39.2	2.2E+05	0.062	0.170	0.487	1.08	2.98	8.78	43.1	2.4E+05	0.061	0.170	0.499		
1.44	3.99	12.02	49.9	2.9E+05	0.060	0.167	0.503	1.47	4.13	11.72	49.8	2.8E+05	0.063	0.177	0.502		
1.36	3.69	10.48	46.9	2.7E+05	0.064	0.174	0.496	0.89	2.43	7.03	38.9	2.2E+05	0.063	0.170	0.492		
1.00	2.78	8.21	41.3	2.4E+05	0.061	0.170	0.500	1.22	3.57	9.96	46.7	2.6E+05	0.059	0.173	0.483		
1.12	3.04	9.09	43.2	2.5E+05	0.063	0.170	0.508	1.16	3.24	9.38	45.2	2.5E+05	0.060	0.168	0.486		
0.71	1.92	5.51	34.0	1.9E+05	0.064	0.174	0.497	0.68	1.90	5.28	33.7	1.9E+05	0.063	0.177	0.492		
0.89	2.50	7.32	38.7	2.2E+05	0.062	0.174	0.509	0.91	2.52	7.03	38.7	2.2E+05	0.065	0.179	0.498		
1.01	2.76	8.16	41.2	2.4E+05	0.062	0.170	0.502	1.21	3.26	9.73	45.0	2.5E+05	0.063	0.171	0.510		
1.17	3.22	9.71	45.1	2.6E+05	0.060	0.165	0.497	1.07	2.93	8.58	42.8	2.4E+05	0.062	0.170	0.496		
1.29	3.61	10.22	46.4	2.7E+05	0.062	0.175	0.495	0.66	1.86	5.33	33.7	1.9E+05	0.062	0.174	0.499		
1.33	3.86	11.99	49.4	2.8E+05	0.057	0.165	0.514	1.23	3.56	10.26	46.6	2.6E+05	0.060	0.174	0.501		
0.70	1.94	5.49	33.8	1.9E+05	0.065	0.178	0.503	1.42	4.05	11.33	49.5	2.8E+05	0.062	0.175	0.490		
1.09	3.07	8.98	42.8	2.4E+05	0.062	0.175	0.511	0.94	2.82	7.92	41.0	2.3E+05	0.059	0.178	0.499		
Configuration: 8	Test: 1		T = 298 K		ρ = 0.99 kg/m^3				Test: 2		T = 297 K			ρ = 1.0 kg/m^3			
D1 (N)	*D2 (N)*	*D3 (N)*	*V (m/s)*	*Re*	C_{d1}	C_{d2}	C_{d3}	*D1 (N)*	*D2 (N)*	*D3 (N)*	*V (m/s)*	*Re*	C_{d1}	C_{d2}	C_{d3}		
1.65	13.33	1.74	49.7	2.8E+05	0.070	0.569	0.074	1.60	13.35	1.68	49.2	2.8E+05	0.069	0.574	0.072		
1.04	8.36	1.05	38.9	2.2E+05	0.072	0.584	0.073	1.35	11.57	1.41	45.2	2.6E+05	0.069	0.591	0.072		
1.39	11.41	1.45	45.1	2.5E+05	0.072	0.591	0.075	1.09	9.51	1.10	41.3	2.3E+05	0.067	0.584	0.068		
1.49	11.71	1.49	46.6	2.6E+05	0.073	0.569	0.072	1.44	11.99	1.42	46.5	2.6E+05	0.070	0.580	0.069		
1.15	9.22	1.16	41.0	2.3E+05	0.072	0.577	0.073	1.29	10.22	1.27	43.1	2.4E+05	0.073	0.577	0.072		
0.76	6.27	0.77	33.7	1.9E+05	0.071	0.583	0.072	0.75	6.34	0.77	33.9	1.9E+05	0.068	0.578	0.070		
1.27	9.97	1.30	42.8	2.4E+05	0.073	0.576	0.075	1.04	8.28	1.03	38.6	2.2E+05	0.073	0.581	0.072		
1.00	8.10	1.04	38.5	2.2E+05	0.071	0.575	0.074	1.16	9.08	1.12	41.0	2.3E+05	0.072	0.566	0.070		
1.55	13.10	1.64	49.3	2.8E+05	0.068	0.570	0.071	1.01	8.11	1.02	38.6	2.2E+05	0.071	0.571	0.072		
1.32	10.93	1.39	44.9	2.5E+05	0.069	0.572	0.073	1.23	10.04	1.23	42.7	2.4E+05	0.070	0.575	0.070		
1.20	10.12	1.30	42.9	2.4E+05	0.069	0.582	0.075	1.42	11.64	1.40	46.4	2.6E+05	0.069	0.567	0.068		
1.46	11.76	1.47	46.5	2.6E+05	0.071	0.576	0.072	1.56	12.93	1.60	49.3	2.8E+05	0.067	0.559	0.069		
1.06	9.13	1.11	41.0	2.3E+05	0.067	0.576	0.070	1.33	11.06	1.30	44.9	2.5E+05	0.069	0.575	0.068		
0.73	6.16	0.72	33.5	1.9E+05	0.069	0.579	0.068	0.74	6.16	0.75	33.7	1.9E+05	0.068	0.569	0.069		

Figure A.4: Wind tunnel results from partial loads tests with 40 ft. well cars. Re and C_d calculated with $L = 10.48cm$ and $A_D = 191.8cm^2$

40 ft. Partial Loads Results Continued																
Configuration: 9	Test: 1		T = 299 K		ρ = 0.99 kg/m^3			Test: 2		T = 298 K			ρ = 0.99 kg/m^3			
D1 (N)	*D2 (N)*	*D3 (N)*	*V (m/s)*	*Re*	C_{d1}	C_{d2}	C_{d3}	*D1 (N)*	*D2 (N)*	*D3 (N)*	*V (m/s)*	*Re*	C_{d1}	C_{d2}	C_{d3}
1.65	2.33	12.80	49.8	2.8E+05	0.070	0.099	0.541	1.43	2.02	10.94	45.2	2.6E+05	0.074	0.104	0.563
1.20	1.77	9.63	43.2	2.4E+05	0.068	0.100	0.543	1.70	2.33	13.07	49.6	2.8E+05	0.073	0.100	0.561
1.07	1.49	7.99	39.1	2.2E+05	0.074	0.103	0.553	1.03	1.48	8.00	39.2	2.2E+05	0.070	0.102	0.550
1.33	1.89	10.58	45.1	2.5E+05	0.069	0.098	0.547	1.15	1.60	9.10	41.3	2.3E+05	0.071	0.099	0.562
1.46	2.05	11.30	46.8	2.6E+05	0.070	0.099	0.544	1.21	1.73	9.95	43.1	2.4E+05	0.069	0.099	0.567
1.16	1.63	8.88	41.3	2.3E+05	0.072	0.101	0.549	1.52	2.08	11.61	46.7	2.6E+05	0.074	0.101	0.565
0.75	1.07	5.94	34.1	1.9E+05	0.068	0.098	0.540	0.79	1.10	6.10	34.0	1.9E+05	0.073	0.101	0.559
1.03	1.44	8.00	38.7	2.2E+05	0.072	0.101	0.561	1.60	2.29	12.94	49.4	2.8E+05	0.069	0.099	0.560
1.18	1.69	9.46	42.9	2.4E+05	0.068	0.097	0.542	1.34	1.96	10.82	45.3	2.5E+05	0.069	0.101	0.557
0.74	1.07	5.92	33.7	1.9E+05	0.069	0.100	0.551	1.09	1.57	8.88	41.3	2.3E+05	0.067	0.098	0.552
1.33	1.91	10.66	45.3	2.5E+05	0.068	0.098	0.549	1.22	1.78	9.71	43.0	2.4E+05	0.070	0.102	0.556
1.60	2.26	12.64	49.6	2.8E+05	0.069	0.097	0.542	1.42	2.07	11.50	46.6	2.6E+05	0.069	0.101	0.559
1.10	1.55	8.59	41.1	2.3E+05	0.069	0.097	0.537	1.01	1.48	7.96	38.7	2.2E+05	0.071	0.104	0.561
1.45	2.03	11.36	46.6	2.6E+05	0.071	0.099	0.553	0.72	1.09	5.95	33.8	1.9E+05	0.067	0.102	0.552

Figure A.5: Wind tunnel results from partial loads tests with 40 ft. well cars. Re and C_d calculated with $L = 10.48cm$ and $A_D = 191.8cm^2$

48 ft. Partial Loads Results															
Configuration: 0		Test: 1	T = 299 K		ρ = 1.0 kg/m^3			Test: 2		T = 299 K			ρ = 0.99 kg/m^3		
D1 (N)	*D2 (N)*	*D3 (N)*	*V (m/s)*	*Re*	C_{d1}	C_{d2}	C_{d3}	*D1 (N)*	*D2 (N)*	*D3 (N)*	*V (m/s)*	*Re*	C_{d1}	C_{d2}	C_{d3}
4.02	3.98	3.77	41.9	2.4E+05	0.237	0.235	0.223	3.96	3.93	3.77	41.9	2.4E+05	0.237	0.235	0.225
3.79	3.66	3.50	40.2	2.3E+05	0.245	0.237	0.226	5.30	5.27	4.89	48.2	2.7E+05	0.240	0.238	0.221
2.41	2.39	2.26	33.1	1.9E+05	0.230	0.229	0.216	3.80	3.69	3.47	40.3	2.3E+05	0.247	0.239	0.225
5.30	5.31	4.97	48.4	2.7E+05	0.237	0.237	0.222	4.61	4.64	4.25	45.5	2.6E+05	0.234	0.236	0.216
3.21	3.17	2.96	37.7	2.1E+05	0.236	0.233	0.218	4.46	4.41	4.12	44.0	2.5E+05	0.243	0.240	0.224
4.37	4.34	4.09	43.9	2.5E+05	0.237	0.236	0.222	2.55	2.49	2.35	33.2	1.9E+05	0.244	0.238	0.224
4.67	4.63	4.36	45.3	2.6E+05	0.237	0.235	0.222	3.25	3.22	3.02	37.8	2.1E+05	0.239	0.237	0.222
4.26	4.32	4.05	43.9	2.5E+05	0.231	0.234	0.220	4.79	4.68	4.40	45.4	2.5E+05	0.245	0.239	0.225
3.33	3.19	3.04	37.6	2.1E+05	0.245	0.235	0.224	3.23	3.23	3.06	37.8	2.1E+05	0.238	0.238	0.226
4.64	4.63	4.38	45.0	2.6E+05	0.239	0.239	0.226	2.47	2.43	2.27	32.9	1.8E+05	0.239	0.236	0.220
3.67	3.58	3.39	39.9	2.3E+05	0.241	0.235	0.223	3.58	3.59	3.39	40.0	2.2E+05	0.236	0.237	0.223
5.36	5.26	4.91	48.0	2.7E+05	0.243	0.239	0.223	4.28	4.35	4.01	44.0	2.5E+05	0.234	0.238	0.219
2.47	2.46	2.29	32.9	1.9E+05	0.239	0.237	0.221	5.32	5.24	4.88	48.3	2.7E+05	0.241	0.237	0.221
4.05	3.95	3.75	41.6	2.4E+05	0.244	0.238	0.225	3.88	3.93	3.68	41.9	2.3E+05	0.234	0.237	0.222
Configuration: 1		Test: 1	T = 298 K		ρ = 1.0 kg/m^3			Test: 2		T = 298 K			ρ = 1.0 kg/m^3		
D1 (N)	*D2 (N)*	*D3 (N)*	*V (m/s)*	*Re*	C_{d1}	C_{d2}	C_{d3}	*D1 (N)*	*D2 (N)*	*D3 (N)*	*V (m/s)*	*Re*	C_{d1}	C_{d2}	C_{d3}
5.54	1.38	8.98	43.8	2.5E+05	0.301	0.075	0.487	6.09	1.59	10.01	45.2	2.6E+05	0.307	0.080	0.505
4.83	1.18	7.71	40.0	2.3E+05	0.315	0.077	0.502	5.66	1.44	9.03	43.7	2.5E+05	0.306	0.078	0.488
3.09	0.73	4.96	33.0	1.9E+05	0.296	0.070	0.475	4.00	1.00	6.47	37.8	2.2E+05	0.290	0.072	0.468
6.80	1.69	10.78	48.0	2.7E+05	0.307	0.076	0.487	3.16	0.78	5.14	32.9	1.9E+05	0.301	0.075	0.491
5.94	1.47	9.56	45.2	2.6E+05	0.304	0.075	0.490	4.64	1.22	7.63	39.8	2.3E+05	0.303	0.080	0.497
4.04	1.01	6.66	37.7	2.1E+05	0.296	0.074	0.488	5.06	1.28	8.13	41.7	2.4E+05	0.301	0.076	0.484
4.98	1.24	8.09	41.7	2.4E+05	0.300	0.074	0.486	6.86	1.77	11.10	48.2	2.8E+05	0.305	0.079	0.494
5.76	1.41	9.05	43.7	2.5E+05	0.315	0.077	0.495	4.73	1.23	7.55	39.9	2.3E+05	0.308	0.080	0.491
6.02	1.45	9.61	45.1	2.6E+05	0.309	0.075	0.494	5.76	1.50	9.34	45.0	2.6E+05	0.294	0.076	0.477
4.94	1.17	8.06	41.5	2.4E+05	0.299	0.071	0.489	6.84	1.80	11.06	47.9	2.7E+05	0.309	0.081	0.500
6.68	1.65	10.67	48.0	2.7E+05	0.302	0.075	0.483	3.86	0.97	6.39	37.4	2.1E+05	0.285	0.071	0.472
3.08	0.73	5.05	32.8	1.9E+05	0.299	0.071	0.489	5.61	1.46	9.19	43.5	2.5E+05	0.306	0.080	0.502
4.59	1.21	7.68	39.8	2.3E+05	0.302	0.079	0.504	3.04	0.77	4.93	32.7	1.9E+05	0.295	0.074	0.478
4.07	0.97	6.51	37.4	2.1E+05	0.303	0.072	0.485	5.05	1.29	8.20	41.4	2.4E+05	0.305	0.078	0.495
Configuration: 2		Test: 1	T = 297 K		ρ = 1.0 kg/m^3			Test: 2		T = 298 K			ρ = 1.0 kg/m^3		
D1 (N)	*D2 (N)*	*D3 (N)*	*V (m/s)*	*Re*	C_{d1}	C_{d2}	C_{d3}	*D1 (N)*	*D2 (N)*	*D3 (N)*	*V (m/s)*	*Re*	C_{d1}	C_{d2}	C_{d3}
6.80	1.82	10.61	45.2	2.6E+05	0.342	0.092	0.534	5.53	1.49	8.93	41.9	2.4E+05	0.326	0.088	0.527
5.75	1.59	9.21	42.0	2.4E+05	0.337	0.093	0.540	5.09	1.41	8.39	40.1	2.3E+05	0.329	0.091	0.542
7.61	2.15	12.30	48.2	2.8E+05	0.339	0.096	0.547	4.53	1.25	7.30	37.8	2.2E+05	0.329	0.091	0.531
5.22	1.44	8.45	40.1	2.3E+05	0.336	0.093	0.544	5.99	1.62	9.55	43.6	2.5E+05	0.327	0.088	0.521
4.47	1.23	7.15	37.6	2.2E+05	0.327	0.090	0.523	3.34	0.92	5.51	33.1	1.9E+05	0.317	0.087	0.523
6.08	1.80	9.88	43.6	2.5E+05	0.330	0.098	0.537	6.39	1.73	10.48	45.1	2.6E+05	0.326	0.088	0.535
3.45	0.99	5.56	32.9	1.9E+05	0.330	0.095	0.531	7.37	2.06	12.18	48.3	2.7E+05	0.331	0.093	0.546
5.56	1.55	8.94	41.4	2.4E+05	0.335	0.094	0.539	5.00	1.41	8.09	40.0	2.3E+05	0.325	0.092	0.525
6.14	1.73	9.97	43.7	2.5E+05	0.333	0.094	0.541	7.42	2.08	11.88	48.1	2.7E+05	0.334	0.094	0.535
7.48	2.08	11.90	47.8	2.7E+05	0.339	0.094	0.539	6.68	1.87	10.89	45.1	2.6E+05	0.342	0.096	0.557
5.15	1.46	8.27	39.9	2.3E+05	0.336	0.095	0.539	6.18	1.74	10.14	43.5	2.5E+05	0.340	0.096	0.557
3.40	0.94	5.39	32.8	1.9E+05	0.327	0.091	0.518	3.27	0.92	5.49	32.9	1.9E+05	0.314	0.088	0.527
4.48	1.23	7.20	37.4	2.1E+05	0.333	0.091	0.535	5.43	1.52	8.92	41.5	2.4E+05	0.327	0.092	0.538
6.54	1.81	10.61	45.0	2.6E+05	0.335	0.093	0.542	4.35	1.26	7.22	37.5	2.1E+05	0.323	0.093	0.535

Figure A.6: Wind tunnel results from partial loads tests with 48 ft. well cars. Re and C_d calculated with $L = 10.48cm$ and $A_D = 191.8cm^2$

48 ft. Partial Loads Results Continued															
Configuration: 3		Test: 1	T = 297 K		ρ = 1.0 kg/m^3			Test: 2		T = 299 K			ρ = 1.0 kg/m^3		
D1 (N)	*D2 (N)*	*D3 (N)*	*V (m/s)*	*Re*	C_{d1}	C_{d2}	C_{d3}	*D1 (N)*	*D2 (N)*	*D3 (N)*	*V (m/s)*	*Re*	C_{d1}	C_{d2}	C_{d3}
0.88	7.91	1.13	37.7	2.2E+05	0.064	0.575	0.082	0.96	8.81	1.30	40.1	2.3E+05	0.062	0.568	0.084
1.17	10.64	1.59	43.9	2.5E+05	0.063	0.573	0.086	1.44	13.28	2.04	48.5	2.7E+05	0.064	0.589	0.090
0.66	6.05	0.87	32.8	1.9E+05	0.063	0.583	0.084	0.94	9.50	1.39	42.0	2.4E+05	0.056	0.562	0.082
1.30	11.27	1.74	45.2	2.6E+05	0.066	0.570	0.088	0.81	7.70	1.20	37.7	2.1E+05	0.059	0.563	0.088
1.48	12.86	1.96	48.1	2.8E+05	0.066	0.575	0.088	1.27	11.55	1.78	45.0	2.6E+05	0.065	0.594	0.092
1.04	9.58	1.46	41.7	2.4E+05	0.062	0.573	0.088	0.55	5.91	0.84	32.9	1.9E+05	0.053	0.569	0.081
0.95	8.87	1.33	39.8	2.3E+05	0.062	0.580	0.087	1.12	10.55	1.65	43.8	2.5E+05	0.061	0.575	0.090
0.63	5.76	0.88	32.7	1.9E+05	0.061	0.559	0.085	1.20	11.26	1.73	45.2	2.6E+05	0.061	0.574	0.088
1.02	8.65	1.33	39.6	2.3E+05	0.067	0.570	0.088	0.86	8.58	1.32	39.9	2.3E+05	0.056	0.562	0.087
1.64	13.04	1.99	48.0	2.7E+05	0.074	0.591	0.090	1.00	9.35	1.43	41.6	2.4E+05	0.060	0.564	0.086
0.88	7.62	1.17	37.4	2.1E+05	0.066	0.566	0.087	1.16	10.45	1.60	43.6	2.5E+05	0.064	0.576	0.088
1.10	9.64	1.47	41.5	2.4E+05	0.067	0.582	0.089	1.41	12.70	1.95	47.7	2.7E+05	0.065	0.582	0.089
1.25	11.03	1.65	44.9	2.6E+05	0.064	0.567	0.085	0.80	7.58	1.16	37.5	2.1E+05	0.060	0.564	0.086
1.18	10.43	1.62	43.6	2.5E+05	0.065	0.569	0.088	0.57	5.70	0.82	32.7	1.8E+05	0.055	0.558	0.080
Configuration: 4		Test: 1	T = 298 K		ρ = 1.0 kg/m^3			Test: 2		T = 298 K			ρ = 1.0 kg/m^3		
D1 (N)	*D2 (N)*	*D3 (N)*	*V (m/s)*	*Re*	C_{d1}	C_{d2}	C_{d3}	*D1 (N)*	*D2 (N)*	*D3 (N)*	*V (m/s)*	*Re*	C_{d1}	C_{d2}	C_{d3}
2.00	2.40	12.75	49.8	2.8E+05	0.085	0.101	0.539	1.58	1.97	10.69	45.4	2.6E+05	0.080	0.100	0.539
1.59	1.92	10.51	44.3	2.5E+05	0.085	0.103	0.564	1.77	2.24	11.88	48.3	2.7E+05	0.079	0.100	0.532
1.37	1.67	8.89	42.3	2.4E+05	0.081	0.098	0.524	0.76	0.99	5.60	33.0	1.9E+05	0.073	0.095	0.536
1.19	1.44	7.60	38.2	2.1E+05	0.086	0.104	0.550	1.22	1.53	8.51	40.1	2.3E+05	0.079	0.099	0.551
1.66	2.01	10.91	45.7	2.6E+05	0.084	0.101	0.550	1.04	1.33	7.63	37.6	2.1E+05	0.077	0.098	0.563
0.86	1.03	5.72	33.3	1.9E+05	0.082	0.097	0.543	1.47	1.84	10.25	43.7	2.5E+05	0.080	0.100	0.558
1.29	1.52	8.15	40.3	2.3E+05	0.083	0.099	0.529	1.27	1.64	8.91	41.5	2.4E+05	0.076	0.099	0.537
0.86	1.02	5.57	33.1	1.9E+05	0.083	0.099	0.537	1.48	1.84	10.02	43.6	2.5E+05	0.081	0.101	0.550
1.14	1.36	7.63	37.8	2.1E+05	0.085	0.100	0.563	0.73	0.97	5.35	32.8	1.9E+05	0.071	0.094	0.518
1.32	1.66	8.88	41.8	2.3E+05	0.080	0.100	0.535	1.80	2.21	12.12	48.1	2.7E+05	0.081	0.100	0.546
1.28	1.53	8.59	40.1	2.3E+05	0.084	0.100	0.561	1.12	1.48	8.33	39.9	2.3E+05	0.073	0.097	0.547
1.60	1.89	10.24	44.1	2.5E+05	0.087	0.103	0.557	1.31	1.66	9.13	41.5	2.4E+05	0.079	0.101	0.553
1.87	2.25	12.03	48.4	2.7E+05	0.084	0.101	0.541	1.58	1.94	10.69	45.0	2.6E+05	0.081	0.100	0.550
1.70	2.03	10.69	45.5	2.5E+05	0.087	0.104	0.545	1.00	1.32	7.11	37.4	2.1E+05	0.074	0.098	0.529
Configuration: 5		Test: 1	T = 297 K		ρ = 1.0 kg/m^3			Test: 2		T = 299 K			ρ = 1.0 kg/m^3		
D1 (N)	*D2 (N)*	*D3 (N)*	*V (m/s)*	*Re*	C_{d1}	C_{d2}	C_{d3}	*D1 (N)*	*D2 (N)*	*D3 (N)*	*V (m/s)*	*Re*	C_{d1}	C_{d2}	C_{d3}
1.65	2.39	1.82	45.6	2.6E+05	0.082	0.119	0.091	1.65	2.42	1.91	45.5	2.6E+05	0.083	0.122	0.096
0.85	1.21	0.93	33.2	1.9E+05	0.081	0.114	0.088	1.25	1.87	1.44	40.5	2.3E+05	0.079	0.119	0.092
1.93	2.72	2.13	48.3	2.8E+05	0.086	0.121	0.095	0.86	1.26	0.96	33.3	1.9E+05	0.081	0.119	0.090
1.47	2.05	1.60	42.1	2.4E+05	0.087	0.121	0.094	1.44	2.03	1.58	42.1	2.4E+05	0.085	0.120	0.093
1.37	1.91	1.50	40.2	2.3E+05	0.089	0.123	0.097	1.90	2.73	2.13	48.0	2.7E+05	0.087	0.125	0.097
1.53	2.24	1.77	44.0	2.5E+05	0.083	0.121	0.095	1.49	2.20	1.74	44.0	2.5E+05	0.081	0.119	0.094
1.11	1.62	1.25	37.8	2.2E+05	0.081	0.118	0.091	1.15	1.66	1.27	37.9	2.1E+05	0.084	0.121	0.093
1.31	1.86	1.41	39.9	2.3E+05	0.085	0.121	0.092	1.33	1.88	1.44	40.1	2.3E+05	0.087	0.123	0.094
1.12	1.63	1.22	37.6	2.1E+05	0.083	0.120	0.090	1.13	1.65	1.28	37.8	2.1E+05	0.083	0.121	0.093
1.82	2.68	2.05	47.9	2.7E+05	0.083	0.122	0.093	0.83	1.24	0.95	33.0	1.9E+05	0.080	0.119	0.092
1.73	2.45	1.88	45.3	2.6E+05	0.088	0.125	0.096	1.65	2.35	1.83	45.4	2.6E+05	0.084	0.120	0.093
0.88	1.25	0.90	32.8	1.9E+05	0.085	0.121	0.087	1.82	2.62	2.03	48.1	2.7E+05	0.083	0.119	0.092
1.61	2.24	1.73	43.7	2.5E+05	0.088	0.123	0.095	1.36	2.02	1.56	41.9	2.4E+05	0.081	0.120	0.093
1.41	2.04	1.54	41.6	2.4E+05	0.085	0.123	0.093	1.59	2.26	1.74	43.8	2.5E+05	0.087	0.123	0.095

Figure A.7: Wind tunnel results from partial loads tests with 48 ft. well cars. Re and C_d calculated with $L = 10.48cm$ and $A_D = 191.8cm^2$

48 ft. Partial Loads Results Continued															
Configuration: 6		Test: 1	T = 297 K		ρ = 1.0 kg/m^3			Test: 2		T = 295 K		ρ = 1.0 kg/m^3			
D1 (N)	*D2 (N)*	*D3 (N)*	*V (m/s)*	*Re*	C_{d1}	C_{d2}	C_{d3}	*D1 (N)*	*D2 (N)*	*D3 (N)*	*V (m/s)*	*Re*	C_{d1}	C_{d2}	C_{d3}
4.16	1.57	1.00	37.8	2.2E+05	0.301	0.114	0.072	4.27	1.58	0.96	38.0	2.2E+05	0.305	0.113	0.068
5.77	2.25	1.49	43.8	2.5E+05	0.312	0.122	0.080	5.29	2.06	1.32	42.0	2.4E+05	0.310	0.121	0.077
3.19	1.21	0.73	32.9	1.9E+05	0.306	0.116	0.070	7.08	2.74	1.74	48.2	2.8E+05	0.316	0.122	0.077
4.69	1.86	1.24	39.9	2.3E+05	0.306	0.121	0.081	6.22	2.41	1.57	45.4	2.6E+05	0.312	0.121	0.079
6.06	2.39	1.52	45.2	2.6E+05	0.308	0.122	0.078	5.72	2.26	1.46	43.9	2.5E+05	0.308	0.122	0.079
5.02	2.02	1.33	41.7	2.4E+05	0.301	0.121	0.079	3.22	1.22	0.75	33.1	1.9E+05	0.303	0.115	0.071
6.90	2.74	1.80	48.0	2.7E+05	0.311	0.123	0.081	4.74	1.84	1.16	40.1	2.3E+05	0.305	0.118	0.075
4.98	1.95	1.32	41.7	2.4E+05	0.298	0.117	0.079	6.18	2.46	1.59	45.2	2.6E+05	0.314	0.125	0.081
5.55	2.20	1.46	43.6	2.5E+05	0.304	0.120	0.080	6.71	2.64	1.72	47.5	2.7E+05	0.309	0.122	0.079
4.53	1.82	1.14	39.8	2.3E+05	0.297	0.120	0.075	5.73	2.21	1.39	43.8	2.5E+05	0.310	0.120	0.075
4.02	1.59	1.05	37.4	2.1E+05	0.298	0.118	0.078	4.83	1.91	1.24	40.1	2.3E+05	0.312	0.123	0.080
6.61	2.60	1.70	48.1	2.7E+05	0.298	0.117	0.077	3.14	1.19	0.68	32.9	1.9E+05	0.301	0.114	0.065
2.96	1.17	0.71	32.6	1.9E+05	0.289	0.114	0.069	5.29	2.08	1.33	41.7	2.4E+05	0.316	0.125	0.080
5.82	2.29	1.54	44.9	2.6E+05	0.300	0.118	0.079	4.09	1.60	0.99	37.5	2.2E+05	0.300	0.118	0.073
Configuration: 7		Test: 1	T = 300 K		ρ = 0.99 kg/m^3			Test: 2		T = 298 K		ρ = 1.0 kg/m^3			
D1 (N)	*D2 (N)*	*D3 (N)*	*V (m/s)*	*Re*	C_{d1}	C_{d2}	C_{d3}	*D1 (N)*	*D2 (N)*	*D3 (N)*	*V (m/s)*	*Re*	C_{d1}	C_{d2}	C_{d3}
1.49	3.93	12.22	48.1	2.7E+05	0.068	0.179	0.557	0.94	2.44	7.47	37.8	2.2E+05	0.068	0.176	0.540
0.96	2.68	8.44	40.3	2.2E+05	0.062	0.175	0.550	1.04	2.70	8.55	40.1	2.3E+05	0.067	0.174	0.549
0.90	2.45	7.64	37.8	2.1E+05	0.067	0.181	0.565	1.22	3.07	9.50	41.8	2.4E+05	0.072	0.182	0.563
1.29	3.46	10.82	45.4	2.5E+05	0.066	0.178	0.555	1.48	3.61	10.87	45.1	2.6E+05	0.075	0.184	0.553
1.01	2.91	8.83	41.7	2.3E+05	0.061	0.176	0.535	1.63	4.09	12.34	48.1	2.7E+05	0.073	0.183	0.553
1.29	3.35	10.20	43.8	2.4E+05	0.071	0.185	0.563	0.69	1.87	5.67	33.1	1.9E+05	0.065	0.178	0.538
0.62	1.86	5.75	33.1	1.8E+05	0.060	0.179	0.556	1.32	3.23	10.03	43.7	2.5E+05	0.071	0.175	0.544
1.22	3.36	10.32	43.8	2.4E+05	0.068	0.186	0.571	1.15	2.84	8.58	40.0	2.3E+05	0.074	0.184	0.556
0.82	2.38	7.47	37.7	2.1E+05	0.061	0.177	0.555	1.59	3.75	11.15	45.2	2.6E+05	0.081	0.191	0.568
1.47	3.98	12.15	48.3	2.7E+05	0.067	0.181	0.553	0.96	2.43	7.65	37.7	2.1E+05	0.070	0.177	0.558
1.00	2.88	8.86	41.8	2.3E+05	0.061	0.175	0.538	0.71	1.91	5.78	32.9	1.9E+05	0.068	0.183	0.555
0.59	1.79	5.55	33.0	1.8E+05	0.057	0.174	0.539	1.26	3.23	9.98	43.7	2.5E+05	0.069	0.176	0.542
1.24	3.45	10.45	45.3	2.5E+05	0.064	0.178	0.541	1.63	4.07	12.70	48.0	2.7E+05	0.073	0.183	0.572
0.94	2.60	8.01	39.9	2.2E+05	0.063	0.173	0.534	1.21	2.97	9.32	41.7	2.4E+05	0.073	0.178	0.559
Configuration: 8		Test: 1	T = 299 K		ρ = 1.0 kg/m^3			Test: 2		T = 300 K		ρ = 0.99 kg/m^3			
D1 (N)	*D2 (N)*	*D3 (N)*	*V (m/s)*	*Re*	C_{d1}	C_{d2}	C_{d3}	*D1 (N)*	*D2 (N)*	*D3 (N)*	*V (m/s)*	*Re*	C_{d1}	C_{d2}	C_{d3}
0.96	8.66	0.76	37.6	2.2E+05	0.071	0.635	0.056	1.80	14.66	1.52	48.0	2.7E+05	0.082	0.670	0.070
1.83	14.89	1.55	48.0	2.7E+05	0.083	0.672	0.070	1.48	12.61	1.27	45.4	2.5E+05	0.076	0.646	0.065
1.46	12.16	1.20	43.8	2.5E+05	0.079	0.660	0.065	1.33	10.99	1.15	41.9	2.3E+05	0.080	0.660	0.069
1.57	12.65	1.24	45.1	2.6E+05	0.080	0.648	0.064	1.46	11.92	1.21	43.7	2.4E+05	0.081	0.659	0.067
0.73	6.75	0.66	33.1	1.9E+05	0.069	0.641	0.063	1.14	9.85	1.00	40.1	2.2E+05	0.075	0.648	0.065
1.23	10.21	1.06	39.7	2.3E+05	0.081	0.672	0.070	0.99	8.75	0.82	37.7	2.1E+05	0.074	0.652	0.061
1.30	10.88	1.12	41.7	2.4E+05	0.078	0.653	0.067	0.78	6.86	0.68	32.9	1.8E+05	0.076	0.667	0.066
1.05	8.80	0.97	37.5	2.1E+05	0.078	0.649	0.071	1.66	14.06	1.42	48.0	2.7E+05	0.076	0.644	0.065
0.76	6.65	0.67	32.7	1.9E+05	0.073	0.644	0.065	1.56	12.72	1.38	44.9	2.5E+05	0.082	0.669	0.072
1.50	12.03	1.24	43.4	2.5E+05	0.082	0.662	0.068	1.01	8.72	0.90	37.6	2.1E+05	0.075	0.650	0.067
1.19	10.17	1.02	39.7	2.3E+05	0.079	0.672	0.068	0.76	6.73	0.67	32.8	1.8E+05	0.075	0.660	0.066
1.79	14.63	1.51	48.0	2.7E+05	0.081	0.661	0.068	1.38	11.90	1.19	43.7	2.4E+05	0.076	0.659	0.066
1.30	10.87	1.12	41.6	2.3E+05	0.078	0.657	0.067	1.09	9.80	1.02	39.8	2.2E+05	0.073	0.654	0.068
1.53	12.53	1.24	45.1	2.6E+05	0.078	0.640	0.063	1.23	10.55	1.10	41.4	2.3E+05	0.076	0.651	0.068

Figure A.8: Wind tunnel results from partial loads tests with 48 ft. well cars. Re and C_d calculated with $L = 10.48cm$ and $A_D = 191.8cm^2$

48 ft. Partial Loads Results Continued															
Configuration: 9		Test: 1	T = 295 K		ρ = 1.0 kg/m^3			Test: 2		T = 303 K		ρ = 0.99 kg/m^3			
D1 (N)	*D2 (N)*	*D3 (N)*	*V (m/s)*	*Re*	C_{d1}	C_{d2}	C_{d3}	*D1 (N)*	*D2 (N)*	*D3 (N)*	*V (m/s)*	*Re*	C_{d1}	C_{d2}	C_{d3}
1.67	2.11	12.10	45.2	2.6E+05	0.084	0.107	0.611	1.01	1.38	7.82	37.5	2.1E+05	0.075	0.103	0.581
1.26	1.67	9.58	40.4	2.3E+05	0.080	0.106	0.607	1.17	1.57	9.08	39.9	2.2E+05	0.077	0.104	0.600
1.09	1.42	8.23	38.1	2.2E+05	0.078	0.101	0.588	0.74	1.01	5.83	32.8	1.8E+05	0.072	0.099	0.571
0.85	1.09	6.28	33.1	1.9E+05	0.080	0.103	0.594	1.34	1.71	9.82	41.7	2.3E+05	0.082	0.104	0.596
1.95	2.46	14.20	48.5	2.8E+05	0.086	0.109	0.627	1.85	2.29	13.44	48.3	2.7E+05	0.084	0.103	0.608
1.47	1.93	11.05	44.0	2.5E+05	0.079	0.103	0.590	1.46	1.91	11.15	43.8	2.4E+05	0.080	0.105	0.612
1.39	1.80	10.12	42.1	2.4E+05	0.081	0.105	0.592	1.59	2.04	11.93	45.3	2.5E+05	0.082	0.105	0.615
2.06	2.44	14.28	48.3	2.8E+05	0.091	0.108	0.635	1.27	1.72	10.04	41.7	2.3E+05	0.077	0.105	0.609
1.74	2.11	11.87	45.3	2.6E+05	0.088	0.107	0.598	1.54	2.04	11.59	45.1	2.5E+05	0.080	0.106	0.600
1.36	1.76	9.99	41.9	2.4E+05	0.080	0.104	0.590	1.74	2.27	13.12	48.4	2.7E+05	0.078	0.102	0.591
0.76	1.07	6.27	33.0	1.9E+05	0.072	0.101	0.596	1.13	1.56	9.00	39.9	2.2E+05	0.075	0.103	0.598
1.05	1.37	7.86	37.5	2.2E+05	0.077	0.101	0.577	1.42	1.89	10.96	43.6	2.4E+05	0.078	0.104	0.606
1.26	1.56	9.16	39.8	2.3E+05	0.083	0.102	0.599	1.04	1.41	7.99	37.4	2.1E+05	0.079	0.106	0.601
1.51	1.94	11.23	43.8	2.5E+05	0.081	0.105	0.608	0.84	1.08	6.28	32.6	1.8E+05	0.083	0.107	0.623

Figure A.9: Wind tunnel results from partial loads tests with 48 ft. well cars. Re and C_d calculated with $L = 10.48cm$ and $A_D = 191.8cm^2$

50 ft. Partial Loads Results

Configuration: 0	Test: 1	T = 296 K		ρ = 1.0 kg/m^3				Test: 2		T = 297 K		ρ = 1.0 kg/m^3			
D1 (N)	*D2 (N)*	*D3 (N)*	*V (m/s)*	*Re*	C_{d1}	C_{d2}	C_{d3}	*D1 (N)*	*D2 (N)*	*D3 (N)*	*V (m/s)*	*Re*	C_{d1}	C_{d2}	C_{d3}
5.47	3.59	3.66	37.8	2.2E+05	0.390	0.255	0.261	5.52	3.65	3.75	37.7	2.2E+05	0.397	0.262	0.269
6.72	4.43	4.65	42.0	2.4E+05	0.390	0.257	0.270	7.45	4.98	5.20	44.0	2.6E+05	0.394	0.264	0.275
7.38	4.96	5.09	44.0	2.6E+05	0.390	0.262	0.269	6.18	4.13	4.30	40.2	2.3E+05	0.395	0.264	0.274
4.13	2.68	2.89	32.8	1.9E+05	0.392	0.255	0.275	7.94	5.21	5.40	45.4	2.6E+05	0.396	0.260	0.269
8.99	6.05	6.28	48.4	2.8E+05	0.393	0.264	0.274	4.10	2.68	2.86	32.8	1.9E+05	0.391	0.256	0.273
6.23	4.11	4.37	40.2	2.3E+05	0.395	0.261	0.277	8.88	6.03	6.17	48.3	2.8E+05	0.391	0.265	0.272
7.89	5.29	5.56	45.5	2.6E+05	0.392	0.263	0.276	6.66	4.46	4.64	42.0	2.4E+05	0.388	0.260	0.271
6.14	4.07	4.32	40.1	2.3E+05	0.393	0.261	0.277	8.85	5.96	6.17	48.4	2.8E+05	0.389	0.262	0.271
8.98	5.94	6.17	47.9	2.8E+05	0.399	0.264	0.274	4.07	2.67	2.85	32.8	1.9E+05	0.390	0.256	0.274
5.32	3.57	3.82	37.6	2.2E+05	0.385	0.258	0.277	7.37	4.87	5.12	43.9	2.5E+05	0.395	0.261	0.274
4.16	2.74	2.98	32.7	1.9E+05	0.399	0.263	0.286	5.38	3.49	3.79	37.6	2.2E+05	0.392	0.254	0.276
7.30	4.87	5.12	43.7	2.5E+05	0.391	0.261	0.274	6.55	4.33	4.63	41.8	2.4E+05	0.387	0.256	0.274
6.59	4.39	4.70	41.7	2.4E+05	0.390	0.260	0.278	6.03	3.98	4.22	40.1	2.3E+05	0.388	0.256	0.271
7.83	5.20	5.42	45.2	2.6E+05	0.393	0.261	0.272	7.72	5.11	5.47	45.5	2.6E+05	0.385	0.255	0.272
Configuration: 0	Test: 1	T = 300 K		ρ = 1.0 kg/m^3				Test: 2		T = 299 K		ρ = 1.0 kg/m^3			
D1 (N)	*D2 (N)*	*D3 (N)*	*V (m/s)*	*Re*	C_{d1}	C_{d2}	C_{d3}	*D1 (N)*	*D2 (N)*	*D3 (N)*	*V (m/s)*	*Re*	C_{d1}	C_{d2}	C_{d3}
7.65	1.65	8.83	41.9	2.4E+05	0.449	0.097	0.519	9.26	1.98	10.83	45.7	2.6E+05	0.457	0.098	0.535
7.13	1.53	8.20	40.3	2.3E+05	0.456	0.098	0.525	7.24	1.52	8.43	40.6	2.3E+05	0.457	0.096	0.532
9.08	1.93	10.60	45.5	2.6E+05	0.457	0.097	0.533	6.52	1.34	7.59	38.0	2.2E+05	0.465	0.096	0.542
4.74	1.01	5.53	33.1	1.9E+05	0.448	0.096	0.523	4.78	0.97	5.66	33.1	1.9E+05	0.451	0.091	0.533
6.34	1.31	7.45	37.8	2.2E+05	0.460	0.095	0.540	7.66	1.66	9.06	42.1	2.4E+05	0.447	0.097	0.529
10.24	2.20	11.94	48.5	2.7E+05	0.453	0.098	0.529	10.24	2.23	11.98	48.5	2.8E+05	0.451	0.098	0.528
8.37	1.88	9.80	44.0	2.5E+05	0.449	0.101	0.526	8.45	1.79	10.04	44.2	2.5E+05	0.448	0.095	0.533
6.13	1.29	7.20	37.8	2.1E+05	0.445	0.094	0.524	10.19	2.08	11.89	48.5	2.7E+05	0.450	0.092	0.525
7.02	1.48	8.14	40.1	2.3E+05	0.454	0.096	0.527	9.12	1.92	10.62	45.6	2.6E+05	0.455	0.096	0.530
8.31	1.80	9.76	43.8	2.5E+05	0.449	0.097	0.527	8.44	1.71	9.90	43.9	2.5E+05	0.453	0.092	0.532
8.97	1.95	10.43	45.4	2.6E+05	0.454	0.099	0.527	7.21	1.49	8.53	40.3	2.3E+05	0.461	0.095	0.545
4.75	0.99	5.54	33.0	1.9E+05	0.454	0.095	0.530	7.48	1.57	8.92	41.8	2.4E+05	0.443	0.093	0.528
7.54	1.60	8.79	41.7	2.4E+05	0.451	0.096	0.526	4.76	0.92	5.66	33.0	1.9E+05	0.455	0.088	0.540
10.24	2.17	11.90	48.4	2.7E+05	0.456	0.097	0.530	6.18	1.23	7.27	37.7	2.2E+05	0.449	0.089	0.528
Configuration: 0	Test: 1	T = 298 K		ρ = 1.0 kg/m^3				Test: 2		T = 300 K		ρ = 1.0 kg/m^3			
D1 (N)	*D2 (N)*	*D3 (N)*	*V (m/s)*	*Re*	C_{d1}	C_{d2}	C_{d3}	*D1 (N)*	*D2 (N)*	*D3 (N)*	*V (m/s)*	*Re*	C_{d1}	C_{d2}	C_{d3}
10.75	1.36	13.14	48.6	2.8E+05	0.467	0.059	0.571	6.66	0.84	8.04	37.8	2.2E+05	0.480	0.061	0.579
8.11	0.99	9.99	42.1	2.4E+05	0.472	0.058	0.581	7.49	0.94	8.93	40.3	2.3E+05	0.478	0.060	0.570
9.50	1.17	11.52	45.5	2.6E+05	0.474	0.058	0.575	9.61	1.22	11.54	45.5	2.6E+05	0.481	0.061	0.578
7.54	0.91	9.22	40.3	2.3E+05	0.480	0.058	0.586	10.86	1.36	12.98	48.3	2.7E+05	0.485	0.061	0.580
8.91	1.05	10.76	43.9	2.5E+05	0.478	0.056	0.577	8.21	1.02	9.76	42.1	2.4E+05	0.484	0.060	0.576
6.65	0.79	8.12	37.9	2.2E+05	0.478	0.057	0.584	5.00	0.61	6.08	33.1	1.9E+05	0.475	0.058	0.577
5.06	0.58	6.19	32.9	1.9E+05	0.480	0.055	0.587	8.81	1.07	10.46	43.9	2.5E+05	0.475	0.058	0.564
9.50	1.19	11.56	45.5	2.6E+05	0.473	0.059	0.575	8.16	1.03	9.82	41.9	2.4E+05	0.484	0.061	0.582
6.59	0.78	8.15	37.7	2.2E+05	0.478	0.057	0.591	9.36	1.18	11.23	45.3	2.6E+05	0.475	0.060	0.570
5.02	0.58	6.20	32.7	1.9E+05	0.485	0.056	0.598	10.90	1.38	13.05	48.3	2.7E+05	0.485	0.061	0.580
10.82	1.32	13.22	48.3	2.8E+05	0.478	0.058	0.584	7.53	0.92	8.98	40.2	2.3E+05	0.485	0.059	0.579
7.31	0.87	8.90	39.9	2.3E+05	0.473	0.056	0.576	6.55	0.82	7.99	37.7	2.1E+05	0.480	0.060	0.586
8.08	0.96	9.83	41.8	2.4E+05	0.477	0.057	0.580	5.03	0.61	6.08	32.9	1.9E+05	0.482	0.059	0.583
8.80	1.08	10.77	43.8	2.5E+05	0.474	0.058	0.580	9.00	1.08	10.79	43.8	2.5E+05	0.490	0.059	0.587

Figure A.10: Wind tunnel results from partial loads tests with 53 ft. well cars. Re and C_d calculated with $L = 10.48cm$ and $A_D = 191.8cm^2$

50 ft. Partial Loads Results Continued															
Configuration: 0		Test: 1	T = 296 K		ρ = 1.0 kg/m^3			Test: 2		T = 301 K			ρ = 1.0 kg/m^3		
D1 (N)	*D2 (N)*	*D3 (N)*	*V (m/s)*	*Re*	C_{d1}	C_{d2}	C_{d3}	*D1 (N)*	*D2 (N)*	*D3 (N)*	*V (m/s)*	*Re*	C_{d1}	C_{d2}	C_{d3}
2.28	9.59	1.46	40.3	2.4E+05	0.143	0.601	0.092	2.79	11.97	1.85	45.4	2.6E+05	0.139	0.599	0.093
2.81	11.63	1.82	44.1	2.6E+05	0.147	0.611	0.096	2.65	11.25	1.77	44.2	2.5E+05	0.142	0.602	0.095
3.27	13.63	2.14	48.5	2.8E+05	0.142	0.594	0.094	2.23	9.58	1.50	40.4	2.3E+05	0.143	0.613	0.096
2.01	8.74	1.42	38.0	2.2E+05	0.142	0.619	0.101	2.45	10.42	1.62	42.0	2.4E+05	0.145	0.617	0.096
2.46	10.34	1.67	42.1	2.4E+05	0.143	0.601	0.097	3.26	13.73	2.10	48.4	2.7E+05	0.145	0.611	0.093
3.01	12.25	2.00	45.6	2.6E+05	0.149	0.605	0.099	1.99	8.31	1.35	38.0	2.1E+05	0.143	0.600	0.097
2.01	8.30	1.38	37.9	2.2E+05	0.144	0.593	0.098	1.50	6.24	1.06	33.0	1.9E+05	0.143	0.598	0.102
2.48	10.26	1.67	41.9	2.4E+05	0.145	0.600	0.098	2.64	11.41	1.80	43.8	2.5E+05	0.143	0.620	0.098
3.33	13.98	2.19	48.4	2.8E+05	0.146	0.615	0.096	3.15	13.51	2.14	48.4	2.7E+05	0.141	0.604	0.096
2.90	12.40	1.97	45.5	2.6E+05	0.144	0.617	0.098	2.23	9.42	1.52	40.2	2.2E+05	0.145	0.610	0.098
2.74	11.28	1.88	43.9	2.5E+05	0.146	0.602	0.100	1.48	6.29	1.05	33.0	1.9E+05	0.142	0.603	0.100
1.51	6.21	1.09	32.8	1.9E+05	0.144	0.594	0.104	2.74	11.96	1.89	45.3	2.5E+05	0.140	0.608	0.096
2.23	9.50	1.53	39.9	2.3E+05	0.144	0.615	0.099	1.97	8.35	1.37	37.8	2.1E+05	0.144	0.613	0.100
1.93	8.18	1.37	37.5	2.2E+05	0.142	0.600	0.101	2.39	10.04	1.62	41.7	2.3E+05	0.144	0.603	0.097
Configuration: 0		Test: 1	T = 298 K		ρ = 1.0 kg/m^3			Test: 2		T = 299 K			ρ = 1.0 kg/m^3		
D1 (N)	*D2 (N)*	*D3 (N)*	*V (m/s)*	*Re*	C_{d1}	C_{d2}	C_{d3}	*D1 (N)*	*D2 (N)*	*D3 (N)*	*V (m/s)*	*Re*	C_{d1}	C_{d2}	C_{d3}
2.95	2.44	12.00	44.2	2.6E+05	0.155	0.128	0.630	2.94	2.45	11.87	44.3	2.6E+05	0.154	0.128	0.621
3.21	2.61	13.03	46.0	2.6E+05	0.156	0.127	0.635	2.66	2.19	10.91	42.3	2.4E+05	0.154	0.127	0.633
2.51	2.04	10.30	40.5	2.3E+05	0.159	0.128	0.650	2.44	1.99	10.24	40.5	2.3E+05	0.154	0.125	0.645
3.60	2.92	14.88	48.5	2.8E+05	0.158	0.128	0.652	2.24	1.79	8.91	38.0	2.2E+05	0.160	0.128	0.638
1.68	1.34	6.66	33.3	1.9E+05	0.156	0.125	0.620	3.50	2.90	14.62	48.5	2.8E+05	0.154	0.128	0.644
2.64	2.15	10.99	41.9	2.4E+05	0.155	0.126	0.645	3.01	2.53	12.94	45.6	2.6E+05	0.150	0.126	0.645
2.12	1.71	8.87	37.8	2.2E+05	0.153	0.124	0.641	1.70	1.33	7.04	33.3	1.9E+05	0.159	0.124	0.657
2.69	2.17	10.71	42.1	2.4E+05	0.157	0.127	0.626	3.51	2.89	14.24	48.8	2.8E+05	0.153	0.126	0.621
3.14	2.60	12.65	45.6	2.6E+05	0.156	0.129	0.630	2.16	1.75	9.11	38.0	2.2E+05	0.155	0.126	0.654
1.64	1.30	6.88	33.0	1.9E+05	0.156	0.123	0.653	2.94	2.36	12.19	44.1	2.5E+05	0.157	0.126	0.651
2.45	1.99	9.87	40.2	2.3E+05	0.157	0.128	0.633	3.21	2.57	12.95	45.6	2.6E+05	0.160	0.128	0.645
2.13	1.65	8.94	37.6	2.2E+05	0.156	0.121	0.654	2.63	2.13	10.81	42.0	2.4E+05	0.155	0.125	0.636
3.52	2.83	15.07	48.6	2.8E+05	0.155	0.124	0.662	1.67	1.32	6.75	33.2	1.9E+05	0.157	0.124	0.635
2.95	2.32	12.26	44.0	2.5E+05	0.157	0.124	0.654	2.39	1.93	9.75	40.1	2.3E+05	0.153	0.124	0.627
Configuration: 0		Test: 1	T = 297 K		ρ = 1.0 kg/m^3			Test: 2		T = 301 K			ρ = 1.0 kg/m^3		
D1 (N)	*D2 (N)*	*D3 (N)*	*V (m/s)*	*Re*	C_{d1}	C_{d2}	C_{d3}	*D1 (N)*	*D2 (N)*	*D3 (N)*	*V (m/s)*	*Re*	C_{d1}	C_{d2}	C_{d3}
8.46	2.52	1.73	44.0	2.6E+05	0.446	0.133	0.091	8.67	2.58	1.72	44.3	2.5E+05	0.456	0.136	0.091
10.12	3.14	2.10	48.4	2.8E+05	0.443	0.137	0.092	7.20	2.13	1.48	40.6	2.3E+05	0.453	0.134	0.093
8.81	2.68	1.86	45.5	2.6E+05	0.438	0.133	0.092	10.35	3.04	2.07	48.7	2.8E+05	0.455	0.134	0.091
6.27	1.89	1.36	37.9	2.2E+05	0.450	0.136	0.098	9.06	2.65	1.87	45.8	2.6E+05	0.452	0.132	0.093
6.96	2.11	1.56	40.1	2.3E+05	0.444	0.134	0.099	4.89	1.40	1.05	33.3	1.9E+05	0.459	0.132	0.099
7.68	2.30	1.66	41.9	2.4E+05	0.450	0.135	0.097	7.81	2.26	1.61	42.3	2.4E+05	0.455	0.132	0.094
4.73	1.41	1.09	32.8	1.9E+05	0.450	0.134	0.104	6.25	1.81	1.34	38.0	2.2E+05	0.451	0.131	0.097
7.62	2.28	1.65	41.8	2.4E+05	0.450	0.134	0.098	10.27	2.92	2.08	48.6	2.8E+05	0.453	0.129	0.092
4.57	1.38	1.05	32.7	1.9E+05	0.440	0.133	0.101	4.84	1.35	1.06	33.0	1.9E+05	0.462	0.128	0.101
10.19	3.11	2.12	48.4	2.8E+05	0.447	0.136	0.093	7.68	2.23	1.64	42.0	2.4E+05	0.455	0.132	0.097
8.89	2.64	1.90	45.5	2.6E+05	0.444	0.132	0.095	6.32	1.77	1.36	37.8	2.1E+05	0.461	0.129	0.099
6.97	2.07	1.53	40.0	2.3E+05	0.449	0.133	0.099	8.51	2.45	1.77	44.1	2.5E+05	0.458	0.132	0.095
8.29	2.50	1.82	43.9	2.5E+05	0.443	0.133	0.098	8.84	2.64	1.86	45.5	2.6E+05	0.446	0.133	0.094
6.01	1.77	1.35	37.5	2.2E+05	0.442	0.130	0.099	6.98	1.99	1.49	40.1	2.3E+05	0.453	0.129	0.097

Figure A.11: Wind tunnel results from partial loads tests with 53 ft. well cars. Re and C_d calculated with $L = 10.48cm$ and $A_D = 191.8cm^2$

50 ft. Partial Loads Results Continued															
Configuration: 0	Test: 1		T = 300 K		ρ = 1.0 kg/m^3			Test: 2		T = 300 K			ρ = 1.0 kg/m^3		
D1 (N)	*D2 (N)*	*D3 (N)*	*V (m/s)*	*Re*	C_{d1}	C_{d2}	C_{d3}	*D1 (N)*	*D2 (N)*	*D3 (N)*	*V (m/s)*	*Re*	C_{d1}	C_{d2}	C_{d3}
1.63	3.81	10.96	42.2	2.4E+05	0.094	0.221	0.634	1.60	3.75	10.85	42.0	2.4E+05	0.093	0.219	0.634
1.46	3.49	10.12	40.4	2.3E+05	0.093	0.223	0.645	0.97	2.31	6.70	33.0	1.9E+05	0.092	0.219	0.635
0.96	2.30	6.79	33.1	1.9E+05	0.091	0.218	0.642	1.30	3.01	8.94	37.8	2.2E+05	0.094	0.218	0.647
2.10	4.92	14.00	48.6	2.8E+05	0.092	0.216	0.613	1.44	3.47	10.13	40.0	2.3E+05	0.093	0.225	0.656
1.92	4.43	12.85	45.5	2.6E+05	0.096	0.223	0.645	2.11	5.01	14.69	48.5	2.7E+05	0.093	0.222	0.650
1.69	4.12	11.94	44.0	2.5E+05	0.091	0.221	0.641	1.76	4.15	11.99	44.1	2.5E+05	0.094	0.222	0.642
1.26	2.98	8.86	38.1	2.2E+05	0.090	0.214	0.636	1.88	4.47	13.26	45.5	2.6E+05	0.094	0.224	0.665
2.12	5.05	14.72	48.4	2.8E+05	0.094	0.223	0.651	1.46	3.43	10.15	40.0	2.3E+05	0.094	0.222	0.657
1.70	4.10	12.13	44.0	2.5E+05	0.091	0.220	0.651	2.15	5.07	14.92	48.3	2.7E+05	0.096	0.226	0.664
1.47	3.52	10.03	40.4	2.3E+05	0.094	0.225	0.640	1.73	4.06	11.88	44.0	2.5E+05	0.093	0.219	0.640
0.97	2.31	6.81	33.1	1.9E+05	0.092	0.219	0.645	1.58	3.67	10.55	41.8	2.4E+05	0.094	0.219	0.630
1.85	4.35	12.76	45.3	2.6E+05	0.093	0.219	0.642	1.29	3.01	8.80	37.8	2.1E+05	0.094	0.219	0.640
1.31	3.09	9.09	37.7	2.1E+05	0.096	0.226	0.664	1.79	4.33	12.80	45.2	2.6E+05	0.091	0.220	0.649
1.61	3.75	10.94	42.0	2.4E+05	0.095	0.222	0.646	0.98	2.28	6.71	33.0	1.9E+05	0.094	0.218	0.642
Configuration: 0	Test: 1		T = 299 K		ρ = 1.0 kg/m^3			Test: 2		T = 299 K			ρ = 1.0 kg/m^3		
D1 (N)	*D2 (N)*	*D3 (N)*	*V (m/s)*	*Re*	C_{d1}	C_{d2}	C_{d3}	*D1 (N)*	*D2 (N)*	*D3 (N)*	*V (m/s)*	*Re*	C_{d1}	C_{d2}	C_{d3}
1.88	13.95	1.41	45.7	2.6E+05	0.093	0.690	0.070	1.91	13.98	1.31	45.6	2.6E+05	0.095	0.691	0.065
1.02	7.39	0.80	33.2	1.9E+05	0.095	0.692	0.075	1.06	7.65	0.76	33.3	1.9E+05	0.098	0.711	0.071
1.32	9.85	1.02	38.0	2.2E+05	0.095	0.707	0.073	1.34	9.90	0.96	38.0	2.2E+05	0.096	0.708	0.069
1.70	12.93	1.29	44.0	2.5E+05	0.091	0.690	0.069	1.64	12.03	1.13	42.1	2.4E+05	0.096	0.701	0.066
2.11	15.59	1.54	48.4	2.8E+05	0.093	0.691	0.068	2.16	16.09	1.51	48.4	2.8E+05	0.095	0.712	0.067
1.49	10.92	1.13	40.2	2.3E+05	0.096	0.700	0.072	1.76	13.09	1.29	44.3	2.5E+05	0.093	0.692	0.068
1.60	11.88	1.22	41.9	2.4E+05	0.094	0.702	0.072	1.52	10.95	1.08	40.3	2.3E+05	0.097	0.701	0.069
0.99	7.26	0.81	33.0	1.9E+05	0.094	0.690	0.077	1.34	9.88	0.98	37.8	2.2E+05	0.097	0.716	0.071
1.31	9.65	1.03	37.7	2.2E+05	0.096	0.703	0.075	1.61	11.89	1.15	41.9	2.4E+05	0.095	0.702	0.068
1.63	11.87	1.23	41.7	2.4E+05	0.097	0.705	0.073	1.95	14.28	1.38	45.4	2.6E+05	0.098	0.717	0.069
1.90	14.03	1.40	45.3	2.6E+05	0.096	0.709	0.071	1.52	10.98	1.08	40.0	2.3E+05	0.098	0.709	0.070
2.17	15.85	1.58	48.4	2.8E+05	0.096	0.701	0.070	1.00	7.28	0.74	33.0	1.9E+05	0.095	0.692	0.071
1.78	13.20	1.36	43.8	2.5E+05	0.096	0.710	0.073	2.15	15.91	1.45	48.5	2.8E+05	0.095	0.701	0.064
1.49	10.91	1.14	40.0	2.3E+05	0.097	0.708	0.074	1.82	13.16	1.29	43.9	2.5E+05	0.098	0.710	0.069
Configuration: 0	Test: 1		T = 300 K		ρ = 1.0 kg/m^3			Test: 2		T = 296 K			ρ = 1.0 kg/m^3		
D1 (N)	*D2 (N)*	*D3 (N)*	*V (m/s)*	*Re*	C_{d1}	C_{d2}	C_{d3}	*D1 (N)*	*D2 (N)*	*D3 (N)*	*V (m/s)*	*Re*	C_{d1}	C_{d2}	C_{d3}
1.62	1.26	9.29	37.9	2.2E+05	0.116	0.091	0.667	1.64	1.26	9.28	38.0	2.2E+05	0.115	0.089	0.653
1.27	0.95	7.04	33.0	1.9E+05	0.121	0.090	0.669	2.39	1.85	13.61	45.7	2.7E+05	0.117	0.091	0.668
2.37	1.85	13.68	45.6	2.6E+05	0.118	0.092	0.683	1.80	1.40	10.61	40.4	2.3E+05	0.113	0.088	0.667
2.19	1.72	12.79	44.0	2.5E+05	0.117	0.092	0.684	2.23	1.72	12.70	44.2	2.6E+05	0.117	0.090	0.667
1.86	1.43	10.68	40.2	2.3E+05	0.119	0.092	0.687	1.23	0.94	7.13	33.1	1.9E+05	0.116	0.088	0.669
2.67	2.06	15.30	48.5	2.7E+05	0.118	0.091	0.677	2.01	1.53	11.37	42.0	2.4E+05	0.116	0.089	0.659
2.08	1.59	11.80	42.3	2.4E+05	0.122	0.093	0.689	2.59	2.00	15.04	48.3	2.8E+05	0.114	0.088	0.662
1.23	0.94	7.05	33.0	1.9E+05	0.117	0.090	0.673	1.76	1.38	10.57	40.2	2.3E+05	0.112	0.088	0.672
2.23	1.76	13.64	45.4	2.6E+05	0.112	0.089	0.687	1.98	1.51	11.41	41.8	2.4E+05	0.117	0.089	0.671
1.99	1.55	11.63	41.9	2.4E+05	0.118	0.092	0.689	2.63	2.03	15.30	48.4	2.8E+05	0.115	0.089	0.672
1.61	1.25	9.25	37.9	2.1E+05	0.117	0.091	0.672	1.22	0.93	7.09	33.0	1.9E+05	0.115	0.088	0.670
1.89	1.42	10.70	40.2	2.3E+05	0.122	0.091	0.690	1.60	1.23	9.31	37.6	2.2E+05	0.116	0.089	0.674
2.70	2.08	15.43	48.6	2.7E+05	0.119	0.092	0.679	2.35	1.78	13.47	45.4	2.6E+05	0.117	0.089	0.672
2.20	1.67	12.64	44.0	2.5E+05	0.119	0.090	0.681	2.13	1.66	12.56	43.8	2.5E+05	0.114	0.089	0.673

Figure A.12: Wind tunnel results from partial loads tests with 53 ft. well cars. Re and C_d calculated with $L = 10.48cm$ and $A_D = 191.8cm^2$

Load Gap Results											
40 cm gap						20 cm gap					
F_D (lbs.)	T (K)	U (m/s)	ρ (kg/m^3)	Re	C_d	F_D (lbs.)	T (K)	U (m/s)	ρ (kg/m^3)	Re	C_d
0.97	290	33.365983	1.0	2.0E+05	0.397	1.61	291	45.214113	1.0	2.7E+05	0.359
1.32	289	38.288845	1.0	2.3E+05	0.407	1.74	291	46.721606	1.0	2.7E+05	0.364
1.47	290	40.742238	1.0	2.4E+05	0.402	0.88	291	33.939266	1.0	2.0E+05	0.350
1.62	290	42.714987	1.0	2.5E+05	0.404	1.16	291	38.734578	1.0	2.3E+05	0.353
1.79	290	44.602169	1.0	2.6E+05	0.409	1.45	291	42.990029	1.0	2.5E+05	0.357
1.92	290	46.323982	1.0	2.7E+05	0.406	1.96	292	49.631784	1.0	2.9E+05	0.363
2.18	290	49.065677	1.0	2.9E+05	0.411	1.31	292	41.138946	1.0	2.4E+05	0.354
F_D (lbs.)	T (K)	U (m/s)	ρ (kg/m^3)	Re	C_d	F_D (lbs.)	T (K)	U (m/s)	ρ (kg/m^3)	Re	C_d
0.97	290	33.321131	1.0	2.0E+05	0.398	1.15	288	39.13511	1.0	2.3E+05	0.343
1.28	291	38.294389	1.0	2.3E+05	0.397	1.30	289	41.577594	1.0	2.5E+05	0.342
1.49	290	40.840066	1.0	2.4E+05	0.405	1.42	289	43.359995	1.0	2.6E+05	0.345
1.62	290	42.640982	1.0	2.5E+05	0.404	1.90	289	50.011764	1.0	3.0E+05	0.346
1.77	290	44.550818	1.0	2.6E+05	0.406	1.67	290	47.159632	1.0	2.8E+05	0.344
1.90	291	46.133793	1.0	2.7E+05	0.406	1.57	290	45.525014	1.0	2.7E+05	0.346
2.16	291	49.218756	1.0	2.9E+05	0.407	0.84	290	33.783108	1.0	2.0E+05	0.336
F_D (lbs.)	T (K)	U (m/s)	ρ (kg/m^3)	Re	C_d	F_D (lbs.)	T (K)	U (m/s)	ρ (kg/m^3)	Re	C_d
0.98	290	33.500984	1.0	2.0E+05	0.399	1.59	290	45.716322	1.0	2.7E+05	0.348
1.31	291	38.449619	1.0	2.3E+05	0.403	1.70	290	47.144918	1.0	2.8E+05	0.350
1.47	291	40.851161	1.0	2.4E+05	0.403	1.31	291	41.669599	1.0	2.4E+05	0.346
1.61	291	42.663945	1.0	2.5E+05	0.402	1.92	291	50.130896	1.0	2.9E+05	0.351
1.79	291	44.771545	1.0	2.6E+05	0.407	1.41	291	43.335578	1.0	2.5E+05	0.345
1.90	290	46.251321	1.0	2.7E+05	0.404	0.85	291	34.011732	1.0	2.0E+05	0.336
2.16	291	49.301665	1.0	2.9E+05	0.405	1.11	291	38.906851	1.0	2.3E+05	0.337

Figure A.13: Wind tunnel results from container gap tests. Re and C_d calculated with $L = 10.48cm$ and $A_D = 191.8cm^2$

Load Gap Results											
12 cm gap						9 cm gap					
F_D (lbs.)	T (K)	U (m/s)	ρ (kg/m^3)	Re	C_d	F_D (lbs.)	T (K)	U (m/s)	ρ (kg/m^3)	Re	C_d
1.20	297	44.331667	1.0	2.5E+05	0.284	1.11	300	44.011517	1.0	2.5E+05	0.268
1.65	297	50.841457	1.0	2.9E+05	0.297	0.64	301	34.579094	1.0	1.9E+05	0.253
1.44	297	47.951807	1.0	2.7E+05	0.292	1.05	301	42.028274	1.0	2.3E+05	0.281
1.33	298	46.330055	1.0	2.6E+05	0.288	1.57	301	50.652575	1.0	2.8E+05	0.289
0.97	297	40.052748	1.0	2.3E+05	0.281	1.38	301	47.566823	1.0	2.6E+05	0.288
0.73	297	34.865771	1.0	2.0E+05	0.279	0.92	301	39.540544	1.0	2.2E+05	0.277
1.11	297	42.271998	1.0	2.4E+05	0.289	1.27	302	45.972328	1.0	2.5E+05	0.285
F_D (lbs.)	T (K)	U (m/s)	ρ (kg/m^3)	Re	C_d	F_D (lbs.)	T (K)	U (m/s)	ρ (kg/m^3)	Re	C_d
1.10	297	42.469845	1.0	2.4E+05	0.284	1.11	300	44.011517	1.0	2.5E+05	0.268
0.98	298	39.845981	1.0	2.3E+05	0.287	0.64	301	34.579094	1.0	1.9E+05	0.253
1.34	298	46.20954	1.0	2.6E+05	0.292	1.05	301	42.028274	1.0	2.3E+05	0.281
0.72	298	34.641225	1.0	2.0E+05	0.280	1.57	301	50.652575	1.0	2.8E+05	0.289
1.41	298	47.718116	1.0	2.7E+05	0.290	1.38	301	47.566823	1.0	2.6E+05	0.288
1.19	298	43.946131	1.0	2.5E+05	0.288	0.92	301	39.540544	1.0	2.2E+05	0.277
1.61	299	50.83338	1.0	2.9E+05	0.291	1.27	302	45.972328	1.0	2.5E+05	0.285
F_D (lbs.)	T (K)	U (m/s)	ρ (kg/m^3)	Re	C_d	F_D (lbs.)	T (K)	U (m/s)	ρ (kg/m^3)	Re	C_d
1.45	298	47.681962	1.0	2.7E+05	0.295	1.33	300	47.869181	1.0	2.7E+05	0.274
0.73	297	34.548372	1.0	2.0E+05	0.283	1.03	301	42.243072	1.0	2.4E+05	0.273
0.98	297	39.360156	1.0	2.2E+05	0.291	1.55	301	50.691549	1.0	2.8E+05	0.284
1.20	298	43.721889	1.0	2.5E+05	0.291	1.30	301	45.972232	1.0	2.6E+05	0.289
1.33	298	45.843901	1.0	2.6E+05	0.294	1.15	301	43.788236	1.0	2.4E+05	0.283
1.09	298	41.719493	1.0	2.4E+05	0.290	0.94	301	39.497318	1.0	2.2E+05	0.283
1.61	299	50.749017	1.0	2.9E+05	0.291	0.67	301	34.454088	1.0	1.9E+05	0.265

Figure A.14: Wind tunnel results from container gap tests. Re and C_d calculated with $L = 10.48cm$ and $A_D = 191.8cm^2$

Load Gap Results											
5 cm gap						1 cm gap					
F_D (lbs.)	T (K)	U (m/s)	ρ (kg/m^3)	Re	C_d	F_D (lbs.)	T (K)	U (m/s)	ρ (kg/m^3)	Re	C_d
0.66	292	39.355807	1.0	2.3E+05	0.198	0.81	291	50.654474	1.0	3.0E+05	0.145
0.48	292	34.027819	1.0	2.0E+05	0.190	0.71	292	47.773072	1.0	2.8E+05	0.144
0.91	292	45.771949	1.0	2.6E+05	0.202	0.59	292	44.006805	1.0	2.6E+05	0.140
1.12	293	50.28558	1.0	2.9E+05	0.205	0.53	292	42.110955	1.0	2.4E+05	0.137
0.83	293	43.58529	1.0	2.5E+05	0.203	0.46	292	39.447743	1.0	2.3E+05	0.135
0.75	293	41.62742	1.0	2.4E+05	0.201	0.68	293	45.930297	1.0	2.7E+05	0.149
1.00	293	47.178356	1.0	2.7E+05	0.209	0.34	292	34.211063	1.0	2.0E+05	0.132
F_D (lbs.)	T (K)	U (m/s)	ρ (kg/m^3)	Re	C_d	F_D (lbs.)	T (K)	U (m/s)	ρ (kg/m^3)	Re	C_d
0.61	295	34.09665	1.0	2.0E+05	0.240	0.66	290	46.2555	1.0	2.7E+05	0.142
0.86	293	39.328227	1.0	2.3E+05	0.256	0.35	291	34.69428	1.0	2.0E+05	0.135
1.04	295	41.666823	1.0	2.4E+05	0.275	0.80	291	50.749482	1.0	3.0E+05	0.143
1.17	295	43.577136	1.0	2.5E+05	0.283	0.47	292	39.799678	1.0	2.3E+05	0.136
1.26	294	45.788671	1.0	2.7E+05	0.276	0.54	292	42.033453	1.0	2.4E+05	0.141
1.32	295	47.212673	1.0	2.7E+05	0.273	0.70	292	47.722584	1.0	2.8E+05	0.143
						0.58	292	43.988254	1.0	2.6E+05	0.139
F_D (lbs.)	T (K)	U (m/s)	ρ (kg/m^3)	Re	C_d	F_D (lbs.)	T (K)	U (m/s)	ρ (kg/m^3)	Re	C_d
0.65	295	34.137601	1.0	2.0E+05	0.258	0.58	290	44.240441	1.0	2.6E+05	0.137
0.88	296	39.32161	1.0	2.3E+05	0.265	0.70	290	47.867923	1.0	2.8E+05	0.140
1.04	296	41.877119	1.0	2.4E+05	0.274	0.35	291	34.694401	1.0	2.0E+05	0.133
1.10	294	43.739429	1.0	2.5E+05	0.265	0.79	291	50.680158	1.0	3.0E+05	0.142
1.18	296	45.732945	1.0	2.6E+05	0.261	0.54	291	42.157054	1.0	2.5E+05	0.139
1.36	296	47.040241	1.0	2.7E+05	0.285	0.47	291	39.561485	1.0	2.3E+05	0.137
1.52	296	50.266191	1.0	2.9E+05	0.278	0.65	291	46.001951	1.0	2.7E+05	0.141

Figure A.15: Wind tunnel results from container gap tests. Re and C_d calculated with $L = 10.48cm$ and $A_D = 191.8cm^2$

Mixed Loading Results

Configuration: 0	Test: 1		T = 298 K		ρ = 0.99 kg/m^3			Test: 2		T = 296 K			ρ = 0.99 kg/m^3		
D1 (N)	*D2 (N)*	*D3 (N)*	*V (m/s)*	*Re*	C_{d1}	C_{d2}	C_{d3}	*D1 (N)*	*D2 (N)*	*D3 (N)*	*V (m/s)*	*Re*	C_{d1}	C_{d2}	C_{d3}
4.01	4.27	3.99	43.2	2.4E+05	0.225	0.240	0.224	3.73	4.02	3.79	41.5	2.4E+05	0.227	0.244	0.230
4.61	4.95	4.62	46.8	2.6E+05	0.222	0.238	0.222	4.04	4.34	4.12	43.2	2.5E+05	0.227	0.243	0.231
2.46	2.69	2.44	34.0	1.9E+05	0.224	0.245	0.223	5.26	5.49	5.31	49.7	2.8E+05	0.223	0.233	0.226
5.23	5.56	5.27	49.8	2.8E+05	0.223	0.237	0.225	3.24	3.50	3.35	39.2	2.2E+05	0.222	0.239	0.229
3.66	3.91	3.64	41.6	2.3E+05	0.224	0.240	0.223	2.48	2.64	2.48	34.1	1.9E+05	0.224	0.238	0.224
3.15	3.41	3.19	38.9	2.2E+05	0.221	0.238	0.223	4.76	5.11	4.90	47.2	2.7E+05	0.224	0.241	0.231
4.28	4.53	4.23	45.2	2.5E+05	0.222	0.235	0.219	4.45	4.63	4.45	45.3	2.6E+05	0.228	0.237	0.228
3.19	3.44	3.17	39.0	2.2E+05	0.222	0.240	0.220	2.49	2.63	2.50	33.9	1.9E+05	0.227	0.240	0.228
2.41	2.62	2.43	33.9	1.9E+05	0.221	0.241	0.223	5.31	5.60	5.38	49.6	2.8E+05	0.227	0.239	0.230
3.60	3.91	3.61	41.1	2.3E+05	0.225	0.244	0.225	3.18	3.44	3.26	38.7	2.2E+05	0.223	0.241	0.229
4.36	4.63	4.31	45.2	2.5E+05	0.225	0.239	0.223	4.46	4.67	4.42	45.1	2.6E+05	0.230	0.241	0.228
3.86	4.12	3.84	43.0	2.4E+05	0.221	0.236	0.220	3.70	3.89	3.67	41.2	2.3E+05	0.229	0.241	0.227
5.27	5.53	5.20	49.6	2.8E+05	0.227	0.238	0.224	4.70	4.98	4.70	46.5	2.6E+05	0.228	0.242	0.228
4.59	4.90	4.59	46.8	2.6E+05	0.223	0.238	0.223	4.04	4.24	4.04	43.0	2.4E+05	0.230	0.241	0.230
Configuration: 0	Test: 1		T = 298 K		ρ = 0.99 kg/m^3			Test: 2		T = 296 K			ρ = 0.99 kg/m^3		
D1 (N)	*D2 (N)*	*D3 (N)*	*V (m/s)*	*Re*	C_{d1}	C_{d2}	C_{d3}	*D1 (N)*	*D2 (N)*	*D3 (N)*	*V (m/s)*	*Re*	C_{d1}	C_{d2}	C_{d3}
4.92	4.19	3.65	47.2	2.7E+05	0.231	0.196	0.171	4.46	3.85	3.34	45.4	2.6E+05	0.225	0.195	0.169
3.35	2.93	2.59	39.3	2.2E+05	0.227	0.199	0.175	2.55	2.22	1.91	34.1	1.9E+05	0.229	0.199	0.171
2.49	2.21	1.89	34.1	1.9E+05	0.224	0.199	0.170	4.85	4.09	3.61	46.8	2.7E+05	0.231	0.195	0.172
5.44	4.64	4.15	50.0	2.8E+05	0.228	0.194	0.174	3.27	2.83	2.48	39.2	2.2E+05	0.222	0.193	0.169
3.82	3.26	2.83	41.6	2.3E+05	0.231	0.197	0.172	5.46	4.59	4.07	49.7	2.8E+05	0.231	0.194	0.172
4.00	3.53	3.09	43.2	2.4E+05	0.224	0.198	0.173	3.73	3.19	2.80	41.5	2.3E+05	0.226	0.193	0.170
4.51	3.91	3.41	45.5	2.6E+05	0.228	0.198	0.173	4.05	3.48	3.03	43.2	2.4E+05	0.228	0.195	0.171
5.28	4.52	4.01	49.6	2.8E+05	0.226	0.193	0.171	3.24	2.80	2.44	38.9	2.2E+05	0.224	0.194	0.169
2.51	2.26	1.94	34.1	1.9E+05	0.226	0.204	0.175	5.37	4.49	3.98	49.6	2.8E+05	0.228	0.191	0.169
3.25	2.91	2.51	38.9	2.2E+05	0.225	0.202	0.174	4.75	3.99	3.53	46.9	2.6E+05	0.227	0.191	0.169
4.44	3.89	3.40	45.4	2.6E+05	0.226	0.198	0.173	3.69	3.11	2.73	41.2	2.3E+05	0.228	0.192	0.169
3.68	3.27	2.81	41.3	2.3E+05	0.226	0.201	0.172	4.35	3.68	3.31	45.1	2.5E+05	0.225	0.190	0.171
3.97	3.46	3.01	42.9	2.4E+05	0.226	0.197	0.171	2.42	2.13	1.86	33.7	1.9E+05	0.224	0.197	0.171
4.70	4.10	3.53	46.7	2.6E+05	0.226	0.197	0.170	4.04	3.49	3.05	42.9	2.4E+05	0.230	0.198	0.174
Configuration: 0	Test: 1		T = 298 K		ρ = 0.99 kg/m^3			Test: 2		T = 296 K			ρ = 0.99 kg/m^3		
D1 (N)	*D2 (N)*	*D3 (N)*	*V (m/s)*	*Re*	C_{d1}	C_{d2}	C_{d3}	*D1 (N)*	*D2 (N)*	*D3 (N)*	*V (m/s)*	*Re*	C_{d1}	C_{d2}	C_{d3}
3.92	3.89	4.00	47.2	2.7E+05	0.183	0.181	0.187	2.65	2.63	2.74	38.6	2.2E+05	0.185	0.184	0.192
4.50	4.42	4.47	49.9	2.8E+05	0.188	0.185	0.187	3.91	3.79	3.97	46.8	2.7E+05	0.186	0.180	0.188
2.06	2.14	2.13	34.4	2.0E+05	0.181	0.188	0.188	3.29	3.27	3.39	43.2	2.5E+05	0.184	0.183	0.189
3.85	3.67	3.74	45.7	2.6E+05	0.192	0.184	0.187	1.99	2.00	2.06	33.6	1.9E+05	0.184	0.185	0.191
3.07	3.03	3.08	41.6	2.4E+05	0.185	0.183	0.185	4.39	4.22	4.39	49.4	2.8E+05	0.187	0.180	0.187
2.77	2.72	2.74	39.0	2.2E+05	0.190	0.186	0.188	3.60	3.56	3.70	45.3	2.6E+05	0.183	0.181	0.188
3.40	3.33	3.36	43.3	2.5E+05	0.190	0.186	0.188	3.01	3.01	3.08	41.1	2.3E+05	0.185	0.186	0.190
4.39	4.27	4.41	49.7	2.8E+05	0.186	0.181	0.187	3.26	3.25	3.32	42.9	2.4E+05	0.185	0.184	0.188
3.35	3.30	3.36	43.3	2.4E+05	0.187	0.185	0.188	3.67	3.58	3.67	45.1	2.6E+05	0.188	0.184	0.188
2.72	2.72	2.75	39.0	2.2E+05	0.187	0.187	0.189	3.84	3.80	3.90	46.7	2.6E+05	0.184	0.182	0.187
4.00	3.94	3.98	47.0	2.7E+05	0.189	0.186	0.188	2.93	2.95	3.01	41.1	2.3E+05	0.181	0.182	0.186
3.04	3.04	3.05	41.4	2.3E+05	0.186	0.186	0.187	2.55	2.63	2.67	38.5	2.2E+05	0.179	0.185	0.188
2.00	2.05	2.03	33.8	1.9E+05	0.183	0.187	0.185	4.34	4.31	4.47	49.6	2.8E+05	0.184	0.183	0.189
3.71	3.64	3.72	45.3	2.6E+05	0.189	0.185	0.189	1.94	2.02	2.01	33.6	1.9E+05	0.180	0.187	0.187

Figure A.16: Wind tunnel results from mixed loads tests. Re and C_d calculated with $L = 10.48cm$ and $A_D = 191.8cm^2$

Arrowedge Results											
First Well Car without the Arrowedge						First Well Car with the Arrowedge					
F_D (N)	T (K)	U (m/s)	ρ (kg/m^3)	Re	C_d	F_D (N)	T (K)	U (m/s)	ρ (kg/m^3)	Re	C_d
13.09	301	49.1	0.98	2.7E+05	0.574	5.39	300	45.8	0.98	2.5E+05	0.242
14.01	301	50.3	0.98	2.8E+05	0.587	6.17	301	49.0	0.98	2.7E+05	0.245
2.66	301	23.8	0.99	1.3E+05	0.497	2.70	300	31.9	0.98	1.8E+05	0.238
10.78	301	44.8	0.98	2.5E+05	0.570	1.31	300	21.8	0.98	1.2E+05	0.232
11.47	302	46.2	0.98	2.6E+05	0.570	5.03	301	44.1	0.98	2.4E+05	0.244
8.82	302	40.8	0.98	2.3E+05	0.563	4.49	300	41.6	0.98	2.3E+05	0.242
9.59	302	42.5	0.98	2.3E+05	0.565	6.69	301	50.1	0.98	2.8E+05	0.255
5.70	302	33.2	0.98	1.8E+05	0.548	4.10	301	40.0	0.98	2.2E+05	0.239
7.56	302	38.0	0.98	2.1E+05	0.557	3.61	301	37.2	0.98	2.1E+05	0.241
F_D (N)	T (K)	U (m/s)	ρ (kg/m^3)	Re	C_d	F_D (N)	T (K)	U (m/s)	ρ (kg/m^3)	Re	C_d
3.11	299	23.7	0.99	1.3E+05	0.580	2.21	301	27.7	0.99	1.5E+05	0.303
11.17	300	44.7	0.99	2.5E+05	0.589	6.54	302	49.3	0.98	2.7E+05	0.285
8.17	301	38.5	0.99	2.1E+05	0.582	4.04	302	38.4	0.98	2.1E+05	0.292
9.19	301	40.6	0.99	2.3E+05	0.588	1.68	302	23.7	0.98	1.3E+05	0.316
13.21	301	49.2	0.99	2.7E+05	0.578	7.01	303	50.4	0.98	2.8E+05	0.294
6.06	301	33.3	0.99	1.9E+05	0.578	5.44	303	44.8	0.98	2.5E+05	0.288
9.74	301	42.4	0.99	2.4E+05	0.573	4.89	303	42.5	0.98	2.3E+05	0.288
14.24	302	50.3	0.98	2.8E+05	0.596	5.73	303	46.1	0.98	2.5E+05	0.287
11.61	302	46.0	0.98	2.5E+05	0.582	4.43	303	40.6	0.98	2.2E+05	0.286
F_D (N)	T (K)	U (m/s)	ρ (kg/m^3)	Re	C_d	F_D (N)	T (K)	U (m/s)	ρ (kg/m^3)	Re	C_d
10.98	300	43.6	0.98	2.4E+05	0.532	5.69	298	46.6	0.99	2.6E+05	0.275
13.19	301	48.4	0.98	2.7E+05	0.529	3.86	298	38.8	0.99	2.2E+05	0.270
14.29	302	49.8	0.98	2.7E+05	0.544	6.76	299	50.1	0.99	2.8E+05	0.283
8.86	301	39.6	0.98	2.2E+05	0.516	5.24	299	45.0	0.99	2.5E+05	0.273
11.58	302	45.2	0.98	2.5E+05	0.530	4.71	300	42.8	0.99	2.4E+05	0.271
7.80	302	36.8	0.98	2.0E+05	0.521	1.39	299	23.9	0.99	1.3E+05	0.255
5.81	301	31.2	0.98	1.7E+05	0.523	6.36	300	49.4	0.99	2.8E+05	0.274
9.67	302	41.1	0.98	2.3E+05	0.528	4.29	300	41.0	0.99	2.3E+05	0.270
2.93	301	21.4	0.98	1.2E+05	0.516	2.83	300	33.6	0.99	1.9E+05	0.265

Figure A.17: Wind tunnel results from Arrowedge tests. Re and C_d calculated with $L = 10.48cm$ and $A_D = 191.8cm^2$

Trailers Results											
Configuration: 1						Configuration: 2					
Test: 1	$T = 300\ K$		$\rho = 0.99\ kg/m^3$			Test: 1	$T = 300\ K$		$\rho = 0.99\ kg/m^3$		
F_{D1} (N)	F_{D2} (N)	U (m/s)	Re	C_{d1}	C_{d2}	F_{D1} (N)	F_{D2} (N)	U (m/s)	Re	C_{d1}	C_{d2}
9.08	7.71	49.2	2.7E+05	0.396	0.336	6.49	5.56	42.5	2.4E+05	0.379	0.325
6.51	5.60	41.0	2.3E+05	0.409	0.352	5.36	4.57	38.4	2.1E+05	0.386	0.329
5.69	4.94	38.5	2.1E+05	0.406	0.353	7.26	6.05	44.4	2.5E+05	0.390	0.325
4.20	3.70	33.7	1.9E+05	0.392	0.345	4.10	3.46	33.2	1.8E+05	0.393	0.331
8.06	7.00	46.4	2.6E+05	0.398	0.346	8.16	6.57	45.9	2.5E+05	0.411	0.331
6.74	5.84	42.6	2.4E+05	0.393	0.341	8.92	7.37	49.0	2.7E+05	0.394	0.325
7.33	6.43	44.6	2.5E+05	0.390	0.342	5.92	5.11	40.5	2.3E+05	0.382	0.329
5.47	4.84	38.6	2.1E+05	0.390	0.345	7.57	6.46	45.8	2.5E+05	0.382	0.325
8.80	7.71	49.2	2.7E+05	0.385	0.338	6.43	5.49	42.3	2.3E+05	0.380	0.324
6.20	5.46	40.9	2.3E+05	0.393	0.346	7.17	5.94	44.4	2.5E+05	0.386	0.320
4.36	3.76	33.5	1.9E+05	0.412	0.355	6.07	5.14	40.3	2.2E+05	0.395	0.334
7.69	6.88	46.1	2.6E+05	0.383	0.342	5.24	4.53	38.0	2.1E+05	0.385	0.333
6.92	6.00	42.7	2.4E+05	0.404	0.350	8.72	7.40	49.0	2.7E+05	0.386	0.327
7.30	6.34	44.6	2.5E+05	0.390	0.339						
Test: 2	$T = 300\ K$		$\rho = 0.99\ kg/m^3$			Test: 2	$T = 300\ K$		$\rho = 0.99\ kg/m^3$		
F_{D1} (N)	F_{D2} (N)	U (m/s)	Re	C_{d1}	C_{d2}	F_{D1} (N)	F_{D2} (N)	U (m/s)	Re	C_{d1}	C_{d2}
7.03	5.80	43.0	2.4E+05	0.400	0.330	7.60	6.55	46.1	2.6E+05	0.376	0.324
9.17	7.65	49.4	2.8E+05	0.398	0.332	6.05	5.07	40.8	2.3E+05	0.385	0.322
4.38	3.74	34.1	1.9E+05	0.399	0.340	5.64	4.71	38.3	2.1E+05	0.405	0.338
8.27	6.95	46.5	2.6E+05	0.405	0.340	8.84	7.57	49.1	2.7E+05	0.388	0.332
6.51	5.55	41.2	2.3E+05	0.405	0.345	4.06	3.51	33.4	1.9E+05	0.383	0.331
5.66	4.78	38.6	2.2E+05	0.400	0.338	7.39	6.23	44.5	2.5E+05	0.394	0.332
8.10	6.59	44.9	2.5E+05	0.426	0.347	6.75	5.60	42.4	2.4E+05	0.397	0.330
5.68	4.82	38.6	2.2E+05	0.403	0.341	4.20	3.55	33.4	1.9E+05	0.398	0.337
7.58	6.47	44.8	2.5E+05	0.400	0.341	7.18	6.06	44.4	2.5E+05	0.386	0.325
4.29	3.67	33.6	1.9E+05	0.401	0.343	8.92	7.55	49.0	2.7E+05	0.394	0.333
6.37	5.30	41.0	2.3E+05	0.402	0.335	7.68	6.56	46.0	2.6E+05	0.385	0.329
6.83	5.77	42.8	2.4E+05	0.395	0.334	5.25	4.59	38.1	2.1E+05	0.382	0.333
8.20	6.69	46.3	2.6E+05	0.405	0.331	6.50	5.60	42.5	2.4E+05	0.381	0.328
9.42	7.73	49.3	2.7E+05	0.411	0.337	5.89	5.13	40.5	2.2E+05	0.380	0.331
Test: 3	$T = 300\ K$		$\rho = 0.99\ kg/m^3$			Test: 3	$T = 300\ K$		$\rho = 0.99\ kg/m^3$		
F_{D1} (N)	F_{D2} (N)	U (m/s)	Re	C_{d1}	C_{d2}	F_{D1} (N)	F_{D2} (N)	U (m/s)	Re	C_{d1}	C_{d2}
5.54	4.68	38.5	2.2E+05	0.394	0.333	5.49	4.55	38.8	2.2E+05	0.385	0.319
7.60	6.48	44.8	2.5E+05	0.402	0.342	6.64	5.75	42.9	2.4E+05	0.382	0.331
6.89	6.08	42.7	2.4E+05	0.402	0.354	7.96	6.73	46.6	2.6E+05	0.389	0.329
9.10	7.85	49.0	2.7E+05	0.402	0.347	8.82	7.44	49.2	2.7E+05	0.387	0.327
8.03	6.96	46.2	2.6E+05	0.400	0.347	6.06	5.36	41.1	2.3E+05	0.381	0.337
4.19	3.86	33.6	1.9E+05	0.394	0.363	7.21	6.27	45.1	2.5E+05	0.378	0.328
6.27	5.48	40.7	2.3E+05	0.402	0.352	4.38	3.69	33.9	1.9E+05	0.406	0.342
9.11	7.77	49.1	2.7E+05	0.401	0.343	6.60	5.40	40.8	2.3E+05	0.420	0.343
4.18	3.74	33.6	1.9E+05	0.394	0.353	5.41	4.70	38.5	2.1E+05	0.388	0.337
6.94	5.99	42.5	2.3E+05	0.408	0.353	8.97	7.61	49.2	2.7E+05	0.394	0.334
6.27	5.30	40.6	2.3E+05	0.404	0.341	6.89	5.80	42.8	2.4E+05	0.399	0.336
5.63	5.00	38.4	2.1E+05	0.406	0.360	7.36	6.21	44.9	2.5E+05	0.390	0.329
7.41	6.46	44.5	2.5E+05	0.399	0.348	8.04	6.79	46.2	2.6E+05	0.401	0.338
7.82	6.86	46.2	2.5E+05	0.391	0.343	4.08	3.51	33.7	1.9E+05	0.383	0.329

Figure A.18: Wind tunnel results from semitrailer tests. *Re* and C_d calculated with $L = 10.48cm$ and $A_D = 191.8cm^2$

Trailers Results											
Configuration: 3						Configuration: 4					
Test: 1	$T = 300\ K$		$\rho = 0.99\ kg/m^3$			Test: 1	$T = 300\ K$		$\rho = 0.99\ kg/m^3$		
F_{D1} (N)	F_{D2} (N)	U (m/s)	Re	C_{d1}	C_{d2}	F_{D1} (N)	F_{D2} (N)	U (m/s)	Re	C_{d1}	C_{d2}
9.68	7.26	45.0	2.5E+05	0.501	0.376	9.28	7.11	46.1	2.6E+05	0.462	0.354
7.57	5.83	41.1	2.3E+05	0.471	0.362	6.52	4.94	38.6	2.1E+05	0.465	0.352
5.13	4.02	33.8	1.9E+05	0.471	0.370	5.14	3.86	33.5	1.9E+05	0.486	0.365
8.23	6.28	42.8	2.4E+05	0.472	0.360	10.73	7.87	49.0	2.7E+05	0.474	0.348
6.77	5.20	38.4	2.2E+05	0.481	0.370	7.89	6.03	42.5	2.4E+05	0.462	0.353
9.85	7.38	46.1	2.6E+05	0.487	0.365	7.38	5.47	40.6	2.2E+05	0.475	0.352
10.86	8.41	48.9	2.7E+05	0.478	0.370	8.76	6.56	44.7	2.5E+05	0.466	0.349
7.03	5.36	38.3	2.1E+05	0.503	0.383	7.39	5.57	40.6	2.3E+05	0.474	0.358
10.90	8.52	49.2	2.8E+05	0.474	0.370	6.58	4.86	38.2	2.1E+05	0.477	0.353
10.22	7.48	46.1	2.6E+05	0.506	0.371	8.81	6.47	44.4	2.5E+05	0.474	0.349
8.04	6.35	42.8	2.4E+05	0.464	0.366	10.53	7.83	49.0	2.7E+05	0.466	0.346
7.45	5.89	40.7	2.3E+05	0.474	0.375	9.17	6.92	46.0	2.5E+05	0.462	0.349
5.18	4.04	33.5	1.9E+05	0.487	0.380	7.87	5.88	42.3	2.3E+05	0.466	0.348
8.90	6.77	44.5	2.5E+05	0.474	0.360	4.92	3.63	33.4	1.8E+05	0.469	0.345
Test: 2	$T = 300\ K$		$\rho = 0.99\ kg/m^3$			Test: 2	$T = 300\ K$		$\rho = 0.99\ kg/m^3$		
F_{D1} (N)	F_{D2} (N)	U (m/s)	Re	C_{d1}	C_{d2}	F_{D1} (N)	F_{D2} (N)	U (m/s)	Re	C_{d1}	C_{d2}
9.70	7.18	46.1	2.6E+05	0.479	0.355	6.39	4.79	38.4	2.1E+05	0.457	0.342
11.30	8.14	48.8	2.7E+05	0.501	0.361	10.30	7.94	49.2	2.7E+05	0.451	0.347
6.67	5.21	38.4	2.1E+05	0.476	0.372	9.52	6.93	46.2	2.5E+05	0.474	0.345
7.95	5.73	40.5	2.3E+05	0.511	0.368	4.90	3.80	33.7	1.9E+05	0.458	0.355
5.09	3.76	33.2	1.9E+05	0.487	0.360	7.91	6.02	42.6	2.4E+05	0.462	0.352
9.48	6.90	44.2	2.5E+05	0.510	0.372	8.83	6.52	44.5	2.5E+05	0.473	0.350
8.21	5.91	42.3	2.4E+05	0.483	0.347	7.64	5.63	40.8	2.3E+05	0.485	0.357
11.40	8.04	48.9	2.7E+05	0.505	0.356	9.18	6.95	46.0	2.5E+05	0.460	0.348
9.79	7.09	45.9	2.6E+05	0.490	0.355	10.75	7.93	49.2	2.7E+05	0.473	0.349
9.45	6.87	44.4	2.5E+05	0.506	0.368	8.04	6.11	42.5	2.4E+05	0.472	0.358
6.60	4.96	38.2	2.1E+05	0.478	0.359	6.40	4.99	38.3	2.1E+05	0.462	0.360
8.11	6.03	42.3	2.4E+05	0.479	0.356	8.59	6.67	44.3	2.4E+05	0.465	0.360
5.06	3.71	33.2	1.9E+05	0.484	0.356	4.89	3.75	33.3	1.8E+05	0.467	0.358
7.67	5.54	40.3	2.2E+05	0.499	0.360	7.21	5.31	40.5	2.2E+05	0.468	0.344
Test: 3	$T = 300\ K$		$\rho = 0.99\ kg/m^3$			Test: 3	$T = 300\ K$		$\rho = 0.99\ kg/m^3$		
F_{D1} (N)	F_{D2} (N)	U (m/s)	Re	C_{d1}	C_{d2}	F_{D1} (N)	F_{D2} (N)	U (m/s)	Re	C_{d1}	C_{d2}
8.46	6.29	42.6	2.4E+05	0.492	0.366	9.79	7.12	46.2	2.6E+05	0.485	0.353
10.02	7.24	46.2	2.5E+05	0.499	0.360	8.97	6.61	44.9	2.5E+05	0.473	0.348
7.63	5.72	41.0	2.3E+05	0.482	0.361	6.70	4.91	38.6	2.1E+05	0.478	0.350
5.26	4.06	33.6	1.9E+05	0.494	0.381	10.53	8.00	49.2	2.7E+05	0.463	0.352
6.82	5.14	38.5	2.1E+05	0.487	0.367	7.48	5.68	40.9	2.3E+05	0.475	0.360
9.07	6.99	44.7	2.5E+05	0.482	0.371	5.05	3.89	33.6	1.9E+05	0.473	0.364
10.91	8.41	49.2	2.7E+05	0.478	0.368	8.04	6.14	42.5	2.4E+05	0.472	0.360
7.79	5.85	40.9	2.3E+05	0.494	0.371	11.17	7.92	49.1	2.7E+05	0.492	0.349
8.23	6.25	42.4	2.4E+05	0.484	0.367	7.22	5.58	40.7	2.2E+05	0.463	0.358
11.28	8.39	49.0	2.7E+05	0.498	0.371	8.81	6.53	44.7	2.5E+05	0.470	0.349
9.81	7.44	46.0	2.5E+05	0.493	0.374	5.15	3.88	33.5	1.8E+05	0.487	0.367
6.74	5.33	38.5	2.1E+05	0.483	0.382	8.01	5.84	42.3	2.3E+05	0.475	0.346
9.15	6.89	44.4	2.5E+05	0.492	0.370	9.39	6.96	46.1	2.5E+05	0.472	0.350
5.29	4.11	33.6	1.9E+05	0.498	0.386	6.39	4.89	38.4	2.1E+05	0.461	0.353

Figure A.19: Wind tunnel results from semi-trailer tests. Re and C_d calculated with $L = 10.48cm$ and $A_D = 191.8cm^2$

Trailers With Side Skirts Results											
Configuration: 1s						Configuration: 2s					
Test: 1	$T = 300\ K$		$\rho = 0.99\ kg/m^3$			Test: 1	$T = 300\ K$		$\rho = 0.99\ kg/m^3$		
F_{D1} (N)	F_{D2} (N)	U (m/s)	Re	C_{d1}	C_{d2}	F_{D1} (N)	F_{D2} (N)	U (m/s)	Re	C_{d1}	C_{d2}
5.41	4.50	38.2	2.2E+05	0.385	0.321	7.46	6.09	44.9	2.6E+05	0.384	0.313
4.15	3.39	33.4	1.9E+05	0.389	0.317	4.15	3.44	33.8	1.9E+05	0.379	0.314
9.14	7.35	48.9	2.8E+05	0.399	0.321	5.54	4.45	38.5	2.2E+05	0.389	0.313
8.02	6.61	46.1	2.6E+05	0.395	0.326	6.21	4.95	40.8	2.3E+05	0.388	0.309
6.80	5.68	42.5	2.4E+05	0.395	0.330	6.55	5.24	42.6	2.4E+05	0.376	0.300
6.22	5.10	40.5	2.3E+05	0.397	0.325	9.15	7.26	49.4	2.8E+05	0.392	0.311
7.52	6.15	44.4	2.5E+05	0.400	0.327	8.16	6.60	46.3	2.6E+05	0.397	0.321
8.42	6.58	45.9	2.6E+05	0.419	0.327	6.78	5.50	42.6	2.4E+05	0.390	0.316
7.34	6.08	44.4	2.5E+05	0.391	0.324	5.82	4.89	40.7	2.3E+05	0.367	0.308
6.22	5.07	40.5	2.3E+05	0.398	0.324	7.94	6.48	45.9	2.6E+05	0.394	0.321
6.90	5.54	42.1	2.4E+05	0.409	0.329	5.51	4.50	38.2	2.2E+05	0.395	0.323
4.21	3.46	33.1	1.9E+05	0.402	0.330	8.81	7.20	49.1	2.8E+05	0.382	0.313
5.43	4.46	37.9	2.1E+05	0.395	0.324	4.07	3.50	33.3	1.9E+05	0.383	0.329
8.85	7.33	49.1	2.8E+05	0.386	0.319	7.26	5.95	44.4	2.5E+05	0.386	0.316
Test: 2	$T = 300\ K$		$\rho = 0.99\ kg/m^3$			Test: 2	$T = 300\ K$		$\rho = 0.99\ kg/m^3$		
F_{D1} (N)	F_{D2} (N)	U (m/s)	Re	C_{d1}	C_{d2}	F_{D1} (N)	F_{D2} (N)	U (m/s)	Re	C_{d1}	C_{d2}
5.64	4.54	38.4	2.2E+05	0.395	0.318	5.35	4.39	38.6	2.2E+05	0.373	0.306
8.11	6.55	46.3	2.6E+05	0.395	0.319	7.90	6.36	46.3	2.6E+05	0.385	0.310
4.34	3.50	33.8	1.9E+05	0.397	0.320	5.95	5.02	40.8	2.3E+05	0.374	0.316
7.06	5.54	42.7	2.4E+05	0.404	0.317	7.38	6.04	44.7	2.5E+05	0.386	0.316
6.46	5.11	40.9	2.3E+05	0.404	0.319	8.81	7.15	48.9	2.8E+05	0.385	0.313
7.85	6.27	44.6	2.5E+05	0.412	0.329	6.55	5.48	42.7	2.4E+05	0.377	0.316
9.03	7.27	49.1	2.8E+05	0.392	0.316	4.09	3.44	33.5	1.9E+05	0.382	0.321
8.12	6.53	46.2	2.6E+05	0.399	0.321	7.84	6.41	46.1	2.6E+05	0.386	0.315
6.35	5.18	40.8	2.3E+05	0.400	0.327	7.39	5.96	44.5	2.5E+05	0.392	0.316
4.24	3.42	33.3	1.9E+05	0.398	0.322	5.17	4.40	38.2	2.2E+05	0.370	0.315
7.62	6.05	44.5	2.5E+05	0.403	0.320	6.62	5.45	42.6	2.4E+05	0.382	0.314
5.52	4.51	38.1	2.2E+05	0.397	0.324	8.74	7.27	48.9	2.8E+05	0.383	0.319
6.72	5.50	42.4	2.4E+05	0.391	0.320	6.11	5.02	40.7	2.3E+05	0.387	0.318
9.03	7.22	49.0	2.8E+05	0.394	0.315	4.09	3.38	33.4	1.9E+05	0.385	0.318
Test: 3	$T = 300\ K$		$\rho = 0.99\ kg/m^3$			Test: 3	$T = 300\ K$		$\rho = 0.99\ kg/m^3$		
F_{D1} (N)	F_{D2} (N)	U (m/s)	Re	C_{d1}	C_{d2}	F_{D1} (N)	F_{D2} (N)	U (m/s)	Re	C_{d1}	C_{d2}
5.93	4.78	40.4	2.3E+05	0.379	0.306	8.56	7.17	49.4	2.8E+05	0.367	0.307
8.00	6.39	46.0	2.6E+05	0.397	0.318	4.26	3.44	33.8	1.9E+05	0.391	0.316
6.91	5.51	42.3	2.4E+05	0.407	0.324	5.33	4.41	38.5	2.2E+05	0.378	0.312
8.78	7.27	49.1	2.8E+05	0.382	0.316	6.12	5.04	40.8	2.3E+05	0.384	0.316
4.17	3.45	33.4	1.9E+05	0.393	0.325	7.90	6.35	46.2	2.6E+05	0.389	0.312
7.34	5.92	44.5	2.5E+05	0.390	0.315	6.46	5.32	42.6	2.4E+05	0.373	0.307
5.32	4.35	38.0	2.1E+05	0.387	0.316	7.38	5.94	44.6	2.5E+05	0.390	0.314
5.98	4.90	40.4	2.3E+05	0.384	0.315	6.58	5.41	42.6	2.4E+05	0.381	0.313
6.71	5.39	42.1	2.4E+05	0.398	0.320	4.07	3.38	33.5	1.9E+05	0.381	0.316
7.36	6.02	44.1	2.5E+05	0.397	0.325	5.36	4.36	38.3	2.2E+05	0.384	0.313
7.93	6.34	45.8	2.6E+05	0.398	0.319	8.45	6.78	48.1	2.7E+05	0.383	0.308
5.50	4.53	38.0	2.1E+05	0.400	0.330	5.83	4.79	40.5	2.3E+05	0.374	0.308
9.21	7.36	48.9	2.7E+05	0.405	0.324	8.62	7.00	49.1	2.8E+05	0.377	0.306
4.00	3.38	33.2	1.9E+05	0.383	0.323	7.37	6.02	44.5	2.5E+05	0.391	0.319

Figure A.20: Wind tunnel results from semi-trailer tests. *Re* and C_d calculated with $L = 10.48cm$ and $A_D = 191.8cm^2$

Trailers With Side Skirts Results											
Configuration: 3s						Configuration: 4s					
Test: 1	$T = 300\ K$		$\rho = 0.99\ kg/m^3$			Test: 1	$T = 300\ K$		$\rho = 0.99\ kg/m^3$		
F_{D1} (N)	F_{D2} (N)	U (m/s)	Re	C_{d1}	C_{d2}	F_{D1} (N)	F_{D2} (N)	U (m/s)	Re	C_{d1}	C_{d2}
7.94	5.32	40.9	2.3E+05	0.494	0.331	10.51	7.22	49.0	2.8E+05	0.457	0.314
6.86	4.78	38.5	2.2E+05	0.482	0.336	5.12	3.49	33.8	1.9E+05	0.470	0.320
11.61	7.78	49.1	2.8E+05	0.503	0.337	9.46	6.55	46.0	2.6E+05	0.469	0.325
9.95	6.72	46.1	2.6E+05	0.489	0.331	6.49	4.64	38.7	2.2E+05	0.456	0.326
8.69	5.95	42.5	2.4E+05	0.504	0.345	7.21	5.03	40.9	2.3E+05	0.452	0.316
5.25	3.73	33.4	1.9E+05	0.490	0.348	9.00	6.10	44.7	2.5E+05	0.475	0.322
9.26	6.40	44.6	2.5E+05	0.487	0.336	7.83	5.48	42.7	2.4E+05	0.452	0.316
5.24	3.70	33.5	1.9E+05	0.490	0.346	6.81	4.63	38.5	2.2E+05	0.483	0.328
9.91	6.77	46.0	2.6E+05	0.489	0.335	9.55	6.49	46.2	2.6E+05	0.470	0.320
9.28	6.33	44.4	2.5E+05	0.492	0.336	8.19	5.73	42.5	2.4E+05	0.477	0.333
7.02	4.68	38.1	2.2E+05	0.506	0.337	9.06	6.18	44.5	2.5E+05	0.482	0.328
7.69	5.40	40.6	2.3E+05	0.488	0.343	10.68	7.28	49.0	2.7E+05	0.470	0.320
11.33	7.85	48.9	2.8E+05	0.495	0.343	7.34	5.07	40.6	2.3E+05	0.468	0.323
8.51	5.85	42.3	2.4E+05	0.497	0.342	5.11	3.60	33.4	1.9E+05	0.482	0.339
Test: 2	$T = 300\ K$		$\rho = 0.99\ kg/m^3$			Test: 2	$T = 300\ K$		$\rho = 0.99\ kg/m^3$		
F_{D1} (N)	F_{D2} (N)	U (m/s)	Re	C_{d1}	C_{d2}	F_{D1} (N)	F_{D2} (N)	U (m/s)	Re	C_{d1}	C_{d2}
6.85	4.61	38.1	2.2E+05	0.491	0.330	7.19	4.99	40.5	2.3E+05	0.459	0.318
8.58	5.69	42.3	2.4E+05	0.502	0.333	4.74	3.38	33.4	1.9E+05	0.445	0.317
10.11	6.76	45.8	2.6E+05	0.504	0.337	7.81	5.28	42.4	2.4E+05	0.456	0.309
11.40	7.88	49.0	2.8E+05	0.495	0.342	9.41	6.53	45.9	2.6E+05	0.468	0.325
7.88	5.27	40.6	2.3E+05	0.500	0.335	10.89	7.20	49.0	2.8E+05	0.477	0.316
8.93	6.19	44.3	2.5E+05	0.477	0.331	8.78	6.12	44.5	2.5E+05	0.466	0.325
5.09	3.54	33.3	1.9E+05	0.482	0.335	6.35	4.45	38.1	2.1E+05	0.459	0.322
7.65	5.27	40.2	2.3E+05	0.496	0.341	4.76	3.42	33.2	1.9E+05	0.453	0.326
6.57	4.67	38.0	2.1E+05	0.477	0.339	10.96	7.43	49.0	2.7E+05	0.480	0.325
11.23	7.72	48.9	2.8E+05	0.492	0.338	8.22	5.57	42.4	2.4E+05	0.482	0.327
8.31	5.71	42.2	2.4E+05	0.490	0.337	9.32	6.42	45.7	2.6E+05	0.468	0.323
9.36	6.27	44.2	2.5E+05	0.502	0.337	7.19	5.16	40.5	2.3E+05	0.461	0.331
9.78	6.64	45.6	2.6E+05	0.494	0.335	8.55	5.89	44.2	2.5E+05	0.457	0.315
5.08	3.58	32.9	1.9E+05	0.490	0.346	6.19	4.38	38.0	2.1E+05	0.452	0.320
Test: 3	$T = 300\ K$		$\rho = 0.99\ kg/m^3$			Test: 3	$T = 300\ K$		$\rho = 0.99\ kg/m^3$		
F_{D1} (N)	F_{D2} (N)	U (m/s)	Re	C_{d1}	C_{d2}	F_{D1} (N)	F_{D2} (N)	U (m/s)	Re	C_{d1}	C_{d2}
6.64	4.48	38.5	2.2E+05	0.466	0.314	9.25	6.41	45.9	2.6E+05	0.459	0.318
9.36	6.39	46.2	2.6E+05	0.458	0.312	6.45	4.48	38.0	2.1E+05	0.467	0.325
8.05	5.48	42.4	2.4E+05	0.468	0.319	10.71	7.50	48.7	2.7E+05	0.474	0.332
7.41	5.01	40.6	2.3E+05	0.470	0.318	9.29	6.35	44.3	2.5E+05	0.496	0.339
5.17	3.44	33.3	1.9E+05	0.488	0.325	7.15	5.06	40.4	2.3E+05	0.459	0.325
9.08	6.05	44.3	2.5E+05	0.484	0.323	7.76	5.54	42.2	2.4E+05	0.457	0.326
11.62	7.70	48.8	2.8E+05	0.510	0.338	5.02	3.54	33.2	1.9E+05	0.478	0.337
6.46	4.46	38.1	2.1E+05	0.466	0.322	7.60	5.39	42.1	2.4E+05	0.450	0.319
5.09	3.41	33.2	1.9E+05	0.485	0.325	9.06	6.48	45.8	2.6E+05	0.454	0.325
10.19	6.69	45.8	2.6E+05	0.508	0.334	7.43	5.11	40.4	2.3E+05	0.479	0.329
7.56	5.10	40.4	2.3E+05	0.486	0.328	11.01	7.50	48.9	2.7E+05	0.485	0.330
9.00	6.08	44.1	2.5E+05	0.484	0.327	6.43	4.57	38.0	2.1E+05	0.467	0.332
8.29	5.53	42.1	2.4E+05	0.490	0.327	4.73	3.46	33.2	1.9E+05	0.451	0.330
10.78	7.32	48.9	2.7E+05	0.474	0.322	9.00	6.00	44.2	2.5E+05	0.485	0.323

Figure A.21: Wind tunnel results from semi-trailer tests. Re and C_d calculated with $L = 10.48cm$ and $A_D = 191.8cm^2$